AD-A122 299 TSUNAMI RESPONSE OF BARBERS POINT HARBOR HAWAII(U) ARMY ENGINEER WATERWAYS EXPERIMENT STATION VICKSBURG MS HYDRAULICS LAB P D FARRAR ET AL. OCT 82 WES/MP/HL-82-1 1/2

UNCLASSIFIED F/G 8/3 NL

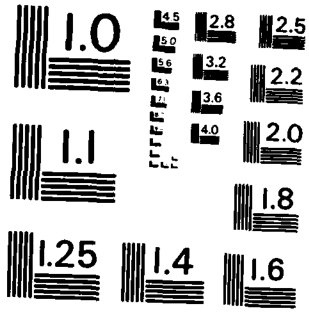

MICROCOPY RESOLUTION TEST CHART
NATIONAL BUREAU OF STANDARDS - 1963 - A

MISCELLANEOUS PAPER HL-82-1

TSUNAMI RESPONSE OF BARBERS POINT HARBOR, HAWAII

by

Paul D. Farrar, James R. Houston

Hydraulics Laboratory
U. S. Army Engineer Waterways Experiment Station
P. O. Box 631, Vicksburg, Miss. 39180

October 1982

Final Report

Prepared for U. S. Army Engineer Division, Pacific Ocean
Fort Shafter, Hawaii 96858

UNCLASSIFIED

SECURITY CLASSIFICATION OF THIS PAGE (When Data Entered)

REPORT DOCUMENTATION PAGE

READ INSTRUCTIONS BEFORE COMPLETING FORM

1. REPORT NUMBER Miscellaneous Paper HL-82-1	2. GOVT ACCESSION NO. A122 299
3. RECIPIENT'S CATALOG NUMBER	
4. TITLE (and Subtitle) TSUNAMI RESPONSE OF BARBERS POINT HARBOR, HAWAII	5. TYPE OF REPORT & PERIOD COVERED Final report
	6. PERFORMING ORG. REPORT NUMBER
7. AUTHOR(s) Paul D. Farrar James R. Houston	8. CONTRACT OR GRANT NUMBER(s)
9. PERFORMING ORGANIZATION NAME AND ADDRESS U. S. Army Engineer Waterways Experiment Station Hydraulics Laboratory, P. O. Box 631 Vicksburg, Miss. 39180	10. PROGRAM ELEMENT, PROJECT, TASK AREA & WORK UNIT NUMBERS
11. CONTROLLING OFFICE NAME AND ADDRESS U. S. Army Engineer Division, Pacific Ocean Fort Shafter, Hawaii 96858	12. REPORT DATE October 1982
	13. NUMBER OF PAGES 136
14. MONITORING AGENCY NAME & ADDRESS(if different from Controlling Office)	15. SECURITY CLASS. (of this report) UNCLASSIFIED
	15a. DECLASSIFICATION/DOWNGRADING SCHEDULE

16. DISTRIBUTION STATEMENT (of this Report)

Approved for public release; distribution unlimited.

17. DISTRIBUTION STATEMENT (of the abstract entered in Block 20, if different from Report)

18. SUPPLEMENTARY NOTES

Available from National Technical Information Service, 5285 Port Royal Road, Springfield, Va. 22151

19. KEY WORDS (Continue on reverse side if necessary and identify by block number)

Barbers Point Harbor
Harbors--Hawaii
Mathematical models
Ocean waves
Tsunamis

20. ABSTRACT (Continue on reverse side if necessary and identify by block number)

This study determines the degree of susceptibility of the proposed Barbers Point Deep-draft Harbor on Oahu Island, Hawaii, to tsunami waves. A finite-difference numerical model was developed to simulate the action of long-period waves within the harbor. This model included the effects of bottom friction, lateral mixing of momentum, radiation losses to the outside ocean, and the flooding of surrounding land areas. A large number of cases were simulated, representing tsunami inputs that could be expected

DD FORM 1 JAN 73 1473 EDITION OF 1 NOV 65 IS OBSOLETE

UNCLASSIFIED

SECURITY CLASSIFICATION OF THIS PAGE (When Data Entered) in the area. The resulting water elevations, land flooding, and water movement are presented.

The response of the harbor to the many different wave cases was combined with a study of the frequency-of-occurrence of tsunamis to obtain frequency-of-occurrence statistics for different harbor response events. This was done both for infrequent large tsunamis and for more frequent small amplitude tsunamis. Conservative probability methods were used for all results.

On the basis of the response modeling and probability studies, the following conclusions were reached: (a) the harbor does amplify incident long-period waves, especially those with a period of around 800 sec, (b) this amplification is, however, much smaller than would be predicted by linear response models, such as that of Durham (1978), which neglects nonlinear effects, such as bottom friction, lateral mixing, and flooding, (c) the nature of the harbor response will depend on the character of the incident wave, and (d) the harbor location chosen is a good location for the mitigation of tsunami hazards.

PREFACE

Authority for the U. S. Army Engineer Waterways Experiment Station (WES) to conduct a tsunami study of the proposed Barbers Point Harbor was granted by the U. S. Army Engineer Division, Pacific Ocean, in Intra-Army Order No. PODSP-CIV-79-11 dated 12 December 1978.

This study was conducted from January 1979 to September 1980 in the Hydraulics Laboratory, WES, under the direction of Mr. H. B. Simmons, Chief of the Hydraulics Laboratory, and Dr. R. W. Whalin, Chief of the Wave Dynamics Division. Mr. P. D. Farrar conducted the study and prepared this report, except for Part IV, the event frequency analysis, which was conducted and written by Dr. J. R. Houston. Mrs. L. W. Chou assisted in the computer programming and graphics preparation.

Dr. C. Bretschneider and Dr. D. Cox of the University of Hawaii provided advice during this study.

COL John L. Cannon, CE, COL Nelson P. Conover, CE, and COL Tilford C. Creel, CE, were Commanders and Directors of WES during the investigation and the preparation and publication of the report. Mr. F. R. Brown was Technical Director.

A

CONTENTS

CONVERSION FACTORS, U. S. CUSTOMARY TO METRIC (SI)
UNITS OF MESUREMENT

U. S. customary units of measurement used in this report can be converted to metric (SI) units as follows:

Multiply	By	To Obtain
acres	4046.9	square metres
feet	0.3048	metres
miles (U. S. statute)	1.6093	kilometres
feet per second	0.3048	metres per second
square feet per second	0.0929	square metres per second

TSUNAMI RESPONSE OF BARBERS POINT HARBOR, HAWAII

PART I: INTRODUCTION

Background

1. The Barbers Point Deep-Draft Harbor was authorized by Congress in Section 301 of the River and Harbor Act of 1965 to provide for the future port needs of Oahu and of the Hawaiian Islands.

2. The harbor site is about 15 miles* west of Honolulu at the southwestern extremity of Oahu (Figure 1) on the Ewa coastal plain near the southern end of the Waianae Range. The plain slopes gently (about 1:300) towards the sea and in the area of the harbor site is about 8 to 16 ft above mean lower low water. The rock is coral limestone reef and breccia with small amounts of volcanic material (tuff and unconsolidated ash) (U. S. Army Engineer District, Honolulu 1977). The site itself is currently largely undeveloped and is mostly covered with native vegetation, except for a large borrow pit. It adjoins the Barbers Point Industrial Park (Figure 2).

3. In 1961 the developers of the Barbers Point Industrial Park dredged a small L-shaped barge harbor on the site. Its dimensions are 520 by 700 ft with a 21-ft depth. Plans for the deep-draft harbor include this harbor as a small side basin (Plate 1).

4. The deep-draft harbor, as authorized by the Rivers and Harbors Act of 1965, was to consist of a 38-ft-deep inshore basin of about 46 acres, an offshore channel 450 ft wide and 42 ft deep, and a separate small-craft harbor. A hydraulic scale model study of various harbor configurations was conducted by the Look Laboratory of the Ocean Engineering Department of the University of Hawaii in 1967-1968 (Palmer 1970).

5. The final design, which makes use of design features tested in the hydraulic model (Palmer 1970), is shown in Plates 1 and 2 from Design Memorandum No. 1 (Honolulu District 1977). The design calls for

---

* A table of factors for converting U. S. Customery units of measurements to metric (SI) units is presented on page 3.

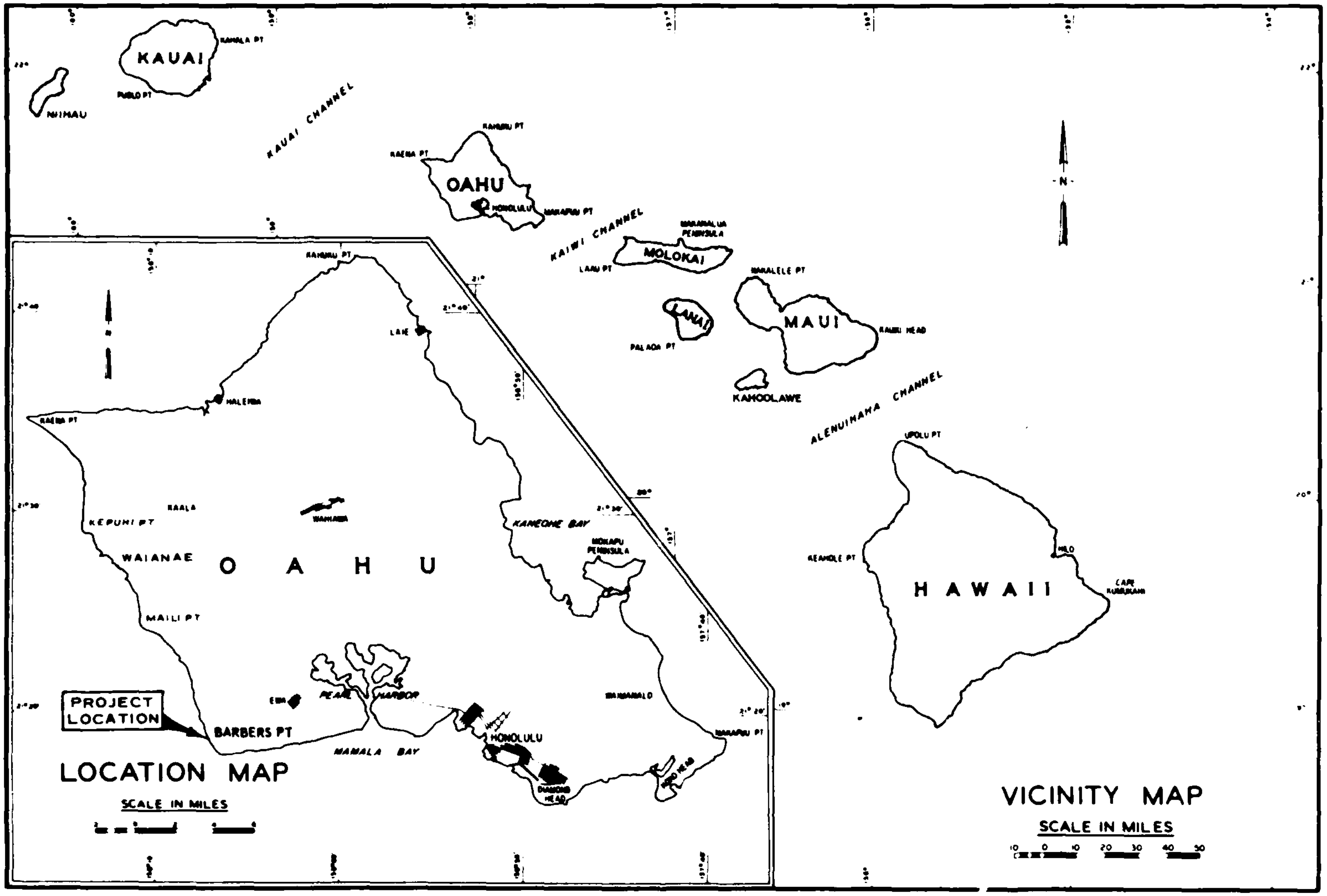

Figure 1. Location of Barbers Point Harbor

Figure 2. Aerial View of Barbers Point Area (from Honolulu, 1977; R. M. Towill Photograph 1974)

a roughly trapezoidal landlocked basin with a 38-ft depth and an area of 92 acres. It would be connected to the offshore region by a dredged channel 4280 ft long, 450 ft wide, and 38 to 42 ft deep. The existing barge harbor would be incorporated as a side basin off the channel. Protection from wind-driven waves would be provided by 4700 lineal ft of wave absorbing structures along the channel and the backs of the two basins in a configuration which performed well in the hydraulic model tests. Dock facilities could be constructed along the northeast, southeast, and southwest sides of the basin.

6. In order to analyze the response of the proposed harbor design to waves of a wide range of periods, the U. S. Army Engineer Waterways Experiment Station conducted a numerical analysis of the linear modes of oscillation of the proposed harbor (Durham 1978). Durham used the finite element method to solve the linear wave equations (as described in paragraphs 7-11). The linear methods used are the best means of identifying resonant modes of the system. However, since nonlinear effects such as friction are eliminated, the predicted response is only accurate for infinitesimally small waves, for which the nonlinear effects become negligible. For larger amplitude waves, the method becomes increasingly inaccurate, especially with respect to resonant amplification. In addition, the model could not take into account flooding and drying of the surrounding land. Therefore, the study reported here was undertaken to investigate the behavior of the harbor in response to tsunami waves of realistic amplitude, taking into account such nonlinear effects as friction and flooding.

Normal Modes of Barbers Point Harbor

7. In order to determine the response of the harbor design to low-frequency waves (20-sec and longer periods), Durham (1978) analyzed the normal modes of long-wave vibration of the harbor. By using the linear long-wave equations, the part of the solution which is not dependent on time is found to be the solution of the Helmholtz equation:

$$\nabla \cdot (h\nabla\phi) + \frac{\omega^2}{g}\phi = 0 \qquad (1)$$

where h is water depth, ω is the angular frequency of the wave, g is the acceleration of gravity, and ϕ, the variable being solved for, is the velocity potential. The amplitude response function $R(x,y,\omega)$ (the wave height amplication factor R is called η in Durham 1978) is determined by

$$R = -\frac{1}{g}\frac{\partial\phi}{\partial t} \qquad (2)$$

8. The system of equations was solved using a finite element model based on that of Chen and Mei (1974). For a group of positions (x, y-constant value), $R(\omega)$ was found by sweeping through ω. The values of ω at which peaks in the $R(\omega)$ curve occurred were the angular frequencies of the various natural resonant modes. An example of one of these curves, for a location in Barbers Point Harbor corresponding to gage 2 for this study, is shown in Figure 3. $R(x,y)$, $u(x,y)$, and $v(x,y)$ were found for the various resonant ω values in order to define the characteristics of each modal response.

9. Since the model equations used by Durham were linear, the $R(\omega)$ curve for each point in the harbor completely determines the linear response at that point. By the definition of linear response, for any two input waves $F_1(\omega_1)$ and $F_2(\omega_2)$ with angular frequencies ω_1 and ω_2 and for a constant c,

$$\begin{gathered} R[F_1(\omega_1 + F_2(\omega_2)] = R[F_1(\omega_1)] + R[F_2(\omega_2)] \ , \\ R[cF_1(\omega_1)] = cR[F_1(\omega_1)] \end{gathered} \qquad (3)$$

Since any input signal meeting Dirichlet's conditions may be Fourier-decomposed into a set of frequencies, the response to any complex signal may be determined by using Equation 3. For a composite signal

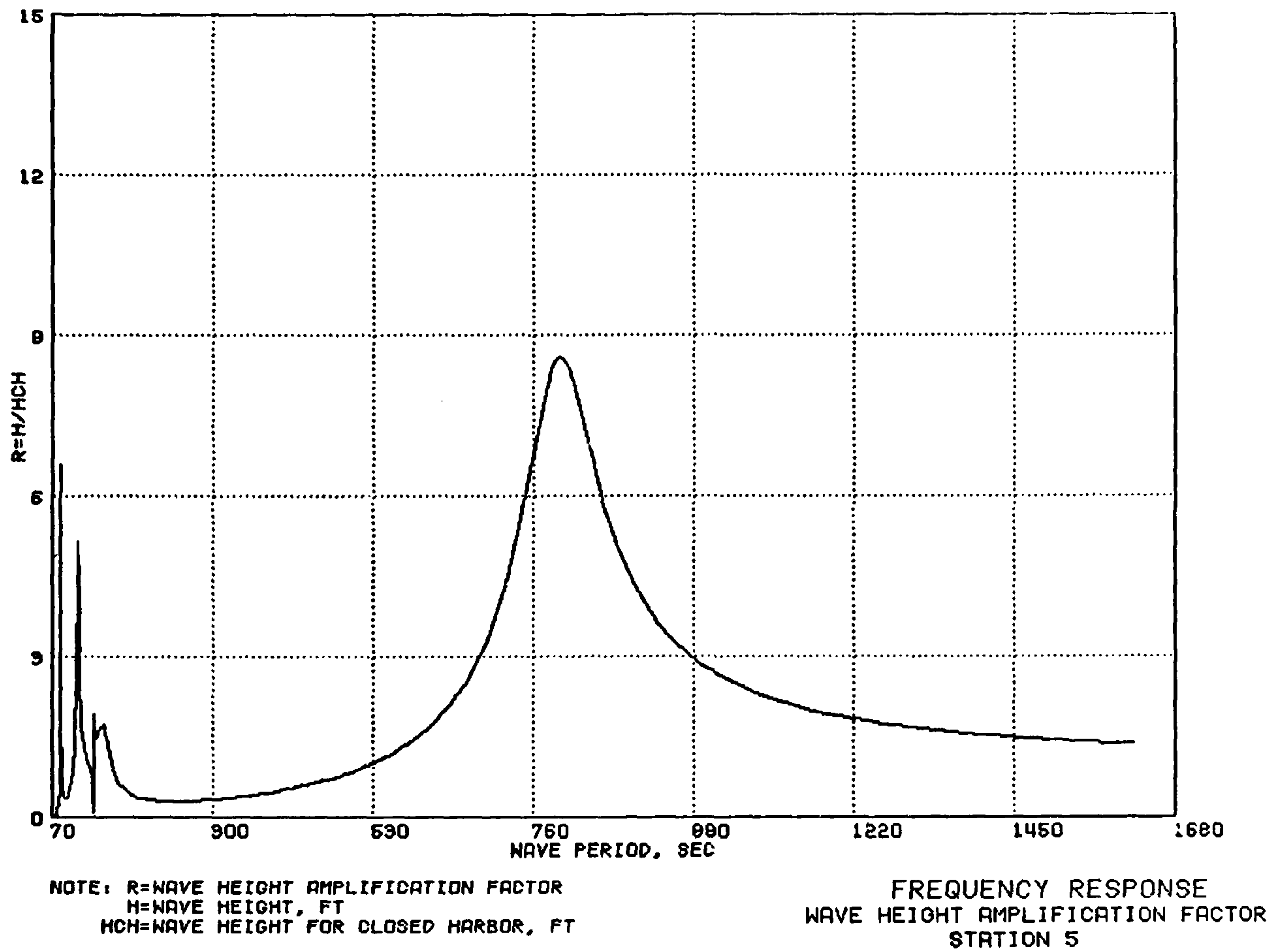

Figure 3. Response found by Durham (1978) at location of gage 2 for this study

$$F(\omega) = \sum_{i=1}^{n} a_i F_i(\omega_i) \ , \tag{4}$$

where a_i and ω_i are the amplitude and frequency of component i, the response is

$$R[F(\omega)] = \sum_{i=1}^{n} a_i R[F_i(\omega_i)] \tag{5}$$

The response to a signal with a continuous spectrum may be determined by converting $R(x,y,\omega)$ into a function of response per unit frequency and taking the convolution of this function with the input spectrum.

10. The responses found by Durham may be divided into two types: (a) a group of rocking or standing wave modes within the harbor and (b) the single fundamental mode of the harbor itself. The first class consists of standing waves having one or more nodal lines within the harbor. These have numerous narrow peaks at periods from 21 to 145 sec. From about a 200-sec period and longer, there is a different type of modal response. There is a large broad peak at 799 sec which corresponds to the fundamental, or Helmholtz, mode (Figure 3). In this mode, the entire surface within the harbor rises and falls together, with no nodal lines within the harbor.

11. This mode is of concern because of the great width of the peak in the response curve, which means that this mode will be excited by any of a large range of wave frequencies. The period range of this peak covers much of the range of tsunami periods, which range from about 8 to 60 min. The peak is at 799 sec (13.3 min). The existence of this peak made further studies of the tsunami response of the proposed harbor desirable.

The Helmholtz Mode

12. A harbor which has a length/width ratio of around unity and

a mouth somewhat narrower than the interior dimensions of the harbor, as at Barbers Point, will have a natural resonant mode in which the entire surface of the inner harbor rises and falls as a unit. This mode is variously referred to as the "zeroth mode," the "fundamental mode," or the "Helmholtz mode," by analogy to the acoustic Helmholtz resonator.

13. The Helmholtz mode may be visualized as a mass-spring oscillator. The vibrating mass is the moving water in and around the harbor mouth, and the restoring force, or spring, is the hydrostatic pressure due to the difference between the surface elevations inside and outside the harbor.

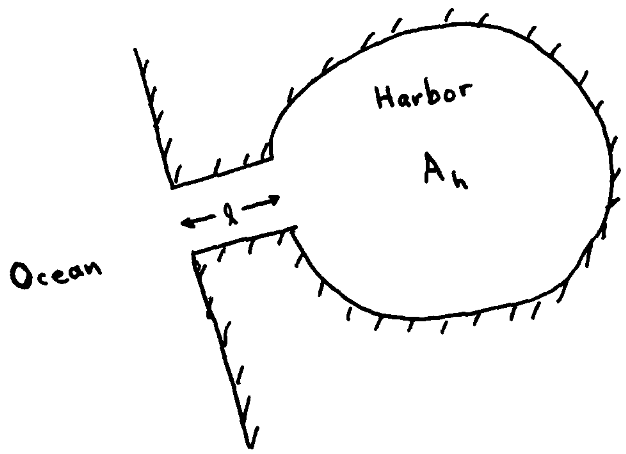

Figure 4. Sample Harbor

Consider a harbor of area A_h connected to an ocean of infinite volume by a channel of length ℓ and cross-sectional area A_c. The mass of water in the channel is $\rho A_c \ell$, where ρ is the density of water. If the water in the channel is moved inward a distance of X, the volume of water in the harbor is increased by $A_c X$, and the surface rises by $A_c X/A_h$. This increases the hydrostatic pressure by $\rho g A_c X/A_h$. Since it acts as a restoring force on the cross-sectional area A_c, the force on the water in the channel is $-\rho g A_c^2 X / A_h$. The equation of motion is

mass × acceleration = force

or

$$\rho A_c \ell \frac{d^2X}{dt^2} = \frac{\rho g A_c^2 X}{A_h} \tag{6}$$

$$\frac{d^2X}{dt^2} + \frac{gA_c}{A_h \ell} X = 0 \tag{7}$$

The solution is of the form $X = X_o e^{-i\omega t}$, where $\omega = (gA_c / A_h \ell)^{1/2}$. The angular frequency ω is the natural resonant frequency of the harbor for the Helmholtz mode of the harbor. The period T equals $2\pi/\omega$, or

$$T = 2\pi \left(\frac{A_h \ell}{gA_c} \right)^{1/2} \tag{8}$$

14. This oscillator is the long-wave equivalent of the acoustic Helmholtz oscillator, an example of which is a soft-drink bottle, in which the mass is the air in the bottle neck and the spring is the acoustic compliance of the air in the body of the bottle.

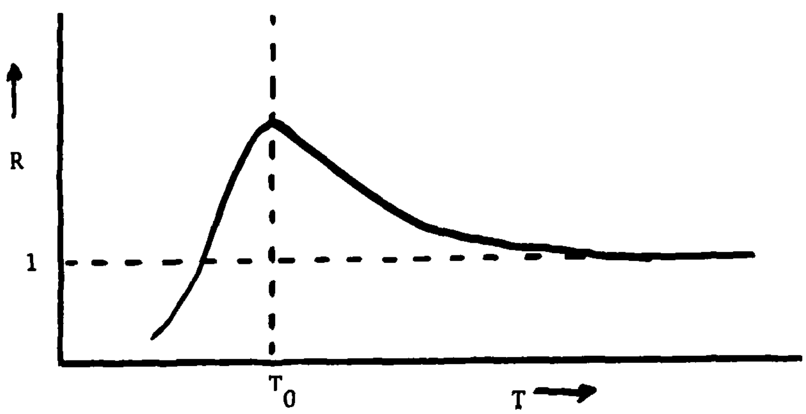

Figure 5. Response of Theoretical Linear Oscillator (R) Versus Forcing Period (T)

15. The above equations give the free or unforced response of the harbor. The forced response to variations in the outside ocean is a considerably more complicated phenomenon. Nevertheless, the general response can be described. The amplitude response function for a linear oscillator is given in Figure 5. For very short-period motions in the ocean, the harbor does not, as a unit, respond at all. As the period lengthens to T_o , the natural period, the harbor responds quite strongly. At this resonance, the interior of the harbor is 180 deg out of phase with the exterior. As the period lengthens further, the response falls, and for very long periods (compared to T_o) the response is unity and is in phase with the exterior. This behavior can be readily seen in the results of Durham (Figure 3). He also found resonant peaks for higher frequencies, but these are for different types of mode, in which the harbor does not respond as a unit.

PART II: THE MODEL

Equations of Motion

16. For this study, the three-dimensional equations of fluid motion may be integrated in the vertical direction to allow solution of a two-dimensional problem. Due to the small lateral extent of the harbor area, the high frequency of the waves under consideration (relative to the frequency of the earth's rotation) and the dominance of frictional effects, the Coriolis forces can be neglected. The fluid may be assumed homogeneous and incompressible and pressure assumed hydrostatic. The resulting equations of motion are

$$\frac{\partial u}{\partial t} + u\frac{\partial u}{\partial x} + v\frac{\partial u}{\partial y} = -g\frac{\partial h}{\partial x} + \frac{\partial}{\partial x} K \frac{\partial u}{\partial x} + \frac{\partial}{\partial y} K \frac{\partial u}{\partial y} - \frac{guQ}{C^2(h + \eta)} \tag{9}$$

and

$$\frac{\partial v}{\partial t} + u\frac{\partial v}{\partial x} + v\frac{\partial v}{\partial y} = -g\frac{\partial \eta}{\partial y} + \frac{\partial}{\partial x} K \frac{\partial v}{\partial x} + \frac{\partial}{\partial y} K \frac{\partial v}{\partial y} - \frac{gvQ}{C^2(h + \eta)} \tag{10}$$

The continuity equation is

$$\frac{\partial \eta}{\partial t} + \frac{\partial}{\partial x}[(h + \eta)u] + \frac{\partial}{\partial y}[(h + \eta)v] = 0 \tag{11}$$

The vertically averaged x and y velocities are u and v, η is the elevation of the water surface above the datum, g is the acceleration of gravity, h is the mean water depth, and $Q = (u^2 + v^2)^{1/2}$ is the current speed. K and C are empirically determined frictional coefficients.

17. The last three terms on the right-hand sides of Equations 9

and 10 model the effects of turbulent mixing of momentum. The lateral mixing of momentum by eddies too small to be resolved in the finite difference representation of Equations 9 and 10 is assumed to occur in a matter analogous to the viscous mixing of momentum. The "eddy-viscosity" coefficient K is not, however, a global constant characteristic of the fluid itself, as the molecular viscosity is, but an empirical coefficient determined for the particular case. The use of an "eddy-viscosity" coefficient is the most widely used method of modeling turbulent mixing and is discussed in detail by Hinze (1959), Launder and Spalding (1972), and Tennekes and Lumley (1972), among others.

18. The effects of vertical turbulent mixing of momentum and of bottom stress are given by the last terms in Equations 9 and 10. Although this form was originally developed for the description of steady flow in an open channel, it may be used in cases such as this, in which u and v vary relatively slowly compared to the time needed for the vertical profile of velocity to adjust its shape for the new u and v. C is the empirical friction coefficient of Chezy (Morris and Wiggert 1972). The value of C may be determined from Manning's n, which is a value characteristic of the particular bottom type, by

$$C = \frac{1.49}{n} R_h^{1/6} , \qquad (12)$$

where R_h is the hydraulic radius.

Boundary Conditions

19. In order to determine the solution of a particular problem governed by the equations of motion and continuity (Equations 9, 10, and 11), it is necessary to prescribe initial and boundary conditions, both internal and external, for the region under consideration. When flooding and drying of cells in the region occurs, the internal boundary conditions will change, so it is necessary to locate the internal boundaries for each time step.

20. The simplest boundary condition is shown in Figure 6a. When the land level of a cell is above the water level in a neighboring cell and there is no preexisting water in the cell, the condition is that of no flow between the cells. Likewise, there is no flow between two dry cells.

21. When the water level in one cell rises above the land level in a neighboring dry cell, it is necessary to move water into the dry cell. This condition is satisfied by prescribing the flow through the boundary using a broad-crested weir equation (Reid and Bodine 1968) giving the volume transport rate per unit width (units of length^2/time):

$$Q_n = \pm C_o D_b \sqrt{g D_b} \tag{13}$$

where Q_n is the volume transport per unit width across the boundary, D_b is the depth of water at the boundary, and C_o is an empirical coefficient. D_b is set equal to η for the wet cell minus z for the dry cell as shown in Figure 6b. The sign is taken as appropriate to give flow in the proper direction.

22. The same equation is used for the situation depicted in Figure 6c, in which water drains from a cell elevated above the water level of its neighbor. This situation may occur during the recession of flood waters. Although there is water in both cells, the use of wave equations to describe this situation is clearly inappropriate, as there is no feedback of information from the lower to the higher cell. In this case, D_b is set to the depth of water in the upper cell.

23. In situations in which there is a very shallow flow over a sill, as depicted in Figures 6d and 6e, the momentum equations are replaced by a head-discharge relation for a submerged weir (Reid and Bodine 1968). This replacement is made in cases in which the water depth on one (Figure 6d) or both (Figure 6e) sides of the boundary are below some critical depth D_c. The equation for volume transport rate per unit width is

$$Q_n = \pm C_1 D_b \sqrt{g \left| \eta_1 - \eta_2 \right|} \, , \tag{14}$$

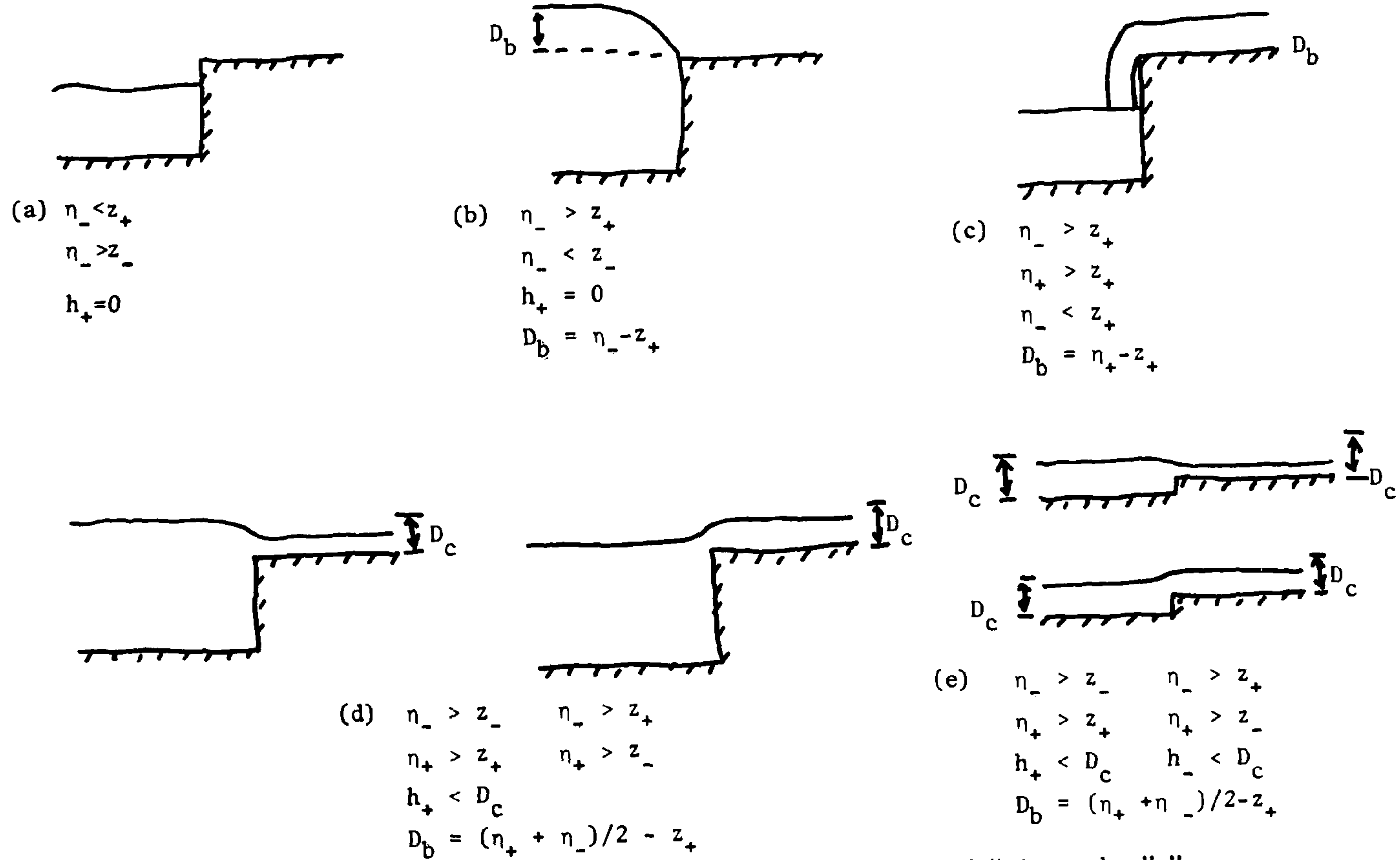

Figure 6. Flooding and drying situations. Higher cell is denoted by "+", lower by "-".

where C_1 is an empirical coefficient, D_b is the water depth over the boundary, and η_1 and η_2 are the surface elevations on either side.

24. In a model of a locality of limited extent, the open ocean will appear to that region to be essentially infinite in extent. The modeling of an area of ocean large enough to appear as if it were practically infinite as well as of the small area under consideration presents great, and usually insuperable, difficulties due to the difference in scale between the open ocean and the small coastal area. One practical method of solving this difficulty is to have two nested models in which the larger open ocean model provides an input boundary condition for the smaller model of the area in which detailed results are desired. Implicit in this approach is the assumption that the smaller area has very little effect on the results in the larger area.

25. The simplest method of describing the seaward boundary condition of a coastal model is to prescribe the surface elevation at that boundary using the given input signal. However, this method does not allow wave energy radiating from the model interior to pass outward through the boundary. Waves travelling outward are reflected back into the region with a phase change of 180 deg.

26. This difficulty can be circumvented by using a boundary condition based on the Sommerfeld radiation condition:

$$\frac{\partial \varepsilon}{\partial t} + C \frac{\partial \varepsilon}{\partial x} = 0 \tag{15}$$

where C is the phase velocity of the waves and ε is any variable (Orlanski 1976). For $\varepsilon = \eta$ and long waves, this condition can be reduced to $Q_n = C\eta$, where $C = \sqrt{gh}$ and Q_n is the outward transport at the boundary (Reid and Bodine 1968, Reid, Vastano, and Reid 1977). For a boundary of zero depth this reduces to $Q_n = 0$, and for a boundary with an infinitely deep ocean the condition produces a node at the boundary (for finite Q_n , $\eta \to 0$ as $C \to \infty$) .

27. For a given input wave $\eta_I(t)$ from outside the boundary, the condition may be written

$$Q_n = C(\eta - \eta_I) \tag{16}$$

if η_I varies only slowly (Reid and Bodine 1968).

Finite Difference Equations

28. The system of wave equations and flooding-drying equations is integrated numerically in time by an explicit finite difference method. The region under study is subdivided into an m by n rectangular grid of square blocks of side Δs. The value of η assigned to each block is located in the center of that block: η_{ij} is at $x = (i - 1/2)\Delta s$, $y = (j - 1/2)\Delta s$ (Figure 7). The values of u and v are located at the borders of each block: u_{ij} is at $x = i\Delta s$, $y = (j - 1/2)\Delta s$ and v_{ij} is at $x = (i - 1/2)\Delta s$, $y = j\Delta s$. Values of bottom elevation z_{ij} are given for the η locations so that the depth h_{ij} is $\eta_{ij} - z_{ij}$.

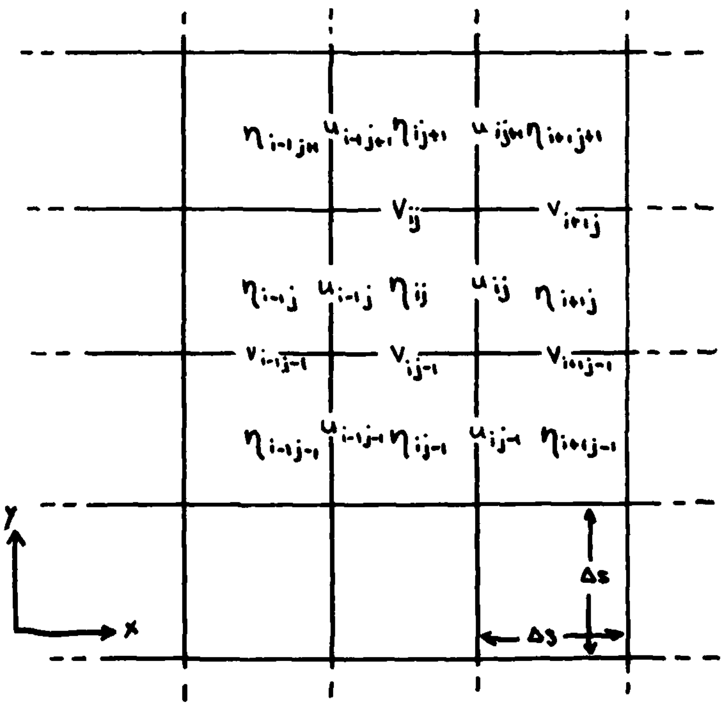

Figure 7. Finite difference grid

The value of a variable at some time $t = k\Delta t$ is denoted by a superscript k. If the superscript is omitted, a value of k should be assumed.

29. Equations 9, 10, and 11 may be written in centered finite difference form using the discrete variables from the finite difference grid. The equations of motion become

$$\frac{u_{ij}^{k+1} - u_{ij}^{k-1}}{2\Delta t} + u_{ij} \frac{u_{i+1j} - u_{i-1j}}{2\Delta s} + \underline{v}_{ij} \frac{u_{ij+1} - u_{ij-1}}{2\Delta s}$$

$$= g \frac{\eta_{i+1j} - \eta_{ij}}{\Delta s} + K \frac{u_{i+1j}^{k-1} + u_{i-1j}^{k-1} + u_{ij+1}^{k-1} + u_{ij-1}^{k-1} - 4u_{ij}^{k-1}}{\Delta s^2} \tag{17}$$

$$- \frac{g u_{ij}^{k+1} Q_{ij}^{k-1}}{C_{ij}^2 (\eta_{ij} - z_{ij})}$$

and

$$\frac{v_{ij}^{k+1} - v_{ij}^{k-1}}{2\Delta t} + \underline{u}_{ij} \frac{v_{i+1j} - v_{i-1j}}{2\Delta s} + v_{ij} \frac{v_{ij+1} - v_{ij-1}}{2\Delta s}$$

$$= g \frac{h_{ij+1} - h_{ij}}{\Delta s} + K \frac{v_{i+1j}^{k-1} + v_{i-ij}^{k-1} + v_{ij+1}^{k-1} + v_{ij-1}^{k-1} - 4v_{ij}^{k-1}}{\Delta s^2} \tag{18}$$

$$- \frac{g v_{ij}^{k+1} Q_{ij}^{k-1}}{C_{ij}^2 (\eta_{ij} - z_{ij})}$$

where

$$\underline{v}_{ij} = (v_{ij} + v_{i+1j} + v_{ij-1} + v_{i+1j-1})/4$$

$$\underline{u}_{ij} = (u_{ij} + u_{ij+1} + u_{i-1j} + u_{i-1j+1})/4$$

$$Q_{ij}^{k-1} = [(u_{ij}^{k-1})^2 + (\underline{v}_{ij}^{k-1})^2]^{1/2} \quad \text{for Equation 17}$$

and

$$Q_{ij}^{k-1} = [(u_{ij}^{k-1})^2 + (v_{ij}^{k-1})^2]^{1/2} \quad \text{for Equation 18}$$

The lateral eddy viscosity term, the second term on the right-hand side of Equations 17 and 18, lags one time step because the numerical scheme in which the term is written for the central time step k is unstable.

30. The continuity equation is

$$\frac{\eta_{ij}^{k+1} - \eta_{ij}^{k-1}}{2\Delta t} + \frac{(uh)_{ij} - (uh)_{i-1j}}{\Delta s} + \frac{(vh)_{ij} - (vh)_{ij-1}}{\Delta s} = 0 \qquad (19)$$

When the values of flow through the side of a block are given by the flooding and drying equations, the uh and vh terms are found directly from these equations. When the flows are determined by the momentum Equations 17 and 18,

$$\begin{aligned}
(uh)_{ij} &= u_{ij}\,(\eta_{i+1j} - z_{i+1j} + \eta_{ij} - z_{ij})/2 \\
(uh)_{i-1j} &= u_{i-1j}\,(\eta_{i-1j} - z_{i-1j} + \eta_{ij} - z_{ij})/2 \\
(vh)_{ij} &= v_{ij}\,(\eta_{ij+1} - z_{ij+1} + \eta_{ij} - z_{ij})/2 \\
(vh)_{ij-1} &= v_{ij-1}\,(\eta_{ij-1} - z_{ij-1} + \eta_{ij} - z_{ij})/2
\end{aligned} \qquad (20)$$

31. For the situation of initial flooding of a dry cell $(i+1, j)$ from cell (i,j), as shown in Figure 6b, the discrete equation is written as follows. When $\eta_{ij} > z_{i+1j}$ for two time steps, set $D_b = (\eta_{ij}^{k} + \eta_{ij}^{k-1})/2 - z_{i+1j}$ and substitute into Equation 13. The use of an average for η is to prevent high-frequency oscillations of water between cells. The one time step delay before flooding is quite negligible due to the shortness of the time steps used. Likewise, for flooding of cell (i, j) from cell $(i+1, j)$, $D_b = (\eta_{i+1j}^{k} + \eta_{i+1j}^{k+1})/2 - z_{ij}$. The sign in Equation 13 is chosen to give flow in the proper direction. Analogous equations are used for flow in the y-direction.

32. In the case in which water drains from an elevated cell $(i+1, j)$ into cell (i, j) as in Figure 6c, Equation 13 is used with $D_b = (\eta^{k+1}_{i+1j} + \eta^{k+1}_{i+1j})/2 - z_{i+1j}$. Equations for flow in other directions are similar.

33. For Equation 14, $D_b = (\eta^{k+1}_{ij} + \eta^{k}_{ij} + \eta^{k+1}_{i+1j} + \eta^{k}_{i+1j})/4 - z_x$, where z_x equals either z_{ij} or z_{i+1j} , depending on which is shallower. The η values used to determine the head difference between cells are $\eta_1 = (\eta^{k}_{ij} + \eta^{k-1}_{ij})/2$ and $\eta_2 = (\eta^{k}_{i+1j} + \eta^{k-1}_{i+1j})/2$. Flow in the y-direction is treated similarly.

34. The values of flow calculated with flooding and drying equations are linked with the wave Equations 17-19 through the continuity equation (19). The values of Q_n are substituted directly into Equation 19 in place of the appropriate $(uh)_{ij}$ or $(vh)_{ij}$ value.

35. For an ocean boundary cell (i, j) , Equation 16 is written

$$Q_n = [g(\eta_{ij} - z_{ij})]^{1/2} (\eta_{ij} - \eta_I) \tag{21}$$

The sign is chosen to give a flow in the proper direction.

Solution Method

36. The numerical integration of Equations 9-11, 13-14, and 16 in time is accomplished as follows. Given the values of u , v , and η at time steps $k-1$ and k and the values of Q_n at time step k , use Equation 19 to predict a new η for time step $k+1$. At this point, η at $k-1$ may be discarded to save storage space since it is no longer needed. Then the flooding and drying equations and the radiation boundary condition are used to find Q_n at $k+1$, which replaces the old Q_n at k in the computer memory. Finally, u and v are found at $k+1$ from Equation 17 and 18, completing a full time step Δt . The process can be repeated for any number of steps to get the values of the hydrodynamic variables at any future time.

37. For stability the time step must be limited to $\Delta t \le \Delta s/(2\ gh_{max})^{1/2}$, where h_{max} is the greatest water depth ever attained. This ensures that numerical information, which propagates with speed $\Delta x/\Delta t$, will propagate faster than the wave being described.

PART III: APPLICATION OF THE MODEL TO BARBERS POINT HARBOR

Model Grid

38. The Barbers Point Harbor and the immediate offshore bottom topography as shown in Plate 1 were discretized on a 47 by 36 grid with a Δs equal to 150 ft. Table 1 gives the elevation of the bottom relative to mean lower low water. The elevation of the land surface for the area around the harbor is shown as 8 ft, but it may be varied to give different experimental conditions. The rows of cells of 100 ft elevation along two edges of the grid are of dummy cells to provide u and v values along those edges. The dredged material disposal sites were given an elevation of 40 ft. Their shape and location are shown in Plate 3, which gives the general layout of the model area. Also shown in Plate 3 are the gage locations at which water elevation time series were recorded during model runs.

Flooding And Drying Coefficients

39. The model has several empirical coefficients, C_o , C_1 , D_c , n , and K , which must be assigned values in order to run the model. C_o , C_1 , and D_c control flooding and drying, and n and K (discussed in the next section) parameterize frictional effects. The value of C_1 may be roughly estimated using Manning's equation,

$$u = \frac{1.49}{n} D^{2/3} S^{1/2} \tag{22}$$

where D is the water depth and S is the water surface slope. Setting $S = |\eta_1 - \eta_2|/\Delta s$, $D = D_b$, and $Q_n = uD_b$ and comparing Equations 14 and 22 yields

$$C_1 = \frac{1.49}{n} \frac{D_b{}^{2/3}}{(g\Delta s)^{1/2}} \tag{23}$$

For $D_b = 1$ ft, $n = 0.025$, $\Delta s = 150$ ft, and $g = 32.2$ ft/sec^2, $C_1 =$ 0.86 . This is only a rough estimate of a reasonable value for C_1 .

In a series of tests, including a verification of the model for the Crescent City, Calif. tsunami of 1964, a value of $C_1 = 1$ was found to work well. Values that are significantly different gave unrealistic results.

40. The value of C_o used in Equation 13 when that equation is used for the initial flooding of a cell is not critical, as Equation 13 is only used for one time step, after which time Equation 14 is used. A value of $C_o = 2$ was found to work well when Equation 13 was used for recession from an elevated cell, as in Figure 6c. This value gave a good match between the wave equations and the flooding-drying equations at the transition between the two regimes as a cell dried.

41. For D_c, the critical depth that distinguishes whether wave equations or flooding-drying equations are used, a value of $D_c = 1$ ft was used for flooding and $D_c = 0.5$ ft was used for drying. When the water level was very low, Equation 23 was used to calculate the flow through the cell boundaries. When the water level rose above 1 ft, the momentum equations (9 and 10) were used. As the water level fell past 1 ft, Equation 9 and 10 were still used until 0.5 ft, at which point Equation 23 was used again. This "hysteresis" is necessary to prevent occasional oscillation between the two model regimes at the critical depth.

Frictional Effects

42. The two frictional coefficients, n and K, supply the frictional damping of the system. Manning's n, is a measure of bottom roughness and may be assigned a constant value characteristic of the bottom surface. A value of $n = 0.025$, which is representative of a moderately smooth surface, was used in this study for both the harbor bottom and the surrounding land. Figure 8 shows the effect of varying n for an input wave of small amplitude. Equations 9, 10, and 11 were linearized and lateral friction was removed, leaving only the wave terms and bottom friction. An incident wave of period 800 sec and amplitude 0.1 ft was used for the harbor model. Since the bottom friction term is

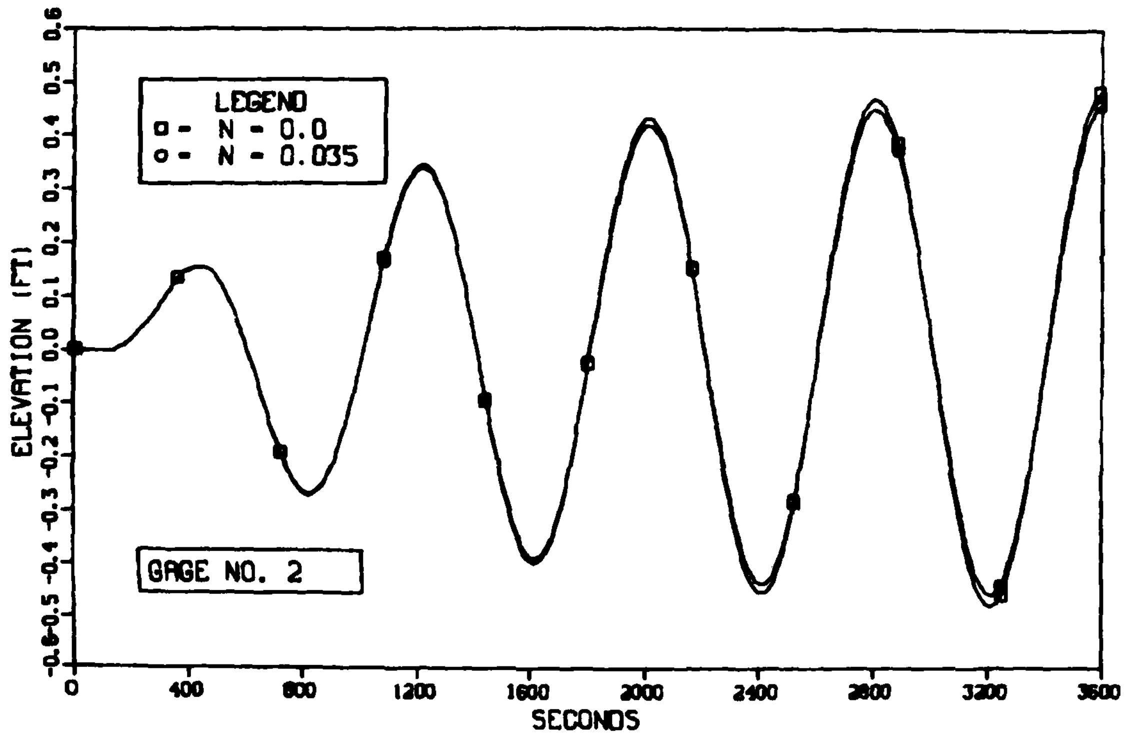

Figure 8. Linear Model with Varying Bottom Friction

quadratic, the effect of this term will increase for larger waves.

43. Unlike n , K is not a constant that may be set a priori. Based on analogies to viscous flow, Prandtl set

$$K = L_m^2 |\nabla u| \tag{24}$$

where L_m is the "mixing length," analogous to the molecular mean free path (Launder and Spalding 1972). This enables determination of K by estimating L_m from the problem dimensions and estimating the velocity gradient. For input wave amplitudes of 1 ft or greater, the velocities in the harbor entrance will be on the order of 5 ft/sec. The distance over which this current decays will be approximately the width of the jet in the entrance, 450 ft. The mixing length may be set to the grid size, 150 ft, as eddies of a significantly larger size, $2\Delta x$, can be resolved by the grid. The resulting K value is 250 ft^2/sec. This is only a rough estimate.

44. Figure 9 shows the response of the linearized model with lateral mixing for K = 0, 100, 200, and 500 ft^2/sec. The input wave is of amplitude = 0.1 ft and period = 800 sec, and no flooding of land is allowed. Figure 10 is for the same conditions with nonlinear terms in the equations and no bottom friction. K is given values of 100, 200, and 500 ft^2/sec.

45. Appendix A gives a verification of the model and coefficients for the Crescent City tsunami of 1964.

Amplitude-Dependent Effects

46. Since several terms in the basic equations of motion and continuity (Equations 9-11) are nonlinear, it is apparent that the amplification of an incident wave will vary according to the magnitude of that wave; i.e., if $R(\omega,\eta_o)$ is the response to a wave of frequency ω and amplitude η_o then for a constant c ,

$$R(\omega, c\eta_o) \neq cR(\omega, \eta_o) \tag{25}$$

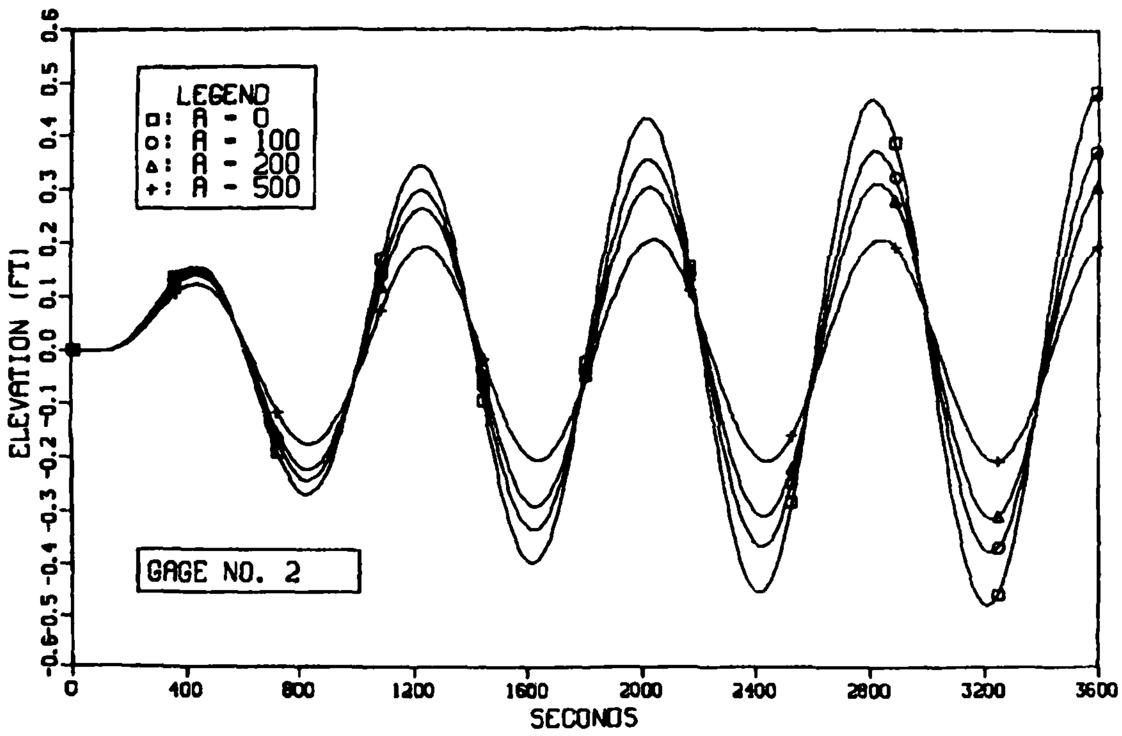

Figure 9. Linear Model with Varying Lateral Mixing

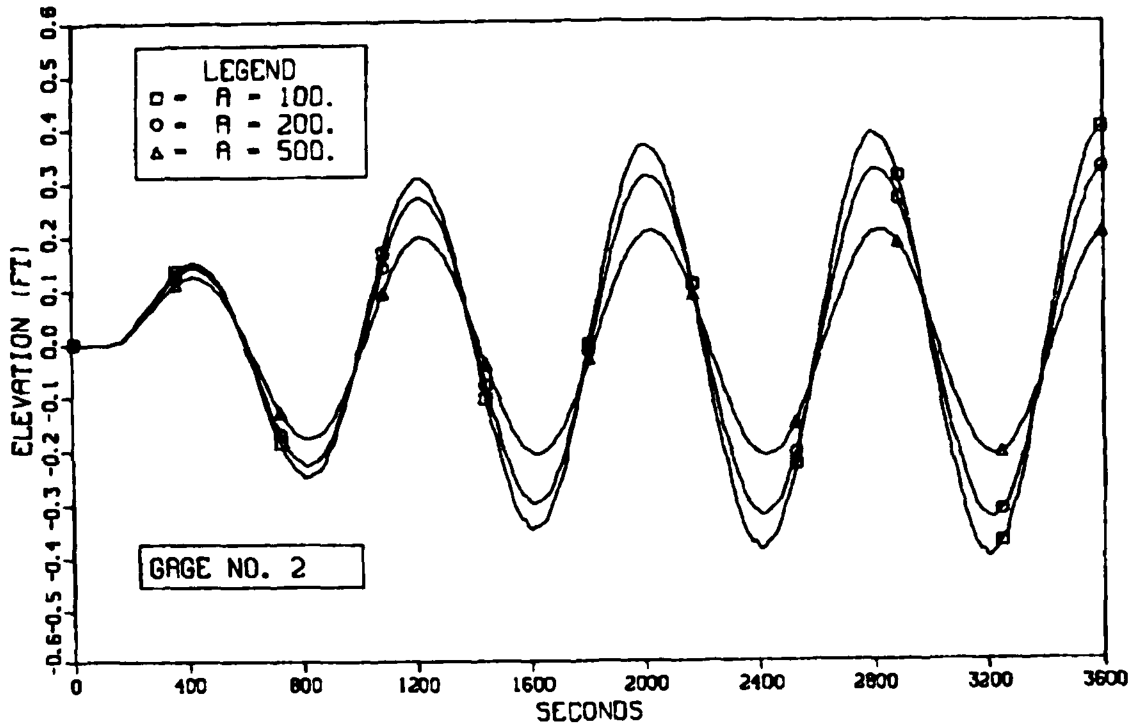

Figure 10. Nonlinear Model with Varying Lateral Mixing

The terms which are nonlinear are the convective acceleration terms ($u \frac{\partial u}{\partial x}$ etc.) and the bottom friction terms in Equation 9 and 10 and the divergence of transport terms ($\frac{\partial}{\partial x}[(h + \eta)u]$ etc.) in Equation 11.

47. The model was run with input waves of 800-sec periods and amplitudes 0.1, 0.3, 1.0, 3.0 and 10.0 ft. The land was given an elevation great enough to prevent any flooding. Table 2 presents the maximum water elevation recorded at each of the harbor gages. Table 3 presents the values of Table 2 divided by the incident amplitude, giving the amplification factor. The results shown in Table 3 illustrate the influence of nonlinear terms in the model. As input amplitude increases, the response amplification factor for any given gage decreases due to the increased relative importance of frictional and advective effects. For a linear model, such as that of Durham (1978), the amplification factor would be constant for each gage, regardless of input amplitude. Flooding and drying not included in Tables 2 and 3 will introduce further nonlinearity into the response.

Flooding Effects

48. One important nonlinear effect determining the Barbers Point Harbor response is the flooding and drying of land areas around the harbor. Whereas other nonlinear effects, such as convective acceleration and bottom friction, may increase their role gradually as the oscillations increase from infinitesimal to large values, flooding and drying effects turn on suddenly at specific water levels.

49. The principal effect is to reduce the amplitude of oscillations. When the water level in the harbor exceeds the elevation of adjacent land areas, water moves laterally into those areas. This water would have, if flooding had not occurred, piled up higher in the harbor, increasing the hydrostatic pressure gradient through the harbor mouth, and thus the restoring force of the oscillating system. Likewise, when the water level drops below its mean level, water may still be draining from the land areas into the harbor, reducing the magnitude of the oscillation. Flooding and drying will reduce the oscillation of the

harbor, but is in itself, however, a hazardous effect.

50. Because of the highly nonlinear behavior of the harbor and the dependence of that behavior on the specific conditions, such as wave amplitude and local topography, each particular case is a unique situation. No generalized solution is possible, as in the case of a system of linear partial differential equations such as those of Durham (1978). However, general features of the response may be discerned by observing a number of cases which are representative of possible designs for areas around the harbor.

51. The model was run for the configuration shown in Plate 3. Land elevations tried were 4, 6, 8, 10, and 12 ft above mean lower low water, except for the dredged material disposal areas, which were set high enough to avoid flooding. Sinusoidal input waves with periods of 800 sec, the resonant period, and amplitudes of 3, 4, 6, 8, 10, and 12 ft were used. Cases in which the amplitude was insufficient for flooding were not used, as the behavior in these cases can be seen from the no-flooding, variable-amplitude series (Tables 2 and 3). The maximum elevation of the water surface at each gage is recorded in Tables 4-31. A value of zero indicates that no water reached that gage location.

52. Gage 2 (Table 5) is at the location within the harbor where the maximum water elevation occurred. Examination of this table shows some of the effects of flooding on response. For a given wave amplitude, the response increases with increasing land elevation. For example, for a 10-ft input wave, the response increases from 8.55 to 12.51 ft as the land elevation increases from 4 to 12 ft. The reason for this is that for greater land elevations flooding does not take place until the water level in the harbor is at a greater height than for lesser land elevations. However, it should be noticed that, although the harbor response is increased, the flooding of adjacent land is reduced as the water elevation above the level of neighboring land is reduced at gage 2 from 4.55 ft for a 4-ft land elevation to 0.51 ft for a 12-ft land elevation.

53. The extent and depth of flooding is information of interest. Plates 4-23 are contour maps showing the flooding of land areas around the harbor. The contour values are the maximum depth of water over the

land. Areas outside the zero contour have no water present. Information about the flooding is also given in Tables 15-31, which give the maximum water surface elevation relative to the mean lower low water datum for the gage locations on land. On some of the contour plots there will be isolated maxima away from the harbor. These are due to standing waves caused by reflections from the dredged material piles.

54. Plates 24-48 show the time series of water elevation for the land and harbor gages for an input wave amplitude of 8 ft and a land elevation of 6 ft. Although the equivalent time series were recorded for each test case, all of this information is not presented here because of its volume. The needed information is adequately supplied by the contour plots, so the time series for only one case is presented to show the character of the response.

Velocity Distribution

55. The distribution of horizontal velocity, u and v , within the harbor is of interest because of its effects on ships. A principal hazard to shipping is presented by small and fairly frequent (relative to the rare large tsunamis) tsunamis which may create fairly significant currents within the harbor. Part IV contains a frequency analysis for these small tsunamis.

56. Plates 49-52 contain vector plots of horizontal current for the harbor area. The input wave has an amplitude of 0.1 ft and a period of 800 sec. There is no flooding. The plots show a series of vector diagrams for approximately one wave period after sufficient time has elapsed for the harbor to reach its full resonant response. The length of each arrow is proportional to current speed at the point where the arrow's tail is located. A vector of length equivalent to a speed of 0.5 ft/sec is shown on each plot. Each arrow points in the direction of the current. Since u and v occur at different points in the grid, to construct a vector it is necessary to interpolate their values to a common point. The velocity is determined at the center point of each grid cell by averaging the values of u and v on each face of the

cell:

$$\overline{u}_{ij} = (u_{ij} + u_{i-1j})/2$$

$$\overline{v}_{ij} = (v_{ij} + v_{ij-1})/2$$

where $\overline{u}$ and $\overline{v}$ are used to construct the vectors.

57. As expected for the Helmholtz mode of oscillation, the current velocity is strongly concentrated in the mouth of the harbor. The velocity distribution shown indicates the hazards to ships. On the sides of the harbor away from the entrance, the water motion will be small up and down movements (around 0.3 ft for this case). Ships moored at these locations would be affected relatively little. For locations near the mouth, the water motion consists of large horizontal movements. Ships moored near here may experience surging (longitudinal) movements, especially for larger amplitude inputs.

58. Since the model is fairly close to being linear for small waves, the velocity distribution for waves of different amplitude may be found from Plates 49-52 by multiplying the arrow length by the increase in amplitude and by a factor given by the ratio of the response factors for the two waves. For example, for a 1-ft input wave, multiply by 10 for the increase of input amplitude and by 2.52/3.03 for the ratio of response (from gage 2, Table 3). This method should be used with caution for input waves of over 1 ft, where nonlinearity becomes quite significant. However, even for these cases, the velocity distribution patterns will be quite similar. Table 32 presents the maximum velocities at several gages in the harbor and its entrance (see Plate 3 for gage locations) for small tsunamis of 800-sec periods.

Period-Dependent Effects

59. The effect of different input wave periods is shown in Plates 53 and 54. These plates show the flooding for input waves of 1000- and 1600-sec periods, respectively, and a 10-ft amplitude. Plate 16 shows the response for a period of 800 sec. The land elevation for all

three cases is 8 ft. Durham (1978) showed a very broad peak in the response curves. In general, nonlinear effects tend to further broaden the period range of response. Plate 54 shows reduced, but still noticeable, resonant effects (that is, amplification) for a 1600-sec period. Because the harbor surface remains elevated for a longer period of time, flooding is more extensive. But since the amplification by harbor resonance is reduced, the flooding will not be as deep. The limiting case would be an input wave of infinite period; i.e., a rise of 10 ft in the sea level. For this case, all of the land will be flooded to a depth of 2 ft.

PART IV: TSUNAMI ELEVATION FREQUENCIES OF OCCURRENCE

Large Tsunamis

60. Houston, Carver, and Markle (1977) predicted tsunami elevation frequencies of occurrence for the entire coastline of the Hawaiian Islands using data for historical tsunamis since 1837. Table 33 presents elevations predicted by them for the 10 largest tsunamis since 1837 on the open coast near the proposed Barbers Point Harbor. These elevations are relatively small. For example, the 100-year elevation (8.1 ft) predicted by Houston, Carver, and Markle (1977) on the open coast near Barbers Point Harbor, based upon the data in Table 33, is in the bottom 20 percent of 100-year elevations predicted by them for the seven major islands of the Hawaiian Islands and in the bottom 30 percent predicted for the island of Oahu. The open coast historical tsunami elevations presented in Table 33 will be used to determine tsunami elevation frequencies of occurrence within Barbers Point Harbor.

61. The response of Barbers Point Harbor to tsunami excitation is dependent upon the period and amplitude of the incident wave and on the topography surrounding the harbor (provided the incident wave is sufficiently large that the tsunami overflows the confines of the harbor). Since the frequencies of occurrence of different tsunami periods were unknown, it was assumed that all the wave energy was concentrated at the period of maximum response of the harbor. Thus, the results presented are conservative.

62. Figure 11 presents the response of Barbers Point Harbor (at the gage 2 location presented in an earlier section) to tsunami excitation as calculated by the numerical model presented in Part II. The amplification factor is defined as the tsunami amplitude within the harbor divided by the open coast amplitude. There are separate curves in Figure 11 for different dock heights for the larger tsunami amplitudes since the amplification factor is a function of the dock height surrounding the harbor once land flooding begins. Gage 2 is at the location

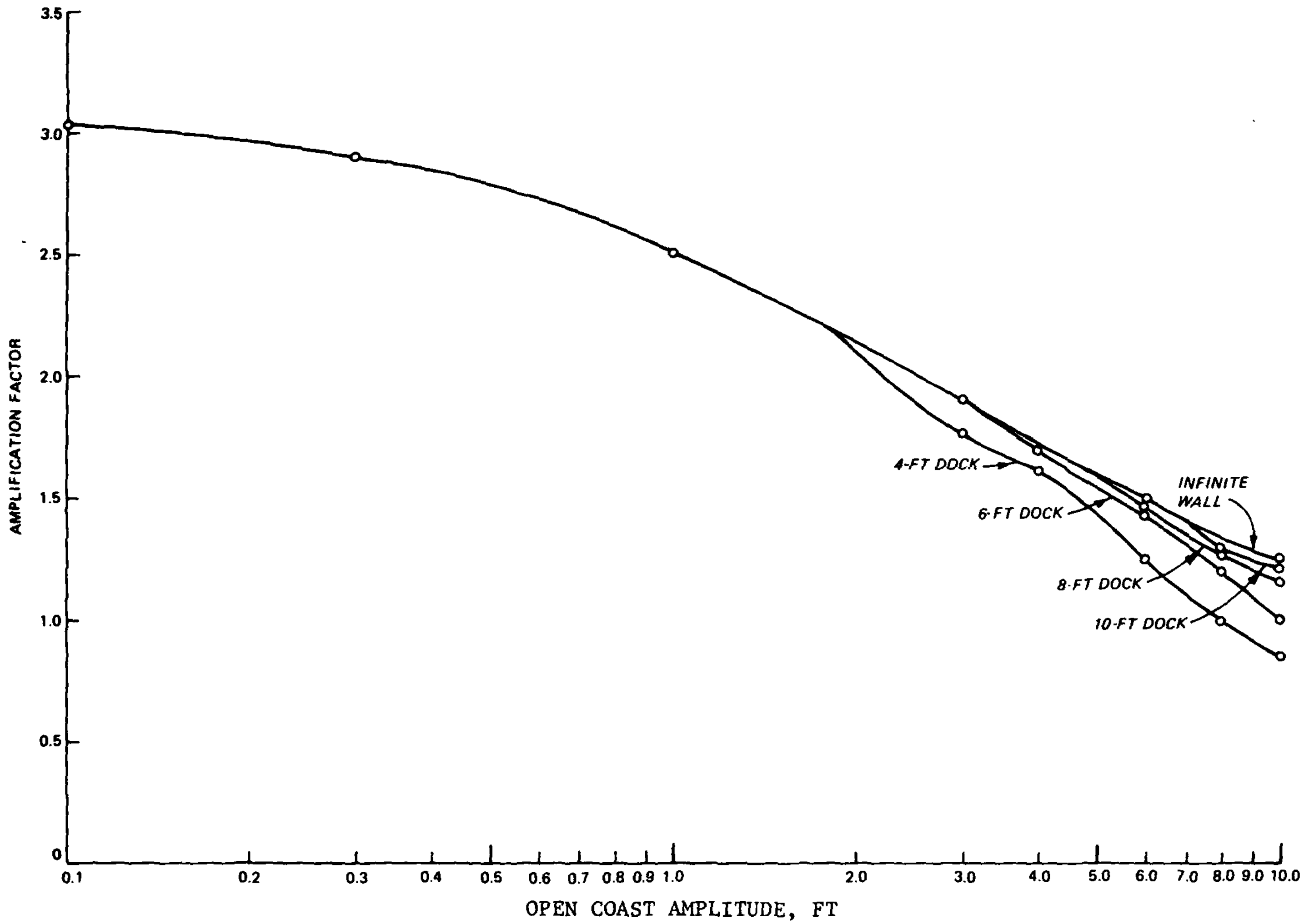

Figure 11. Amplification Factor at Gage 2 Within the Ha:bor

where Durham (1978) found the response of the harbor to be maximum (using linear equations in the computations). The analysis presented in this section will be for the gage 2 location.

63. Figure 11 was used to determine the response of Barbers Point Harbor to the historical tsunamis presented in Table 33. The open coast amplitudes of these historical tsunamis (Table 33) were multiplied by the amplification factors presented in Figure 11 to determine the maximum tsunami amplitudes within the harbor. Table 33 shows these amplitudes within the harbor and indicates that, the greater the dock height, the larger the amplitude of a tsunami within the harbor. This increase in tsunami amplitude with increasing dock height results from the fact that once a tsunami overflows the confines of the harbor the amplification factor decreases significantly. Thus, the lower the dock height, the smaller the tsunami amplitude.

64. Frequency of occurrence curves for tsunamis at Barbers Point were determined by fitting the data presented in Table 33 to logarithmic distributions. Cox (1964) found that the logarithm of the tsunami mean exceedance frequency was linearly related to tsunami elevations for the 10 largest tsunamis occurring from 1837 to 1964 in Hilo, Hawaii. Earthquake intensity and mean exceedance frequency have been similarly related by Gutenburg and Richter (1965). Rascon and Villarreal (1975) demonstrated that a linear relationship between the logarithm of the mean exceedance frequency and recorded tsunami elevations held for historical tsunamis on the west coast of Mexico (data from 1732) and on the Pacific West Coast of North America, excluding Mexico. Wiegel (1965) used the same relationship for tsunamis at San Francisco and Crescent City, Calif,; Adams (1970) for tsunamis at Kahuku Point, Oahu; and Houston, Carver, and Markle (1977) for tsunamis in the Hawaiian Islands.

65. The tsunami amplitude H is related to the frequency of occurrence F by a relationship with the following form:

$$H = B - A \log F \tag{26}$$

Table 34 presents amplitude-frequency equations determined for different dock heights using a least squares analysis to fit the data of Table 33 with the logarithmic distribution of Equation 26. Figure 12 presents the A and B coefficients of Equation 26 for different dock heights. Equation 26 can be used to predict tsunami elevations for various frequencies of occurrence. For example, $F = 0.01$ for a 100-year tsunami. Since $\log 0.01 = -2$, $H = B + 2A$ for a 100-year tsunami. Figure 13 shows 100-year elevations calculated for the varying dock heights using this formula. Again, the greater the dock height, the larger the 100-year tsunami. However, as shown in Figure 14, the greater the dock height, the smaller the depth of flooding of the 100-year tsunami over the dock. Although the 100-year tsunami elevation grows with increasing dock height, it does not grow as fast as the increase in dock height and thus the flooding level over the dock decreases with increasing dock height.

66. The elevation-frequency equations presented in Table 34 cannot be used to determine tsunami elevations for return periods significantly outside the 143-year record from 1837 to 1979. Extrapolation much beyond the limits of the data base (in this case above return periods of 143 years) is therefore questionable. Thus, it is not valid to determine the largest expected tsunami at Barbers Point Harbor by calculating the height for a rare event such as the "million-year" tsunami. In addition, return periods much less than 15 years are below the lower limits of the data base, and the analysis presented in the next section was required.

Small Tsunamis

67. The response of the proposed Barbers Point Harbor to excitation by small-amplitude tsunamis is important, since these tsunamis are not as strongly dissipated as larger tsunamis and thus experience greater amplification by the harbor (Figure 11). Small-amplitude tsunamis also arrive fairly often in the Hawaiian Islands (average of one per year during the period from 1945 to 1975). Although the vertical movement of water during small tsunamis is relatively minor and gradual, fairly high

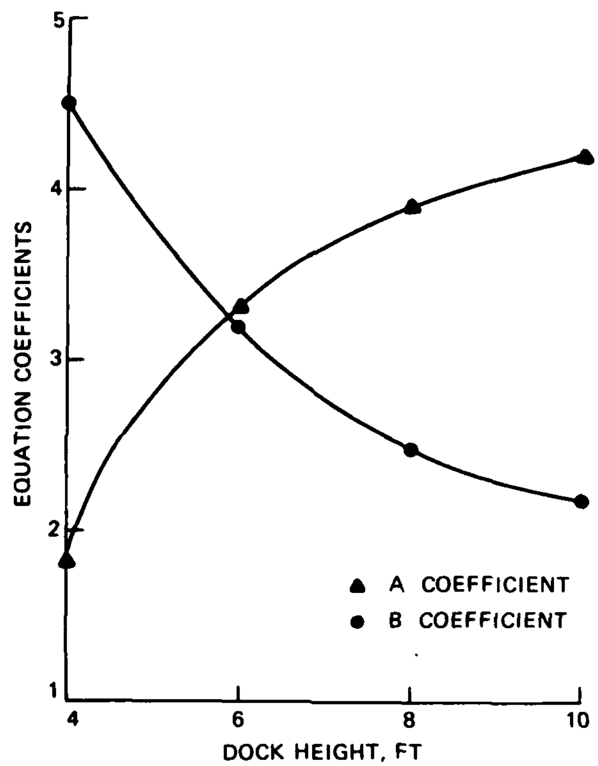

Figure 12. A and B coefficients for Different Dock Heights

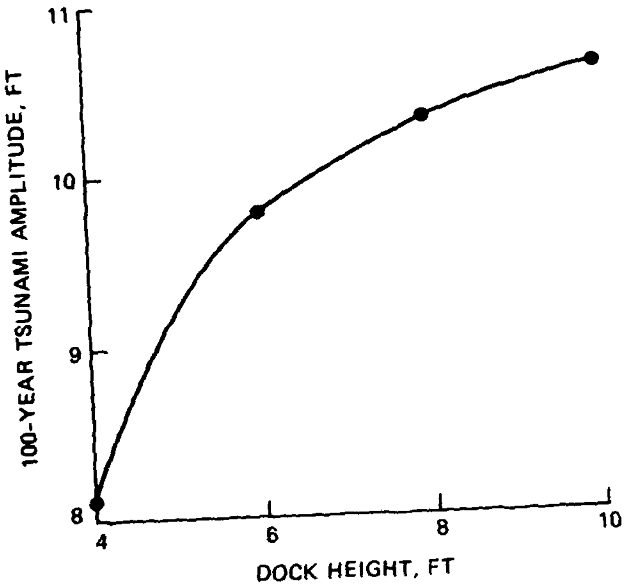

Figure 13. 100-year Tsunami Amplitudes for Different Dock Heights

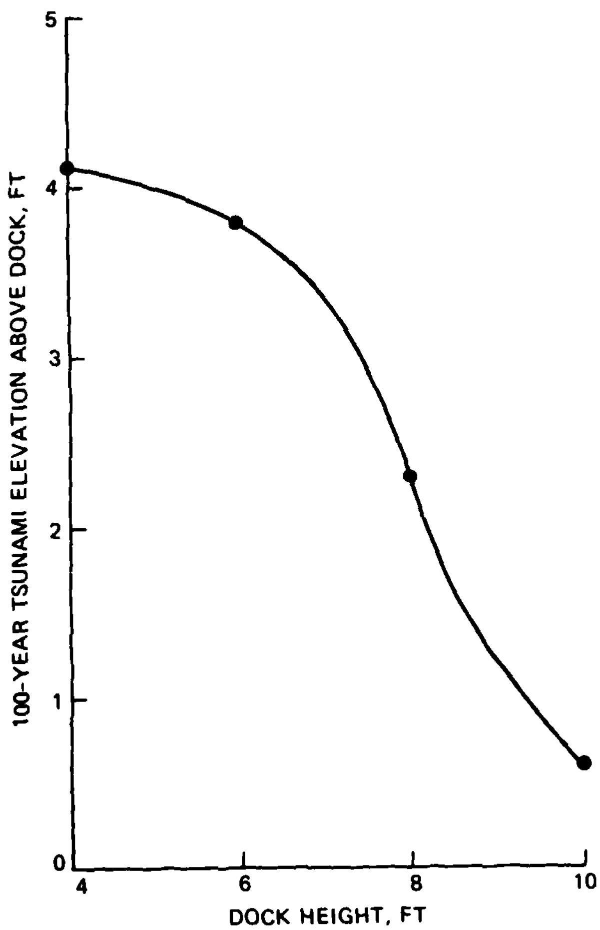

Figure 14. 100-year Tsunami Flooding Elevation Above Dock

horizontal water velocities may develop at the mouth of the proposed harbor. These currents may interfere with (and even pose a safety hazard to) ship movement in and out of the harbor during the arrival of a small tsunami. The 1960 tsunami at Los Angeles and Long Beach Harbors, Calif., illustrates the deleterious effects of small tsunamis. This tsunami had an amplitude of only 2 to 3 ft within the harbors; however, it produced large currents with velocities up to 15 knots reported, sunk 30 to 40 small craft, and produced a million dollars in damage to boats and slips (U. S. Army Engineer District, Los Angeles, 1960).

68. Small tsunamis are defined for the purpose of this report as those recorded at Honolulu that are not among the 10 largest tsunamis listed in Table 33. Of course, there undoubtedly were many small tsunamis in the 19th century that were not reported at Honolulu. In fact, only two tsunamis with heights less than 0.6 m were reported in Honolulu Harbor during the 19th century. Thus, the period of time considered in a frequency analysis cannot extend from 1837 to the present (as was the case for large tsunamis). The earliest tsunami with a height less than 0.6 m that was reported in Honolulu Harbor was recorded in 1883 and had a height of 0.2 m. This tsunami apparently was produced by an atmospheric pressure wave from the eruption of the volcano at Krakatoa in Indonesia. The other 19th century tsunami with a height less than 0.6 m was recorded in 1896 and had a height of 0.1 m. Since the 1883 event was atypical and of unknown probability and since tsunami recordings after 1896 probably have been reliable, the year 1896 was taken as the start of the time period for the frequency analysis of small tsumanis. A tsunami catalog for the Hawaiian Islands (Pararas-Carayannis 1977) reports tsunamis to the year 1975. Thus, the 80-year period from 1896 to 1975 was considered in the frequency analysis.

69. In order to determine the height of small tsunamis at Barbers Point Harbor, it was necessary to relate tsunamis on the open coast near Barbers Point Harbor to tsunamis within Honolulu Harbor. Tsunamis at these two locations were related using the finite element numerical model employed by Houston, Carver, and Markle (1977) to calculate the interaction of tsunamis with the Hawaiian Islands. Houston, Carver, and

Markle (1977) showed that this model accurately simulated the interaction of actual historical tsunamis with the Hawaiian Islands.

70. The accuracy of the finite element numerical model in simulating the interaction of a tsunami with an island was demonstrated in this study by comparisons with an analytical solution. Figure 15 shows the case considered. Hom-ma (1950) solved the problem of the interaction of long waves with the circular island on a paraboloidal shoal shown in Figure 15. Figure 16 shows the finite element grid used to simulate the interaction of long waves with this circular island on a paraboloidal shoal (actually, only half of the island and shoal had to be modeled due to symmetry). The grid cells telescope in size so that a constant resolution of the tsunami can be maintained as it enters shallow water and its wavelength decreases; Figure 17 shows a comparison between the finite element solution and Hom-ma's analytical solution at points around the shoreline of the island. The agreement is excellent with only slight differences for the short-period (4-min) wave. These differences are due to the lower resolution of the short-period wave and can be eliminated by decreasing the grid cell size.

71. Figure 18 shows the finite element grid used to model the interaction of tsunamis with the Island of Oahu. The other islands of the Hawaiian Islands were not included in the grid since Honolulu Harbor and Barbers Point Harbor are relatively close together, Oahu is distant from the other islands, and only relative heights are desired. A grid covering only Oahu also allows very detailed representation of the bathymetry and shoreline configuration.

72. The finite element grid was used to relate tunamis within Honolulu Harbor to tsunamis on the open coast at Barbers Point Harbor. The finite element model took into account the major processes that would cause different tsunami elevations at Honolulu and the open coast at Barbers Point Harbor. That is, the model calculated shoaling, refraction, diffraction, and reflection.

73. Tsunamis with trough to crest heights greater than or equal to 0.1 m in Honolulu Harbor were considered in the analysis of small tsunamis. Heights less than 0.1 m were not considered, since Pararas-

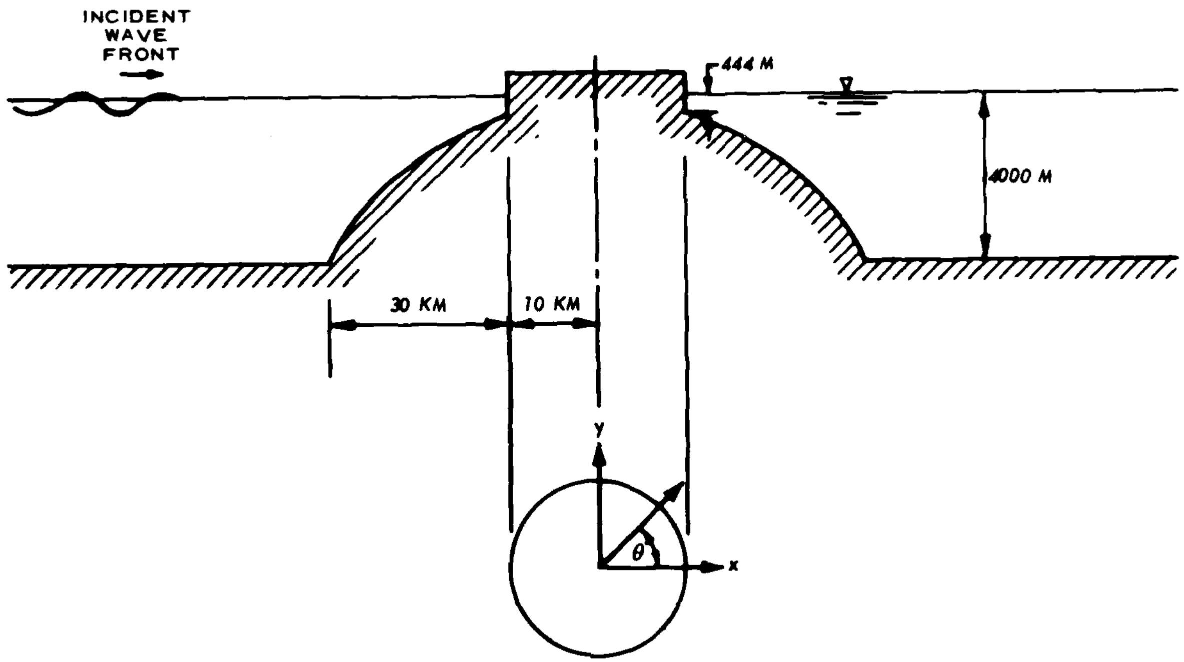

Figure 15. Circular Island on a Paraboloidal Shoal

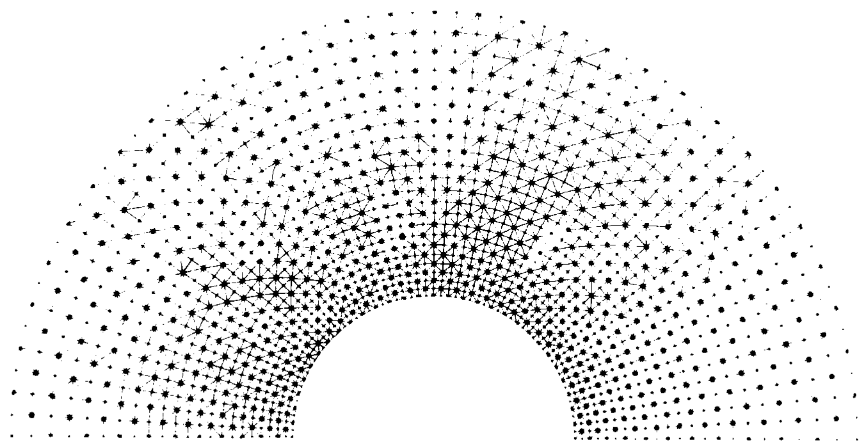

Figure 16. Finite Element Grid for a Circular Island on a Paraboloidal Shoal

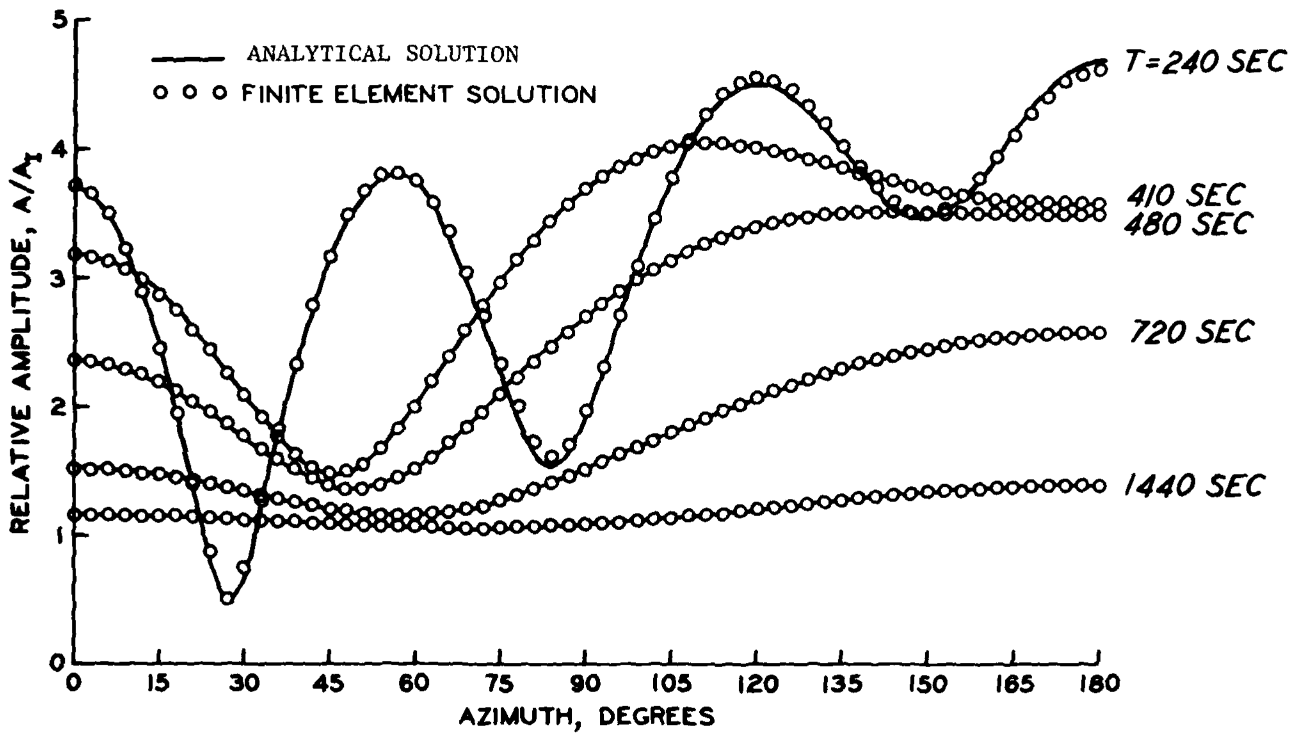

Figure 17. Comparison of Finite Element and Analytical Solution, 2640 Element Grid

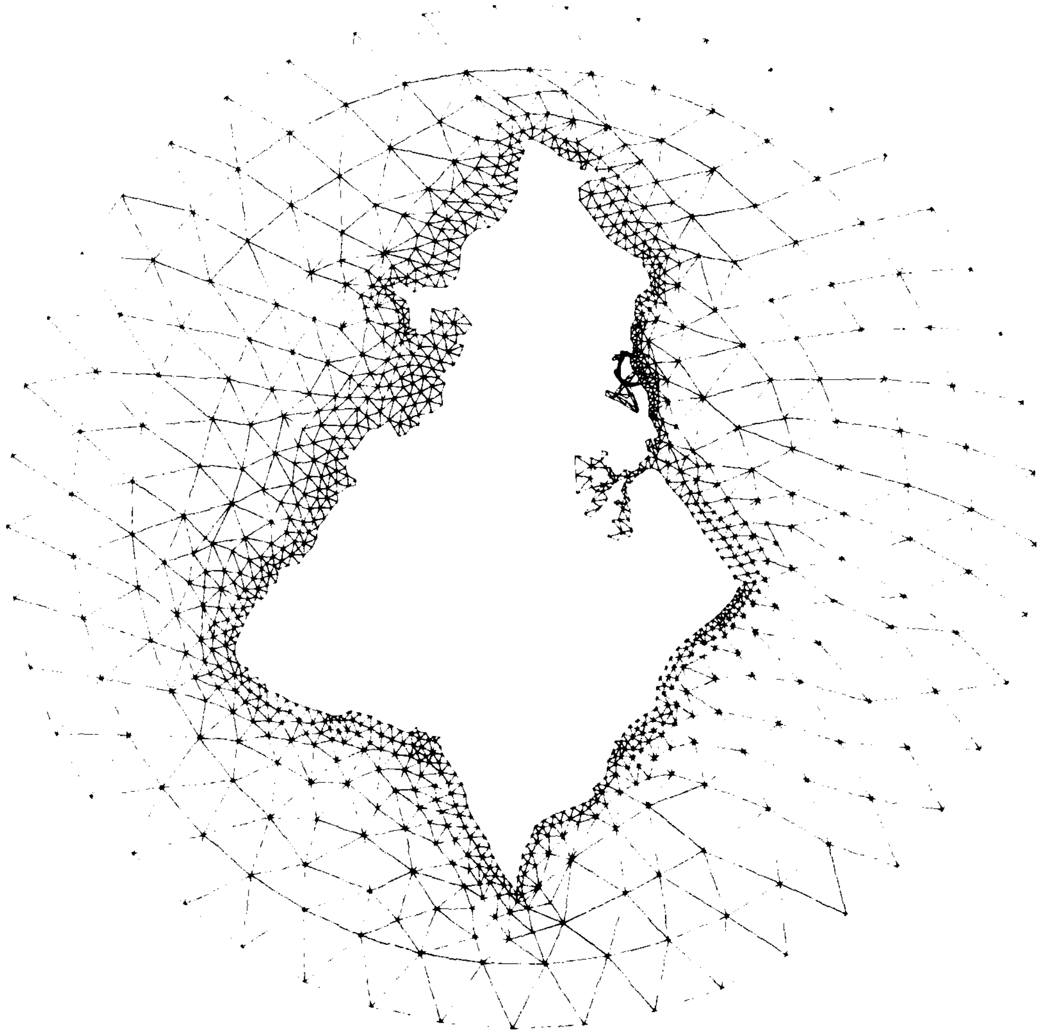

Figure 18. Finite Element Grid for Island of Oahu

Carayannis (1977) does not specify the actual heights of these tsunamis (they are just listed as being less than 0.1 m). The region of generation of each tsunami was taken from Pararas-Carayannis (1977), and the direction of approach to Oahu of each tsunami was determined. The finite element model was used to calculate the interation of all the tsunamis with Oahu. The ratio of the height calculated at Barbers Point Harbor to the height calculated at the tide gage location at Honolulu was then multiplied by the height recorded at the tide gage at Honolulu to determine a height on the open coast at Barbers Point Harbor. Table 35 shows the tsunamis considered in the analysis, the height (in metres) recorded in Honolulu Harbor, and the height (in metres) calculated on the open coast at Barbers Point Harbor. The tsunamis are arranged in order from largest to smallest at Barbers Point Harbor. Some of the heights are as much as four times larger at Barbers Point Harbor than in Honolulu Harbor, although one is smaller.

74. The relationship between tsunami height within Barbers Point Harbor and height on the open coast is a function of wave height on the open coast. The greater the open coast height, the smaller the amplification (due to greater dissipation). The open coast heights at Barbers Point (column 3, Table 35) were converted to units of feet, divided by two (to convert height to amplitude), and finally multiplied by the amplification factors given in Figure 11. The result (column 4 of Table 35 is the assumed tsunami amplitude within Barbers Point Harbor if that harbor had existed at the time of these historic tsunamis. Frequencies of occurrence were determined by including in the analysis the six large tsunamis that occurred during the period from 1896 to 1975. The largest small tsunami (the 1923 tsunami listed in Table 33) was thus the seventh largest tsunami during the 80-year period, and the probability of a tsunami of this height or larger occurring was equal to the ratio of the rank of the tsunami (7) divided by the number of years considered (80).

75. Cox (1964) demonstrated that for small tsunamis at Hilo, Hawaii, the logarithm of the frequency per year of tsunami occurrence was linearly related to the logarithm of tsunami height. The same

relationship was assumed to be valid for Barbers Point Harbor. Only tsunamis with open coast amplitudes at Barbers Point of 0.3 m or greater were used to determine the amplitude-occurrence frequency relationship. The reason for this is that historic catalogs do not give the size of tsunamis of height less than 0.1 m for Honolulu. Since tsunamis of this size may be amplified to give open coast heights of 0.2 m or so at Barbers Point, heights less than approximately 0.3 m that are listed in Table 35 are not a complete population. Thus, only heights greater than 0.3 m on the open coast of Barbers Point are used to determine the frequency curve.

76. Figure 19 shows a log-log plot of tsunami amplitude within Barbers Point Harbor versus frequency per year of tsunami occurrence and a linear least squares fit of the data. The following equation was determined using these data:

$$H = 0.42F^{-0.89} \tag{27}$$

The following tabulation shows the amplitudes of small tsunamis within Barbers Point Harbor determined for various return periods using Equation 27: It is important to note that these amplitudes are probably

Tsunami Return Period (years)	Tsunami Amplitude, ft
1	0.4
5	1.8
10	3.3

upper limits since the amplification factors presented in Figure 11 were determined assuming that the tsunamis had a wave period that produced the maximum harbor response. Actually, only part of the energy of a tsunami would be concentrated at this particular period. However, the energy distributions of tsunamis and the frequencies of occurrence of these distributions are unknown. Thus, this conservative approach must be used.

77. Equation 27 is valid only for small tsunamis (1- to 10-year return periods). Equation 26 of the previous section must be used for

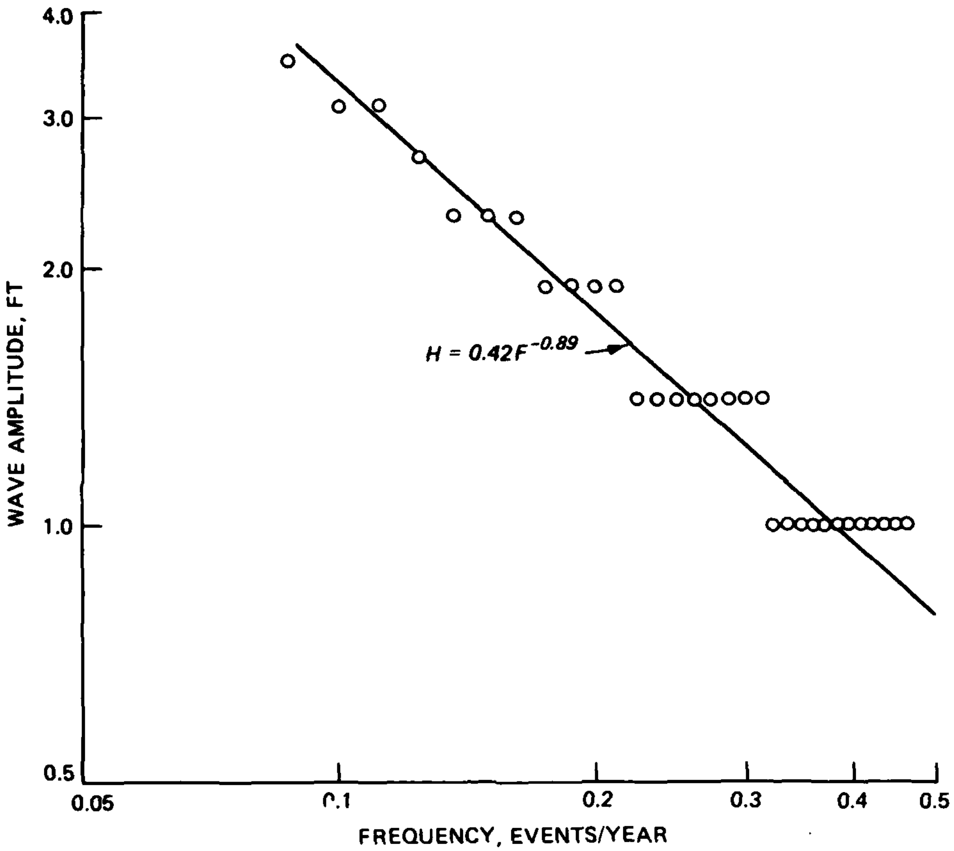

Figure 19. Wave Amplitude vs. Event Frequency for Small Amplitude Tsunamis

larger tsunamis (15- to 150-year return periods). These two equations do not overlap during the return period interval from 10 to 15 years. Part of the reason that the two equations appear not to be consistent is the fact that Equation 27 does not include the effect of the astronomical tide, but Equation 26 does implicitly (since the historical data used by Houston, Carver, and Markle (1977) included the effect of tides). Houston and Garcia (1974, 1978) and Houston (1980) showed that if tsunami heights are large compared with the astronomical tide, the effect of the tides on the exceedance frequency distribution is negligible. However, the astronomical tide has a significant effect on the total combined tsunami and astronomical tide elevation for the case of small tsunamis. Since tsunamis persist for days, the largest combined tsunami and astronomical tide elevation for small tsunamis probably occurs at a tide stage of mean higher high water (mhhw). An elevation of approximately 1 ft (elevation of mhhw over mean sea level) must be added to the tsunami amplitudes in paragraph 76 to produce a combined tsunami and astronomical tide elevation. In addition, the two equations are based upon different time intervals. If the heights of small tsunamis from 1837 to 1896 were known at Barbers Point Harbor, these heights could be included in the small tsunami analysis, and the two equations would be consistent. The following tabulation shows tsunami elevations within Barbers Point Harbor (1 ft added to small tsunamis to include effect of astronomical tides) for various return periods and dock heights:

Tsunami Return Period, years	Elevation, ft, at Cited Dock Heights, ft			
	4	6	8	10
1	1.4	1.4	1.4	1.4
5	2.8	2.8	2.8	2.8
10	4.3	4.3	4.3	4.3
15	6.6	7.1	7.1	7.1
25	7.0	7.8	8.0	8.1
50	7.6	8.8	9.1	9.3
100	8.1	9.8	10.3	10.6

PART V: SUMMARY AND CONCLUSIONS

78. The results of this study may be summarized as follows:

a. The proposed Barbers Point Harbor has a Helmholtz-type resonant mode with a period of about 800 sec. This mode is characterized by a rising and falling movement as a unit of the harbor interior with strong horizontal currents in the area of the harbor mouth.

b. This resonant mode amplifies the wave height of incident waves of a broad range of periods with a peak at about 800 sec. Due to nonlinear effects, primarily frictional, the degree of amplification decreases with increasing incident wave height. Incident waves of period = 800 sec and amplitude = 0.1 ft are amplified by a factor of 3.03 at the maximum, and waves of period = 800 sec and amplitude = 10 ft are amplified by 1.26. If flooding of land occurs, these factors will be further reduced.

c. The amplification factor is dependent on period as well. As the period of the incident wave increases to infinity, the amplification factor goes to unity. The model shows some amplification at the 1600-sec period. The width of the resonant peak is such that the harbor will respond to a large portion of the tsunami period range. For periods significantly shorter than the resonant peak, the harbor will not respond as a unit.

d. Flooding of the area around the harbor can occur under many circumstances. This flooding will decrease the amplitude of the harbor response as the water from the harbor will spread out laterally rather than pile up in the harbor. The effect of flooding depends on both the incident wave characteristics and upon the specific topography of the area. A number of different cases have been presented in this study.

e. The effect of increasing the elevation of the land areas around the harbor will be to decrease the likelihood and the magnitude of flooding of these areas. However, this will be at the price of increasing the water movement within the harbor, the vertical oscillation in the main body, and the horizontal velocities in the mouth.

f. Helmholtz-type resonant response is a characteristic of all harbors with a large interior region and a constricted entrance. Since such a configuration is typical of almost all harbors, the constricted entrance being necessary to protect shipping from short-period, wind-driven waves, this type of response is found in most harbors. The period of resonance is dependent upon the harbor geometry, and for harbors suitable for ocean-going shipping the dimensions are such that the resonant period will fall within the period range of tsunamis. It is no coincidence that "tsunami" is Japanese for "harbor wave." It should be stressed that Helmholtz-type resonant response is not peculiar to the specific design chosen for the Barbers Point Harbor.

g. The analysis of harbor response to particular waves is combined in Part IV with well established tsunami frequency of occurrence prediction methods to establish the frequency of occurrence of various events. This is done for small-amplitude, relatively frequent tsunamis as well as for the large, rare tsunamis such as those of 1946 and 1960. The lack of observational data at Barbers Point before the mid-19th century prevents analysis for events of frequency much less than about 0.01 per year.

h. The harbor location chosen is relatively good as far as tsunamis are concerned, as Barbers Point has relatively small open coast tsunami amplitudes. Houston (1977) found that the site is in the bottom 20 percent of predicted 100-year elevations for the seven major islands and in the bottom 30 percent for Oahu.

i. In order to reduce the hazard due to tsunamis, it is important to take the response of the harbor into account. For ships and docks, the primary risk is from large currents in the area close to the mouth. The large horizontal water movements may produce surging motion in moored ships and cause maneuvering problems for ships under way. Ships moored well away from the entrance will experience vertical movement of a scale dependent on the size of the tsunami. For onshore port facilities, the main danger is due to flooding.

j. Procedures to be followed in the event a tsunami is expected should be developed by the harbor operator. Such procedures have already been implemented for many coastal areas of Hawaii, which is a high tsunami-risk state. Full use should be made of existing warning systems, especially the Pacific Tsunami Warning Center, which is based in Hawaii and has an ocean-wide warning net of gages and seismographs. There are two fairly distinct threats, whose frequency analyses are treated separately in Part IV. For small tsunamis, the ability to do damage is fairly low, but warning times may be short. As the main threat would be from currents in the entrance, the best response may be to keep ships clear of the entrance area. For large tsunamis, the warning time will be much longer, as these are generated in such areas as Alaska, Chile, etc. The longer lead time may be needed to prepare for the much larger effects of these tsunamis, including flooding, by the evacuation of ships and personnel and the removal of vehicles, containers, and other cargo from the flood prone areas.

REFERENCES

Adams, W. M. 1970. "Tsunami Effects and Risk at Kahuku Point, Oahu, Hawaii," Engineering Geology Case Histories, Geological Society of America, No. 8, pp 63-70.

Chen, H. S., and Mei, C. C. 1974. "Oscillations and Wave Forces in an Offshore Harbor (Application of the Hybrid Finite Element Method to Water-Wave Scattering)," Report No. 190, Massachusetts Institute of Technology, Cambridge, Mass.

Cox, D. C. 1964. "Tsunami Height-Frequency Relationship of Hilo," unpublished paper, Hawaii Institute of Geophysics, University of Hawaii, Honolulu, Hawaii.

Durham, D. L. 1978. "Numerical Analysis of Harbor Oscillations for Barbers Point Deep-Draft Harbor," Technical Report H-78-20, U. S. Army Engineer Waterways Experiment Station, CE, Vicksburg, Miss.

Gutenberg, B., and Richter, C. F. 1965. Seismicity of the Earth and Associated Phenomena, Hafner Publishing Co., New York.

Hinze, J. O. 1959. Turbulence, McGraw-Hill, New York.

Hom-ma, S. 1950. "On the Behavior of Seismic Sea Waves Around a Circular Island," Geophysical Magazine, Vol 21, pp 199-208.

Houston, J. R. 1980. "Type 19 Flood Insurance Study: Tsunami Predictions for Southern California," Technical Report HL-80-18, U. S. Army Engineer Waterways Experiment Station, CE, Vicksburg, Miss.

Houston, J. R., Carver, R. D., and Markle, D. G. 1977. "Tsunami-Wave Elevation Frequency of Occurrence for the Hawaiian Islands," Technical Report H-77-16, U. S. Army Engineer Waterways Experiment Station, CE, Vicksburg, Miss.

Houston, J. R. and Garcia, A. W. 1974. "Type 16 Flood Insurance Study: Tsunami Predictions for Pacific Coastal Communities," Technical Report H-74-3, U. S. Army Engineer Waterways Experiment Station, CE, Vicksburg, Miss.

__________. 1978. "Type 16 Flood Insurance Study: Tsunami Predictions for the West Coast of the Continental United States," Technical Report H-78-26, U. S. Army Engineer Waterways Experiment Station, CE, Vicksburg, Miss.

Launder, B. E. and Spalding, D. B. 1972. Mathemetical Models of Turbulence, Academic Press, New York.

Magoon, O. T. 1965. "Structural Damage by Tsunamis," Coastal Engineering, Santa Barbara Specialty Conference, American Society of Civil Engineers, pp 35-68.

Morris, H. M. and Wiggert, J. M. 1972. Applied Hydraulics in Engineering, The Ronald Press Co., New York.

Orlanski, I. 1976. "A Simple Boundary Condition for Unbounded Hyperbolic Flows," Journal of Computational Physics, Vol 21, pp 251-269.

Palmer, R. Q. 1970. "Study of Proposed Barbers Point Harbor, Hawaii: Hydraulic Model Investigation," Technical Report No. 8, U. S. Army Engineer District, Honolulu, Hawaii.

Pararas-Carayannis, G. 1977. "Catalog of Tsunamis in Hawaii," Report SE-4, World Data Center A for Solid Earth Geophysics, Boulder, Colo.

Rascon, O. A. and Villarreal, A. G. 1975. "On a Stochastic Model to Estimate Tsunami Risk," Journal of Hydraulic Research, Vol 13, No. 4, pp 383-403.

Reid, R. O. and Bodine, B. R. 1968. "Numerical Model for Storm Surges in Galveston Bay," Journal of The Waterways and Harbors Division, American Society of Civil Engineers, Vol 94, No. WW1, pp 33-57.

Reid, R. O., Vastano, A. C., and Reid, T. J. 1977. "Development of SURGE II Program with Application to the Sabine-Calcasieu Area for Hurricane Carla and Design Hurricanes," Technical Paper No. 77-13, U. S. Army Coastal Engineering Research Center, CE, Fort Belvoir, Va.

Tennekes, H. and Lumley, J. L. 1972. A First Course in Tubulence, MIT Press, Cambridge, Mass.

U. S. Army Engineer District, Honolulu, CE. 1977. "Design Memorandum No. 1, Phase II Project Design, for Barbers Point Deep-Draft Harbor, Island of Oahu, Hawaii," Honolulu, Hawaii.

U. S. Army Engineer District, Los Angeles, CE. 1960. "Effect of Tsunami of 23 May 1960 in the Los Angeles District," unpublished memorandum, Los Angeles, Calif.

Wiegel, R. L. 1965. "Protection of Crescent City, California, from Tsunami Waves," Consultant's Report, The Redevelopment Agency of the City of Crescent City, Crescent City, Calif.

Wilson, B. W. and Tørum, A. 1968. "The Tsunami of the Alaskan Earthquake, 1964: Engineering Evaluation," Technical Memorandum No. 25, U. S. Army Corps of Engineers Coastal Engineering Research Center, CE, Fort Belvoir, Va.

TABLE 1

Land Elevation (ft), Barbers Point Harbor Model

I — rows; J — columns

I \ J	1	2	3	4	5	6	7	8	9	10	11	12	13	14	15	16	17	18
1	100.	100.	100.	100.	100.	100.	100.	100.	100.	100.	100.	100.	100.	100.	100.	100.	100.	100.
2	100.	8.	8.	40.	40.	40.	40.	40.	8.	40.	40.	40.	40.	40.	40.	40.	40.	40.
3	100.	8.	8.	40.	40.	40.	40.	40.	8.	40.	40.	40.	40.	40.	40.	40.	40.	40.
4	100.	8.	8.	40.	40.	40.	40.	40.	8.	40.	40.	40.	40.	40.	40.	40.	40.	40.
5	100.	8.	8.	8.	40.	40.	8.	8.	8.	8.	8.	8.	8.	8.	8.	8.	8.	8.
6	100.	8.	8.	8.	8.	8.	8.	8.	8.	8.	8.	8.	8.	8.	8.	8.	8.	8.
7	100.	8.	8.	8.	8.	8.	8.	8.	8.	8.	8.	8.	8.	8.	8.	8.	8.	8.
8	100.	8.	8.	8.	8.	8.	8.	8.	8.	-38.	-38.	-38.	-38.	8.	8.	8.	8.	8.
9	100.	8.	8.	8.	8.	8.	8.	-38.	-38.	-38.	-38.	-38.	-38.	-38.	-38.	-38.	-38.	-38.
10	100.	8.	8.	8.	8.	8.	-38.	-38.	-38.	-38.	-38.	-38.	-38.	-38.	-38.	-38.	-38.	-38.
11	100.	8.	8.	8.	8.	8.	-38.	-38.	-38.	-38.	-38.	-38.	-38.	-38.	-38.	-38.	-38.	-38.
12	100.	8.	8.	8.	8.	8.	-38.	-38.	-38.	-38.	-38.	-38.	-38.	-38.	-38.	-38.	-38.	-38.
13	100.	8.	8.	8.	8.	8.	-38.	-38.	-38.	-38.	-38.	-38.	-38.	-38.	-38.	-38.	-38.	-38.
14	100.	8.	8.	8.	8.	8.	-38.	-38.	-38.	-38.	-38.	-38.	-38.	-38.	-38.	-38.	-38.	-38.
15	100.	8.	8.	8.	8.	8.	-38.	-38.	-38.	-38.	-38.	-38.	-38.	-38.	-38.	-38.	-38.	-38.
16	100.	8.	8.	8.	8.	8.	-38.	-38.	-38.	-38.	-38.	-38.	-38.	-38.	-38.	-38.	-38.	-38.
17	100.	8.	8.	8.	8.	8.	8.	-38.	-38.	-38.	-38.	-38.	-38.	-38.	-38.	-38.	-38.	-38.
18	100.	8.	8.	8.	8.	8.	8.	-38.	-38.	-38.	-38.	-38.	-38.	-38.	-38.	-38.	-38.	-38.
19	100.	8.	8.	8.	8.	8.	8.	-38.	-38.	-38.	-38.	-38.	-38.	-38.	-38.	-38.	-38.	-38.
20	100.	8.	8.	8.	8.	8.	8.	-38.	-38.	-38.	-38.	-38.	-38.	-38.	-38.	-38.	-38.	-38.
21	100.	8.	8.	8.	8.	8.	8.	-38.	-38.	-38.	-38.	8.	8.	8.	8.	8.	8.	8.
22	100.	8.	8.	8.	8.	8.	8.	-38.	-38.	-38.	8.	8.	8.	8.	8.	8.	8.	8.
23	100.	8.	8.	8.	8.	8.	8.	-38.	-38.	-38.	-25.	8.	8.	8.	8.	8.	8.	8.
24	100.	8.	8.	8.	8.	8.	8.	-38.	-38.	-38.	-25.	-21.	-21.	-21.	8.	8.	8.	8.
25	100.	-7.	-2.	8.	8.	8.	8.	-38.	-38.	-38.	-29.	-21.	-21.	8.	8.	8.	8.	8.

(continued)

(sheet 1 of 4)

TABLE 1 (Continued)

I | J

I	19	20	21	22	23	24	25	26	27	28	29	30	31	32	33	34	35	36
1	100.	100.	100.	100.	100.	100.	100.	100.	100.	100.	100.	100.	100.	100.	100.	100.	100.	100.
2	40.	40.	8.	8.	8.	8.	8.	8.	8.	8.	8.	8.	8.	8.	8.	8.	8.	8.
3	40.	40.	8.	8.	8.	8.	8.	8.	8.	8.	8.	8.	8.	8.	8.	8.	8.	8.
4	40.	40.	40.	40.	40.	40.	8.	8.	8.	8.	8.	8.	8.	8.	8.	8.	8.	8.
5	8.	40.	40.	40.	40.	40.	40.	40.	40.	8.	8.	8.	8.	8.	8.	8.	8.	8.
6	8.	8.	8.	8.	8.	8.	40.	40.	40.	8.	8.	8.	8.	8.	8.	8.	8.	8.
7	8.	8.	8.	8.	8.	8.	8.	8.	8.	8.	8.	8.	8.	8.	8.	8.	8.	8.
8	8.	8.	8.	8.	8.	8.	8.	8.	8.	8.	8.	8.	8.	8.	8.	8.	8.	8.
9	-38.	-38.	8.	8.	8.	8.	8.	8.	8.	8.	8.	8.	8.	8.	8.	8.	8.	8.
10	-38.	-38.	8.	8.	8.	8.	8.	8.	8.	8.	8.	8.	8.	8.	8.	8.	8.	8.
11	-38.	-38.	8.	8.	8.	8.	[illegible]	8.	8.	8.	8.	8.	8.	8.	8.	8.	8.	8.
12	-38.	-38.	8.	8.	8.	8.	8.	8.	8.	8.	8.	8.	8.	8.	8.	8.	8.	40.
13	-38.	-38.	8.	8.	8.	8.	8.	8.	8.	8.	8.	8.	8.	8.	8.	8.	8.	40.
14	-38.	-38.	8.	8.	8.	8.	8.	8.	8.	8.	8.	8.	8.	8.	8.	8.	8.	40.
15	-38.	-38.	8.	8.	8.	8.	8.	8.	8.	8.	8.	8.	8.	8.	8.	8.	8.	40.
16	-38.	-38.	8.	8.	8.	8.	8.	8.	8.	8.	8.	8.	8.	8.	8.	8.	8.	40.
17	-38.	-38.	8.	8.	8.	8.	8.	8.	8.	8.	8.	8.	8.	8.	8.	8.	8.	40.
18	-38.	-38.	8.	8.	8.	8.	8.	8.	8.	8.	8.	8.	8.	8.	8.	8.	8.	40.
19	-38.	-38.	8.	8.	8.	8.	8.	8.	8.	8.	8.	8.	8.	8.	8.	8.	8.	40.
20	-38.	-38.	8.	8.	8.	8.	8.	8.	8.	8.	8.	8.	8.	8.	8.	8.	8.	40.
21	8.	8.	8.	8.	8.	8.	8.	8.	8.	8.	8.	8.	8.	8.	8.	8.	40.	40.
22	8.	8.	8.	8.	8.	8.	8.	8.	8.	8.	40.	8.	8.	8.	8.	8.	40.	40.
23	8.	8.	8.	8.	8.	8.	8.	8.	8.	40.	40.	40.	40.	40.	8.	8.	40.	40.
24	8.	8.	8.	8.	8.	8.	8.	8.	8.	8.	40.	40.	40.	40.	40.	40.	40.	40.
25	8.	8.	8.	8.	8.	8.	8.	8.	8.	8.	8.	8.	40.	40.	40.	40.	40.	40.

(continued)

(sheet 2 of 4)

TABLE 1 (Continued)

I	J																	
	1	2	3	4	5	6	7	8	9	10	11	12	13	14	15	16	17	18
26	100.	[illegible]	[illegible]	-5.	8.	8.	8.	-38.	-38.	-38.	-25.	-21.	8.	8.	8.	8.	8.	8.
27	100.	-15.	-14.	-11.	-8.	-2.	-1.	-39.	-39.	-39.	8.	8.	8.	8.	8.	8.	8.	8.
28	100.	-16.	-16.	-14.	-13.	-11.	[illegible]	-39.	-39.	-39.	8.	8.	8.	8.	8.	8.	8.	8.
29	100.	-18.	-18.	-17.	-16.	-14.	-26.	-39.	-39.	-39.	-20.	-5.	-4.	-3.	8.	8.	8.	8.
30	100.	-22.	-20.	-20.	-20.	-20.	-28.	-40.	-40.	-40.	-25.	-25.	-12.	-11.	-8.	-5.	8.	8.
31	100.	-24.	-22.	-22.	-21.	-20.	-30.	-40.	-40.	-40.	-27.	-15.	-15.	-15.	-13.	-11.	-8.	-6.
32	100.	-25.	-24.	-23.	-21.	-21.	-31.	-40.	-40.	-40.	-28.	-17.	-17.	-17.	-15.	-14.	-12.	-10.
33	100.	-26.	-25.	-23.	-22.	-22.	-31.	-41.	-41.	-41.	-29.	-18.	-18.	-18.	-16.	-15.	-14.	-13.
34	100.	-26.	-25.	-24.	-23.	-22.	-32.	-41.	-41.	-41.	-29.	-20.	-20.	-19.	-18.	-17.	-17.	-14.
35	100.	-27.	-25.	-24.	-24.	-23.	-32.	-41.	-41.	-41.	-30.	-21.	-21.	-21.	-20.	-18.	-18.	-15.
36	100.	-27.	-26.	-25.	-24.	-24.	-33.	-42.	-42.	-42.	-30.	-21.	-21.	-21.	-21.	-20.	-19.	-17.
37	100.	-26.	-26.	-25.	-25.	-25.	-33.	-42.	-42.	-42.	-30.	-21.	-21.	-21.	-21.	-21.	-20.	-20.
38	100.	-25.	-25.	-26.	-26.	-26.	-33.	-42.	-42.	-42.	-31.	-22.	-22.	-22.	-22.	-22.	-21.	-21.
39	100.	-25.	-25.	-25.	-25.	-25.	-33.	-42.	-42.	-42.	-31.	-22.	-22.	-22.	-22.	-22.	-21.	-21.
40	100.	-24.	-24.	-24.	-24.	-24.	-34.	-42.	-42.	-42.	-31.	-22.	-22.	-22.	-22.	-22.	-21.	-21.
41	100.	-24.	-24.	-24.	-24.	-24.	-34.	-42.	-42.	-42.	-32.	-23.	-23.	-23.	-23.	-22.	-22.	-22.
42	100.	-25.	-25.	-25.	-25.	-25.	-34.	-42.	-42.	-42.	-32.	-23.	-23.	-23.	-23.	-22.	-22.	-22.
43	100.	-29.	-28.	-28.	-28.	-28.	-35.	-42.	-42.	-42.	-32.	-23.	-23.	-23.	-23.	-23.	-22.	-22.
44	100.	-34.	-34.	-35.	-35.	-35.	-38.	-42.	-42.	-42.	-33.	-24.	-24.	-24.	-23.	-23.	-23.	-23.
45	100.	[illegible]	[illegible]	-40.	-40.	[illegible]	[illegible]	-42.	-42.	-42.	-33.	-24.	-24.	-24.	-23.	-23.	-23.	-23.
46	100.	-42.	-42.	-42.	-42.	-42.	-42.	-42.	-42.	-42.	-33.	-25.	-25.	-24.	-24.	-24.	-24.	-24.
47	100.	-42.	-42.	-42.	-42.	-42.	-42.	-42.	-42.	-42.	-35.	-30.	-25.	-25.	-25.	-24.	-24.	-24.

(continued)

TABLE 1 (Concluded)

I \ J	19	20	21	22	23	24	25	26	27	28	29	30	31	32	33	34	35	36
26	8.	8.	8.	8.	8.	8.	9.	8.	8.	8.	8.	8.	8.	8.	40.	40.	40.	40.
27	8.	8.	8.	8.	8.	8.	8.	6.	8.	8.	8.	8.	8.	8.	8.	8.	40.	40.
28	8.	8.	8.	8.	8.	8.	8.	8.	8.	8.	8.	8.	8.	8.	8.	8.	8.	8.
29	8.	8.	8.	8.	8.	8.	8.	9.	8.	8.	8.	8.	8.	8.	8.	8.	[illegible]	8.
30	8.	8.	8.	8.	8.	8.	8.	8.	8.	8.	8.	8.	8.	8.	8.	8.	8.	8.
31	-5.	8.	8.	8.	8.	8.	8.	8.	8.	8.	8.	8.	8.	8.	8.	8.	8.	8.
32	-9.	-9.	-2.	8.	8.	8.	8.	8.	8.	8.	8.	8.	8.	8.	8.	8.	8.	8.
33	-12.	-11.	-9.	-1.	8.	8.	8.	8.	8.	8.	8.	8.	8.	8.	8.	8.	8.	8.
34	-13.	-12.	-11.	-7.	-5.	-2.	9.	8.	8.	8.	8.	8.	8.	8.	8.	8.	8.	8.
35	-14.	-14.	-13.	-10.	-9.	-5.	-3.	8.	8.	8.	8.	8.	8.	8.	8.	8.	8.	8.
36	-15.	-14.	-14.	-12.	-11.	-9.	-5.	8.	8.	8.	8.	8.	8.	8.	8.	8.	8.	8.
37	-18.	-17.	-16.	-14.	-13.	-12.	-9.	-4.	-4.	8.	8.	8.	8.	8.	8.	8.	8.	8.
38	-21.	-20.	-17.	-15.	-14.	-14.	-12.	-11.	-9.	-8.	-7.	8.	8.	8.	8.	8.	8.	8.
39	-21.	-2[illegible].	-18.	-17.	-15.	-15.	-14.	-13.	-12.	-10.	-9.	-9.	-8.	8.	8.	8.	8.	8.
40	-21.	-21.	-20.	-19.	-17.	-16.	-15.	-14.	-14.	-12.	-12.	-11.	-10.	-10.	-10.	-10.	-10.	-10.
41	-22.	-22.	-21.	-20.	-19.	-17.	-16.	-15.	-15.	-14.	-14.	-13.	-12.	-12.	-12.	-12.	-12.	-12.
42	-22.	-22.	-22.	-21.	-21.	-19.	-17.	-17.	-17.	-16.	-16.	-14.	-14.	-14.	-14.	-14.	-14.	-14.
43	-22.	-22.	-22.	-22.	-21.	-20.	-20.	-19.	-19.	-18.	-18.	-16.	-16.	-16.	-16.	-16.	-16.	-16.
44	-23.	-23.	-23.	-22.	-22.	-21.	-21.	-21.	-20.	-20.	-20.	-18.	-18.	-18.	-18.	-18.	-18.	-18.
45	-23.	-23.	-23.	-23.	-22.	-22.	-22.	-21.	-21.	-21.	-20.	-20.	-20.	-20.	-20.	-20.	-20.	-20.
46	-24.	-24.	-23.	-23.	-23.	-23.	-23.	-22.	-22.	-22.	-22.	-22.	-22.	-22.	-22.	-22.	-22.	-22.
47	-24.	-24.	-24.	-24.	-24.	-24.	-24.	-24.	-24.	-24.	-24.	-24.	-24.	-24.	-24.	-24.	-24.	-24.

(sheet 4 of 4)

TABLE 2

Maximum Water-Surface Elevation

Gage	Maximum Water-Surface Elevation at Cited Amplitude, ft 0.1	0.3	1.0	3.0	10.0
1	0.298	0.854	2.48	5.62	12.52
2	0.303	0.866	2.52	5.71	12.55
3	0.295	0.844	2.45	5.56	12.28
4	0.269	0.770	2.24	5.04	11.26
5	0.211	0.605	1.77	4.09	9.93
6	0.211	0.607	1.78	4.10	9.96
7	0.169	0.485	1.43	3.30	8.90
8	0.124	0.357	1.04	2.47	7.08

Note: T = 800-sec incident wave height.
All elevations are in feet referred to NGVD.

TABLE 3

Amplification Factor

Gage	Amplitude, ft 0.1	0.3	1.0	3.0	10.0
1	2.98	2.84	2.48	1.87	1.25
2	3.03	2.89	2.52	1.90	1.26
3	2.95	2.67	2.45	1.85	1.23
4	2.69	2.57	2.24	1.68	1.13
5	2.11	2.02	1.77	1.36	.99
6	2.11	2.02	1.78	1.37	1.00
7	1.69	1.62	1.43	1.10	.89
8	1.24	1.19	1.04	.82	.71

Note: T = 800-sec incident wave height.
All elevations are in feet referred to NGVD.

TABLE 4

Maximum Water-Surface Elevation, Gage 1

Wave Amplitude, ft	Maximum Water-Surface Elevation at Cited Land Elevation, ft				
	4	6	8	10	12
3	5.28				
4	6.19	6.71			
6	7.07	8.20	8.68		
8	7.77	9.23	9.96	10.18	
10	8.50	9.78	11.02	11.96	12.48
12	9.87	10.51	12.11	13.18	14.17

Note: Wave period = 800 sec.
All elevations are in feet referred to NGVD.

TABLE 5

Maximum Water-Surface Elevation, Gage 2

Wave Amplitude, ft	Maximum Water-Surface Elevation at Cited Land Elevation, ft				
	4	6	8	10	12
3	5.31				
4	6.47	6.78			
6	7.48	8.61	8.80		
8	7.96	9.59	10.20	10.37	
10	8.55	9.92	11.55	12.22	12.51
12	10.14	10.65	12.15	13.53	14.53

Note: Wave period = 800 sec.
All elevations are in feet referred to NGVD.

TABLE 6

Maximum Water-Surface Elevation, Gage 3

Wave Amplitude, ft	Maximum Water-Surface Elevation at Cited Land Elevation, ft				
	4	6	8	10	12
3	5.18				
4	5.98	6.61			
6	6.98	7.87	8.53		
8	7.65	8.70	9.53	10.00	
10	8.36	9.53	10.90	11.70	12.25
12	9.44	10.52	11.81	13.06	13.83

Note: Wave period = 800 sec.
All elevations are in feet referred to NGVD.

TABLE 7

Maximum Water-Surface Elevation, Gage 4

Wave Amplitude, ft	Maximum Water-Surface Elevation at Cited Land Elevation, ft				
	4	6	8	10	12
3	4.70				
4	5.38	6.03			
6	6.26	7.12	7.79		
8	6.88	8.28	8.87	9.23	
10	7.63	8.91	10.24	10.86	11.24
12	8.58	9.48	11.02	12.09	12.75

Note: Wave period = 800 sec.
All elevations are in feet referred to NGVD.

TABLE 8

Maximum Water-Surface Elevation, Gage 5

Wave Amplitude, ft	Maximum Water-Surface Elevation at Cited Land Elevation, ft				
	4	6	8	10	12
3	3.90				
4	4.50	5.00			
6	5.44	6.25	6.66		
8	6.38	7.11	7.79	7.98	
10	7.15	8.30	8.96	9.75	9.93
12	8.04	9.16	10.15	10.89	11.71

Note: Wave period = 800 sec.
All elevations are in feet referred to NGVD.

TABLE 9

Maximum Water-Surface Elevation, Gage 6

Wave Amplitude, ft	Maximum Water-Surface Elevation at Cited Land Elevation, ft				
	4	6	8	10	12
3	3.91				
4	4.53	5.03			
6	5.50	6.24	6.64		
8	6.35	7.02	7.82	8.00	
10	7.21	8.30	8.98	9.78	9.96
12	8.07	9.08	10.22	10.93	11.75

Note: Wave period = 800 sec.
All elevations are in feet referred to NGVD.

TABLE 10

Maximum Water-Surface Elevation, Gage 7

Wave Amplitude, ft	Maximum Water-Surface Elevation at Cited Land Elevation, ft				
	4	6	8	10	12
3	3.27				
4	3.89	4.00			
6	4.89	5.50	5.53		
8	6.29	6.45	7.12	7.13	
10	7.50	8.06	8.36	8.91	8.90
12	8.98	9.45	9.73	10.30	10.66

Note: Wave period = 800 sec.
All elevations are in feet referred to NGVD.

TABLE 11

Maximum Water-Surface Elevation, Gage 8

Wave Amplitude, ft	Maximum Water-Surface Elevation at Cited Land Elevation, ft				
	4	6	8	10	12
3	2.48				
4	3.00	3.10			
6	4.22	4.26	4.27		
8	5.69	5.46	5.60	5.59	
10	7.19	6.98	6.94	7.07	7.08
12	8.45	8.60	8.16	8.47	8.60

Note: Wave period = 800 sec.
All elevations are in feet referred to NGVD.

TABLE 12

Maximum Water-Surface Elevation, Gage 9

Wave Amplitude, ft	Maximum Water-Surface Elevation at Cited Land Elevation, ft				
	4	6	8	10	12
3	2.65				
4	3.56	3.56			
6	5.32	5.42	5.42		
8	7.02	7.22	7.31	7.31	
10	8.56	8.92	9.13	9.22	9.22
12	10.23	10.52	10.84	11.06	11.14

Note: Wave period = 800 sec.
All elevations are in feet referred to NGVD.

TABLE 13

Maximum Water-Surface Elevation, Gage 10

Wave Amplitude, ft	Maximum Water-Surface Elevation at Cited Land Elevation, ft				
	4	6	8	10	12
3	3.17				
4	4.18	4.20			
6	6.03	6.22	6.24		
8	7.72	8.03	8.21	8.23	
10	9.41	9.74	10.00	10.16	10.17
12	11.13	11.43	11.73	11.94	12.08

Note: Wave period = 800 sec.
All elevations are in feet referred to NGVD.

TABLE 14

Maximum Water-Surface Elevation, Gage 11

Wave Amplitude, ft	Maximum Water-Surface Elevation at Cited Land Elevation, ft				
	4	6	8	10	12
3	2.67				
4	3.58	3.58			
6	5.39	5.42	5.42		
8	7.12	7.26	7.30	7.31	
10	8.80	9.05	9.14	9.21	9.21
12	10.43	10.77	10.97	11.03	11.13

Note: Wave period = 800 sec.
All elevations are in feet referred to NGVD.

TABLE 15

Maximum Water-Surface Elevation, Gage 12

Wave Amplitude, ft	Maximum Water-Surface Elevation at Cited Land Elevation, ft				
	4	6	8	10	12
3	0.00				
4	0.00	0.00			
6	4.72	0.00	0.00		
8	7.53	6.70	0.00	0.00	
10	9.29	9.31	8.67	0.00	0.00
12	9.75	11.33	11.14	10.60	0.00

Note: Wave period = 800 sec.
All elevations are in feet referred to NGVD.

TABLE 16

Maximum Water-Surface Elevation, Gage 13

Wave Amplitude, ft	Maximum Water-Surface Elevation at Cited Land Elevation, ft				
	4	6	8	10	12
3	4.54				
4	5.45	6.06			
6	6.96	7.08	0.00		
8	7.01	8.72	8.69	0.00	
10	8.24	8.85	10.78	10.69	0.00
12	9.06	10.01	10.95	12.78	12.82

Note: Wave period = 800 sec.
All elevations are in feet referred to NGVD.

TABLE 17

Maximum Water-Surface Elevation, Gage 14

Wave Amplitude, ft	Maximum Water-Surface Elevation at Cited Land Elevation, ft				
	4	6	8	10	12
3	0.00				
4	0.00	0.00			
6	4.89	0.00	0.00		
8	7.62	6.86	0.00	0.00	
10	8.87	9.66	8.85	0.00	0.00
12	10.08	11.01	11.57	10.79	0.00

Note: Wave period = 800 sec.
All elevations are in feet referred to NGVD.

TABLE 18

Maximum Water-Surface Elevation, Gage 15

Wave Amplitude, ft	Maximum Water-Surface Elevation at Cited Land Elevation, ft				
	4	6	8	10	12
3	4.80				
4	6.64	6.36			
6	7.62	8.66	8.35		
8	7.91	9.52	9.50	10.08	
10	8.56	10.24	11.44	11.29	12.09
12	9.82	10.74	12.18	13.69	14.28

Note: Wave period = 800 sec.
All elevations are in feet referred to NGVD.

TABLE 19

Maximum Water-Surface Elevation, Gage 16

Wave Amplitude, ft	Maximum Water-Surface Elevation at Cited Land Elevation, ft				
	4	6	8	10	12
3	4.89				
4	6.38	6.41			
6	7.24	8.29	8.40		
8	7.80	9.21	9.88	10.09	
10	9.02	9.99	11.36	11.90	12.10
12	9.51	10.85	12.20	13.42	14.03

Note: Wave period = 800 sec.
All elevations are in feet referred to NGVD.

TABLE 20

Maximum Water-Surface Elevation, Gage 17

Wave Amplitude, ft	Maximum Water-Surface Elevation at Cited Land Elevation, ft				
	4	6	8	10	12
3	4.97				
4	6.27	6.48			
6	7.37	8.31	8.44		
8	7.98	9.13	9.94	10.07	
10	8.45	9.98	11.19	12.09	12.12
12	9.80	10.56	12.19	13.30	14.44

Note: Wave period = 800 sec.
All elevations are in feet referred to NGVD.

TABLE 21

Maximum Water-Surface Elevation, Gage 18

Wave Amplitude, ft	Maximum Water-Surface Elevation at Cited Land Elevation, ft				
	4	6	8	10	12
3	4.96				
4	6.47	6.48			
6	7.88	8.61	8.45		
8	8.19	9.82	10.16	10.09	
10	8.69	10.18	11.79	12.14	12.14
12	10.47	10.75	12.25	13.84	14.73

Note: Wave period = 800 sec.
All elevations are in feet referred to NGVD.

TABLE 22

Maximum Water-Surface Elevation, Gage 19

Wave Amplitude, ft	Maximum Water-Surface Elevation at Cited Land Elevation, ft				
	4	6	8	10	12
3	5.01				
4	6.48	6.51			
6	7.40	8.58	8.47		
8	8.04	9.44	10.19	10.07	
10	8.94	9.98	11.51	12.38	12.14
12	10.85	10.71	12.09	13.55	14.60

Note: Wave period = 800 sec.
All elevations are in feet referred to NGVD.

TABLE 23

Maximum Water-Surface Elevation, Gage 20

Wave Amplitude, ft	Maximum Water-Surface Elevation at Cited Land Elevation, ft				
	4	6	8	10	12
3	0.00				
4	4.34	0.00			
6	5.03	6.27	0.00		
8	6.52	6.82	8.06	0.00	
10	8.00	8.57	8.75	10.07	0.00
12	9.20	9.91	10.55	10.72	12.08

Note: Wave period = 800 sec.
All elevations are in feet referred to NGVD.

TABLE 24

Maximum Water-Surface Elevation, Gage 21

Wave Amplitude, ft	Maximum Water-Surface Elevation at Cited Land Elevation, ft				
	4	6	8	10	12
3	4.48				
4	5.00	0.00			
6	6.87	6.98	0.00		
8	7.50	8.78	8.73	0.00	
10	7.99	9.60	10.71	10.74	0.00
12	9.02	10.21	11.73	12.90	12.76

Note: Wave period = 800 sec.
All elevations are in feet referred to NGVD.

TABLE 25

Maximum Water-Surface Elevation, Gage 22

Wave Amplitude, ft	Maximum Water-Surface Elevation at Cited Land Elevation, ft				
	4	6	8	10	12
3	0.00				
4	4.39	0.00			
6	6.00	6.30	0.00		
8	6.56	6.92	0.00	0.00	
10	7.41	8.57	8.83	0.00	0.00
12	8.80	9.25	10.35	10.81	12.09

Note: Wave period = 800 sec.
All elevations are in feet referred to NGVD.

TABLE 26

Maximum Water-Surface Elevation, Gage 23

Wave Amplitude, ft	Maximum Water-Surface Elevation at Cited Land Elevation, ft				
	4	6	8	10	12
3	0.00				
4	0.00	0.00			
6	4.62	0.00	0.00		
8	6.13	6.47	0.00	0.00	
10	7.18	7.89	8.37	0.00	0.00
12	8.57	9.10	9.14	10.33	0.00

Note: Wave period = 800 sec.
All elevations are in feet referred to NGVD.

TABLE 27

Maximum Water-Surface Elevation, Gage 24

Wave Amplitude, ft	Maximum Water-Surface Elevation at Cited Land Elevation, ft				
	4	6	8	10	12
3	0.00				
4	0.00	0.00			
6	4.28	0.00	0.00		
8	4.87	6.11	0.00	0.00	
10	6.28	7.04	0.00	0.00	0.00
12	7.32	7.87	8.52	0.00	0.00

Note: Wave period = 800 sec.
All elevations are in feet referred to NGVD.

TABLE 28

Maximum Water-Surface Elevation, Gage 25

Wave Amplitude, ft	Maximum Water-Surface Elevation at Cited Land Elevation, ft				
	4	6	8	10	12
3	0.00				
4	4.09	0.00			
6	4.59	0.00	0.00		
8	5.98	6.40	0.00	0.00	
10	7.44	7.51	8.26	0.00	0.00
12	8.06	9.28	8.84	10.21	0.00

Note: Wave period = 800 sec.
All elevations are in feet referred to NGVD.

TABLE 29

Maximum Water-Surface Elevation, Gage 26

Wave Amplitude, ft	Maximum Water-Surface Elevation at Cited Land Elevation, ft				
	4	6	8	10	12
3	0.00				
4	4.33	0.00			
6	5.07	6.15	0.00		
8	6.68	6.90	0.00	0.00	
10	7.92	8.50	8.72	0.00	0.00
12	9.62	9.90	10.12	10.70	0.00

Note: Wave period = 800 sec.
All elevations are in feet referred to NGVD.

TABLE 30

Maximum Water-Surface Elevation, Gage 27

Wave Amplitude, ft	Maximum Water-Surface Elevation at Cited Land Elevation, ft				
	4	6	8	10	12
3	4.82				
4	6.07	6.27			
6	7.08	7.90	8.14		
8	7.77	9.04	9.07	0.00	
10	8.42	9.84	10.98	11.45	0.00
12	9.62	10.60	11.98	13.04	13.88

Note: Wave period = 800 sec.
All elevations are in feet referred to NGVD.

TABLE 31

Maximum Water-Surface Elevation, Gage 28

Wave Amplitude, ft	Maximum Water-Surface Elevation at Cited Land Elevation, ft				
	4	6	8	10	12
3	4.89				
4	6.44	6.41			
6	7.22	8.37	8.34		
8	7.82	9.57	9.90	10.02	
10	8.71	10.20	11.38	12.24	12.12
12	10.13	10.89	12.66	13.31	14.46

Note: Wave period = 800 sec.
All elevations are in feet referred to NGVD.

TABLE 32

Maximum Velocities at Selected Gages for Small Tsunamis

Gage	Maximum velocities, fps, at Cited Incident Wave Amplitudes, ft		
	0.1	0.3	1.0
3	0.05	0.13	0.39
4	0.19	0.53	1.6
5	0.39	1.1	3.2
8	0.43	1.2	3.6

Note: Wave period = 800 sec.
All elevations are in feet referred to NGVD.

TABLE 33

Predicted Tsunami Amplitudes Based on Historical Data*

Year	Tsunami Amplitude, ft, On Open Coast	Tsunami Amplitude, ft, Within the Harbor at Cited Dock Heights			
		4 ft	6 ft	8 ft	10 ft
1946	8.0	8.0	9.6	10.2	10.4
1960	8.0	8.0	9.6	10.2	10.4
1957	7.0	7.7	9.2	9.5	9.9
1841	6.3	7.6	8.8	9.0	9.3
1837	5.7	7.4	8.4	8.6	8.7
1923	5.0	7.2	7.8	8.0	8.0
1952	5.0	7.2	7.8	8.0	8.0
1877	4.6	7.0	7.4	7.5	7.5
1964	4.0	6.5	6.8	6.9	6.9
1868	3.4	5.7	6.2	6.2	6.2

* Houston, Carver, and Markle (1977).

TABLE 34

Frequency Equations for Various Dock Heights

Dock Height, ft	Amplitude-Frequency Equation
4	$H = 4.5 - 1.8 \log F$
6	$H = 3.2 - 3.3 \log F$
8	$H = 2.5 - 3.9 \log F$
10	$H = 2.2 - 4.2 \log F$

TABLE 35

Small Tsunami Heights and Amplitudes

Year	Tsunami Height, m, at Honolulu*	Tsunami Height, m, at Barbers Point Harbor (open coast)	Tsunami Amplitude, Ft, within Barbers Point Harbor
1923	0.2	0.8	3.5
1918	0.3	0.7	3.1
1929	0.1	0.7	3.1
1951	0.3	0.6	2.7
1968	0.2	0.5	2.3
1943	0.1	0.5	2.3
1963 (Oct 12)	0.2	0.5	2.3
1965	0.1	0.4	1.9
1938	0.1	0.4	1.9
1975	0.18	0.4	1.9
1969	0.15	0.4	1.9
1956	0.1	0.3	1.4
1917	0.3	0.3	1.4
1896	0.1	0.3	1.4
1933	0.1	0.3	1.4
1944	0.1	0.3	1.4
1952	0.1	0.3	1.4
1958 (Jul 10)	0.1	0.3	1.4
1963 (Oct 19)	0.1	0.3	1.4
1922	0.3	0.2	1.0
1971	0.12	0.2	1.0
1913	0.1	0.2	1.0
1931	0.1	0.2	1.0
1958 (Nov 6)	0.1	0.2	1.0
1959	0.1	0.2	1.0
1906	0.1	0.1	0.5
1919	0.1	0.1	0.5
1928	0.1	0.1	0.5
1948	0.1	0.1	0.5
1950	0.1	0.1	0.5
1932	0.1	0.1	0.5

* Pararas-Carayannis (1977).

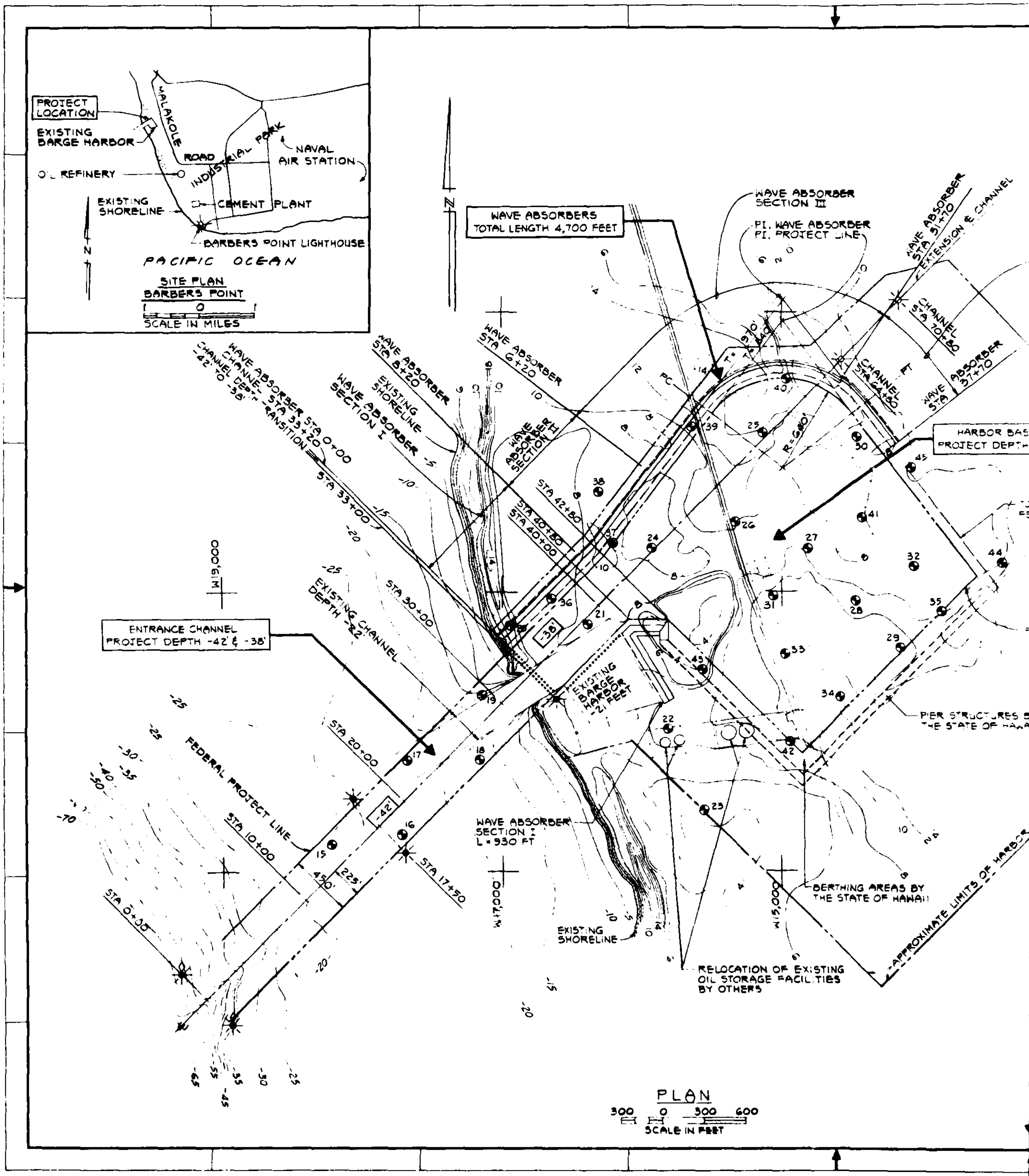

PROJECT LOCATION
EXISTING BARGE HARBOR
OIL REFINERY
MALAKOLE
ROAD
INDUSTRIAL PARK
NAVAL AIR STATION
EXISTING SHORELINE
CEMENT PLANT
BARBERS POINT LIGHTHOUSE
PACIFIC OCEAN
SITE PLAN
BARBERS POINT
SCALE IN MILES
WAVE ABSORBERS
TOTAL LENGTH 4,700 FEET
WAVE ABSORBER SECTION III
PI. WAVE ABSORBER
PI. PROJECT LINE
WAVE ABSORBER STA 51+70
EXTENSION & CHANNEL
CHANNEL STA 70+80
CHANNEL STA 64+80
WAVE ABSORBER STA 57+70
HARBOR BAS
PROJECT DEPTH
WAVE ABSORBER STA 6+20
WAVE ABSORBER STA 8+20
EXISTING SHORELINE
WAVE ABSORBER SECTION I
WAVE ABSORBER SECTION II
WAVE ABSORBER STA 0+00
CHANNEL STA 33+20
CHANNEL DEPTH TRANSITION -42' TO -38'
STA 33+00
STA 42+80
STA 40+80
STA 40+00
STA 30+00
EXISTING CHANNEL DEPTH -22'
ENTRANCE CHANNEL
PROJECT DEPTH -42' & -38'
EXISTING BARGE HARBOR -21 FEET
R=640'
FEDERAL PROJECT LINE
STA 20+00
STA 10+00
STA 17+50
STA 0+00
450'
225'
-42'
-38'
W19,000
W17,000
W15,000
WAVE ABSORBER SECTION I
L = 930 FT
EXISTING SHORELINE
RELOCATION OF EXISTING OIL STORAGE FACILITIES BY OTHERS
BERTHING AREAS BY THE STATE OF HAWAII
PIER STRUCTURES B
THE STATE OF HAWA
APPROXIMATE LIMITS OF HARBOR
PLAN
300 0 300 600
SCALE IN FEET

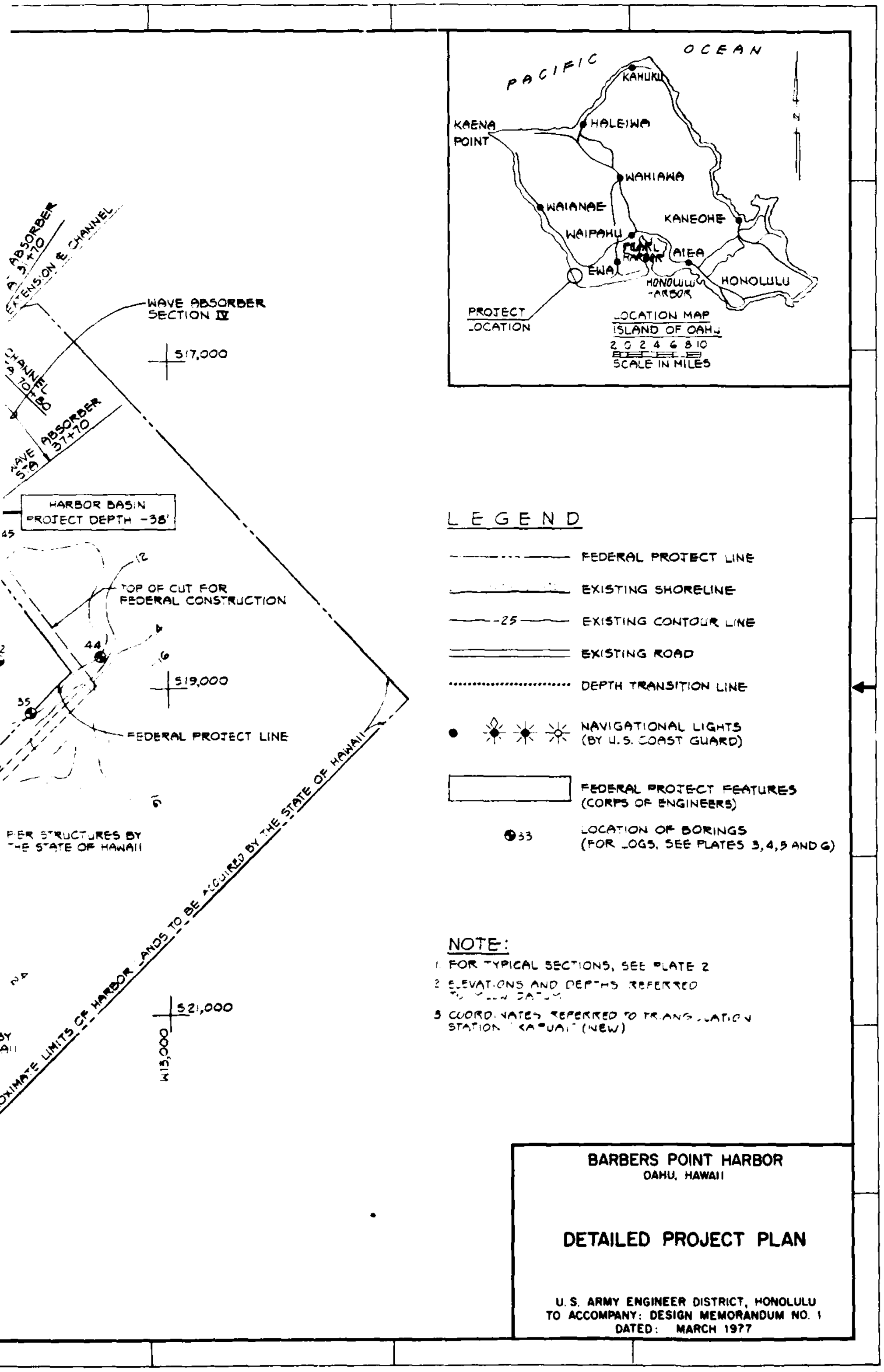
PACIFIC OCEAN
KAHUKU
HALEIWA
KAENA POINT
WAHIAWA
WAIANAE
KANEOHE
WAIPAHU
PEARL HARBOR
AIEA
EWA
HONOLULU HARBOR
HONOLULU
PROJECT LOCATION
LOCATION MAP
ISLAND OF OAHU
SCALE IN MILES
WAVE ABSORBER SECTION IV
EXTENSION & CHANNEL
517,000
HARBOR BASIN
PROJECT DEPTH -38'
TOP OF CUT FOR FEDERAL CONSTRUCTION
519,000
FEDERAL PROJECT LINE
PIER STRUCTURES BY THE STATE OF HAWAII
APPROXIMATE LIMITS OF HARBOR LANDS TO BE ACQUIRED BY THE STATE OF HAWAII
521,000
W13,000
LEGEND
FEDERAL PROJECT LINE
EXISTING SHORELINE
25 EXISTING CONTOUR LINE
EXISTING ROAD
DEPTH TRANSITION LINE
NAVIGATIONAL LIGHTS (BY U.S. COAST GUARD)
FEDERAL PROJECT FEATURES (CORPS OF ENGINEERS)
33 LOCATION OF BORINGS (FOR LOGS, SEE PLATES 3, 4, 5 AND 6)
NOTE:
1. FOR TYPICAL SECTIONS, SEE PLATE 2
2. ELEVATIONS AND DEPTHS REFERRED
3. COORDINATES REFERRED TO TRIANGULATION STATION (NEW)
BARBERS POINT HARBOR
OAHU, HAWAII
DETAILED PROJECT PLAN
U. S. ARMY ENGINEER DISTRICT, HONOLULU
TO ACCOMPANY: DESIGN MEMORANDUM NO. 1
DATED: MARCH 1977

PLATE 1

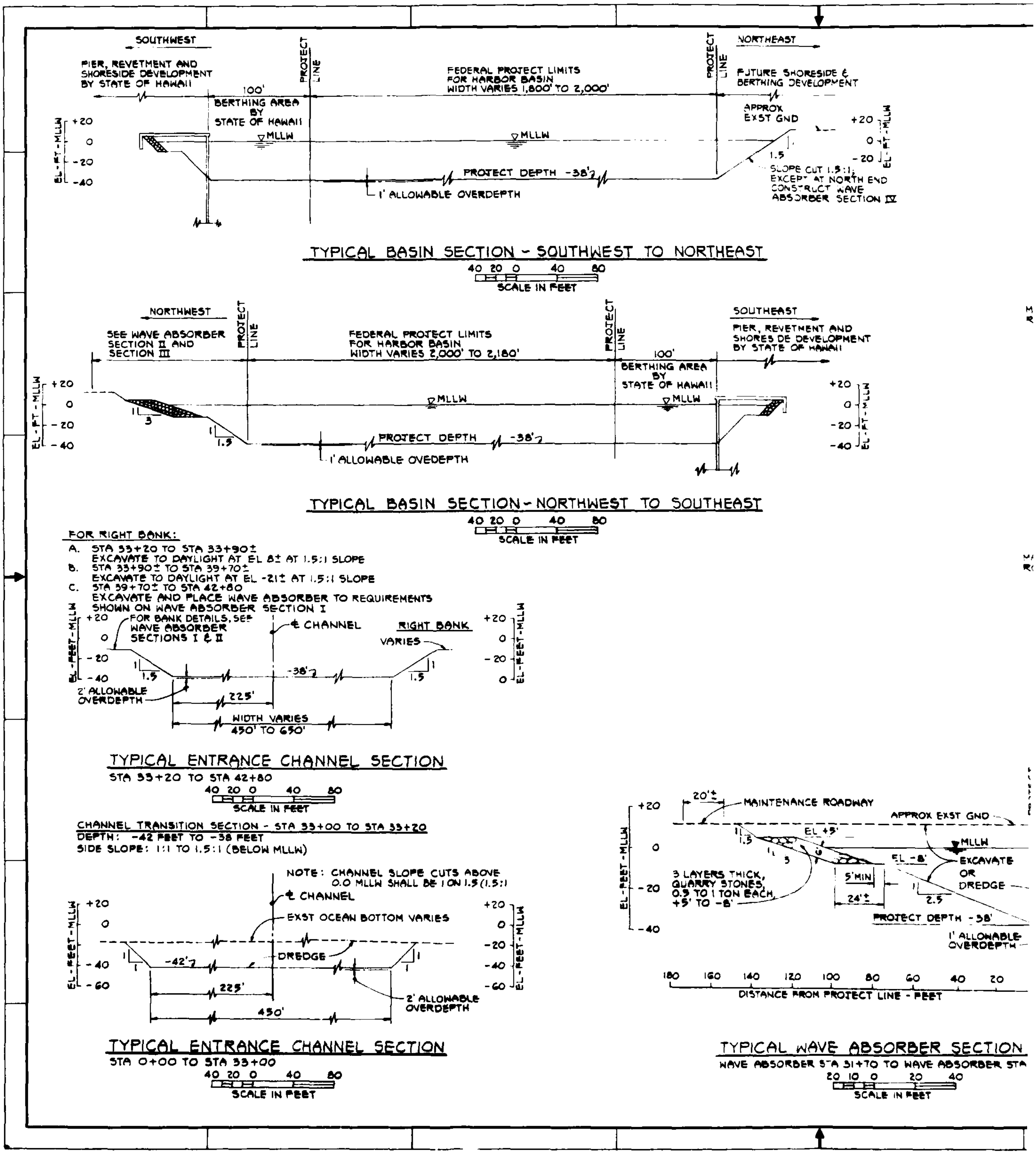
SOUTHWEST
PIER, REVETMENT AND SHORESIDE DEVELOPMENT BY STATE OF HAWAII
PROTECT LINE
100'
BERTHING AREA BY STATE OF HAWAII
FEDERAL PROJECT LIMITS FOR HARBOR BASIN WIDTH VARIES 1,800' TO 2,000'
NORTHEAST
FUTURE SHORESIDE & BERTHING DEVELOPMENT
APPROX EXST GND
MLLW
PROJECT DEPTH -38'
1' ALLOWABLE OVERDEPTH
SLOPE CUT 1.5:1; EXCEPT AT NORTH END CONSTRUCT WAVE ABSORBER SECTION IV
EL-FT-MLLW
TYPICAL BASIN SECTION - SOUTHWEST TO NORTHEAST
SCALE IN FEET
NORTHWEST
SEE WAVE ABSORBER SECTION II AND SECTION III
FEDERAL PROJECT LIMITS FOR HARBOR BASIN WIDTH VARIES 2,000' TO 2,180'
SOUTHEAST
PIER, REVETMENT AND SHORESIDE DEVELOPMENT BY STATE OF HAWAII
100'
BERTHING AREA BY STATE OF HAWAII
PROJECT DEPTH -38'
1' ALLOWABLE OVEDEPTH
TYPICAL BASIN SECTION - NORTHWEST TO SOUTHEAST
SCALE IN FEET
FOR RIGHT BANK:
A. STA 35+20 TO STA 33+90±
EXCAVATE TO DAYLIGHT AT EL 8± AT 1.5:1 SLOPE
B. STA 33+90± TO STA 39+70±
EXCAVATE TO DAYLIGHT AT EL -21± AT 1.5:1 SLOPE
C. STA 39+70± TO STA 42+80
EXCAVATE AND PLACE WAVE ABSORBER TO REQUIREMENTS SHOWN ON WAVE ABSORBER SECTION I
FOR BANK DETAILS, SEE WAVE ABSORBER SECTIONS I & II
℄ CHANNEL
RIGHT BANK
VARIES
-38'
2' ALLOWABLE OVERDEPTH
225'
WIDTH VARIES 450' TO 650'
EL-FEET-MLLW
TYPICAL ENTRANCE CHANNEL SECTION
STA 35+20 TO STA 42+80
SCALE IN FEET
CHANNEL TRANSITION SECTION - STA 35+00 TO STA 35+20
DEPTH: -42 FEET TO -38 FEET
SIDE SLOPE: 1:1 TO 1.5:1 (BELOW MLLW)
NOTE: CHANNEL SLOPE CUTS ABOVE 0.0 MLLW SHALL BE 1 ON 1.5 (1.5:1)
℄ CHANNEL
EXST OCEAN BOTTOM VARIES
DREDGE
-42'
225'
450'
2' ALLOWABLE OVERDEPTH
TYPICAL ENTRANCE CHANNEL SECTION
STA 0+00 TO STA 35+00
SCALE IN FEET
20'±
MAINTENANCE ROADWAY
APPROX EXST GND
EL +5'
MLLW
EL -8'
EXCAVATE OR DREDGE
3 LAYERS THICK, QUARRY STONES, 0.5 TO 1 TON EACH, +5' TO -8'
5'MIN
24'±
2.5
PROJECT DEPTH -38'
1' ALLOWABLE OVERDEPTH
DISTANCE FROM PROJECT LINE - FEET
EL-FEET-MLLW
TYPICAL WAVE ABSORBER SECTION
WAVE ABSORBER STA 31+70 TO WAVE ABSORBER STA
SCALE IN FEET

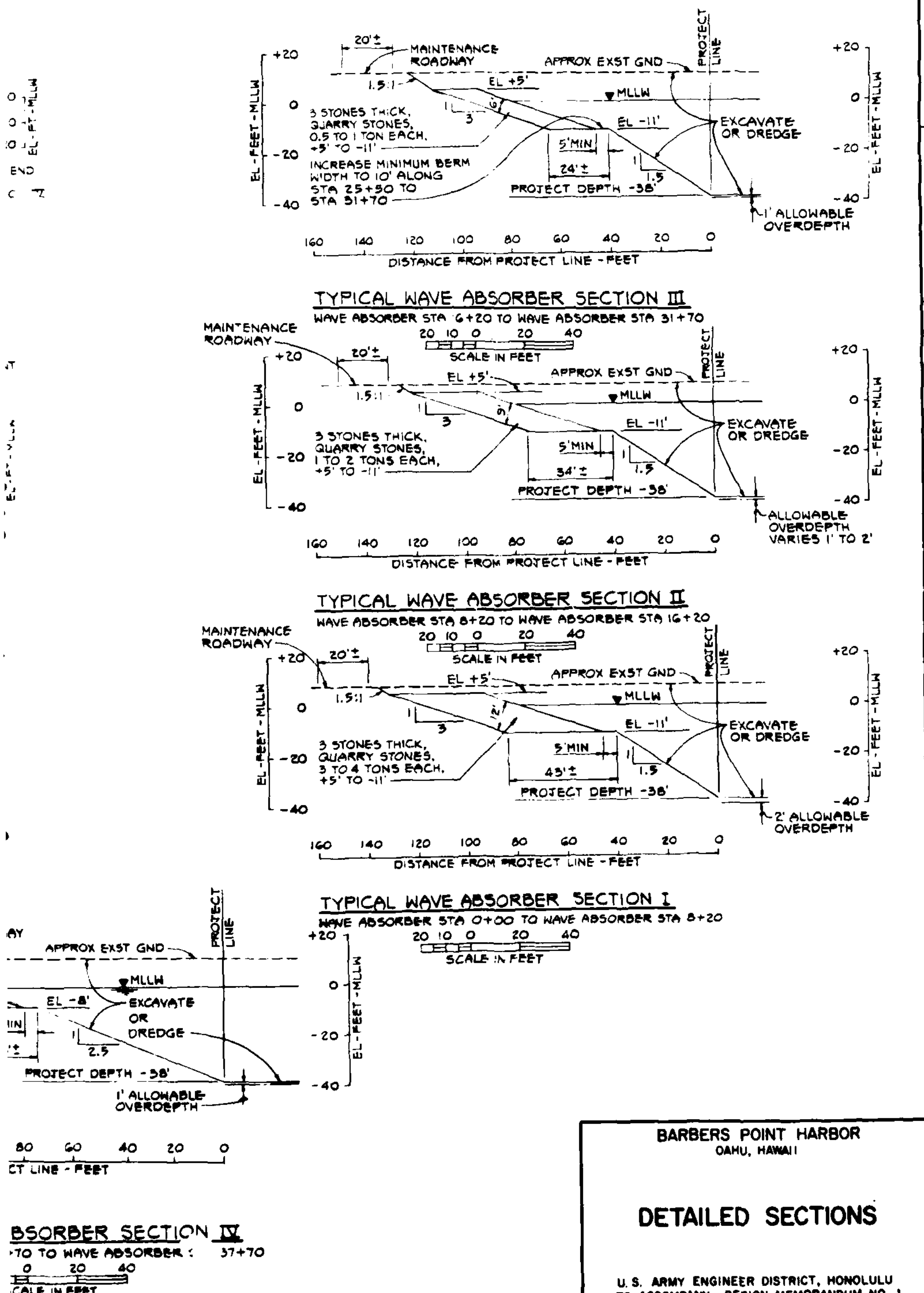

BARBERS POINT HARBOR
OAHU, HAWAII

DETAILED SECTIONS

U. S. ARMY ENGINEER DISTRICT, HONOLULU
TO ACCOMPANY: DESIGN MEMORANDUM NO. 1
DATED: MARCH 1977

PLATE 2

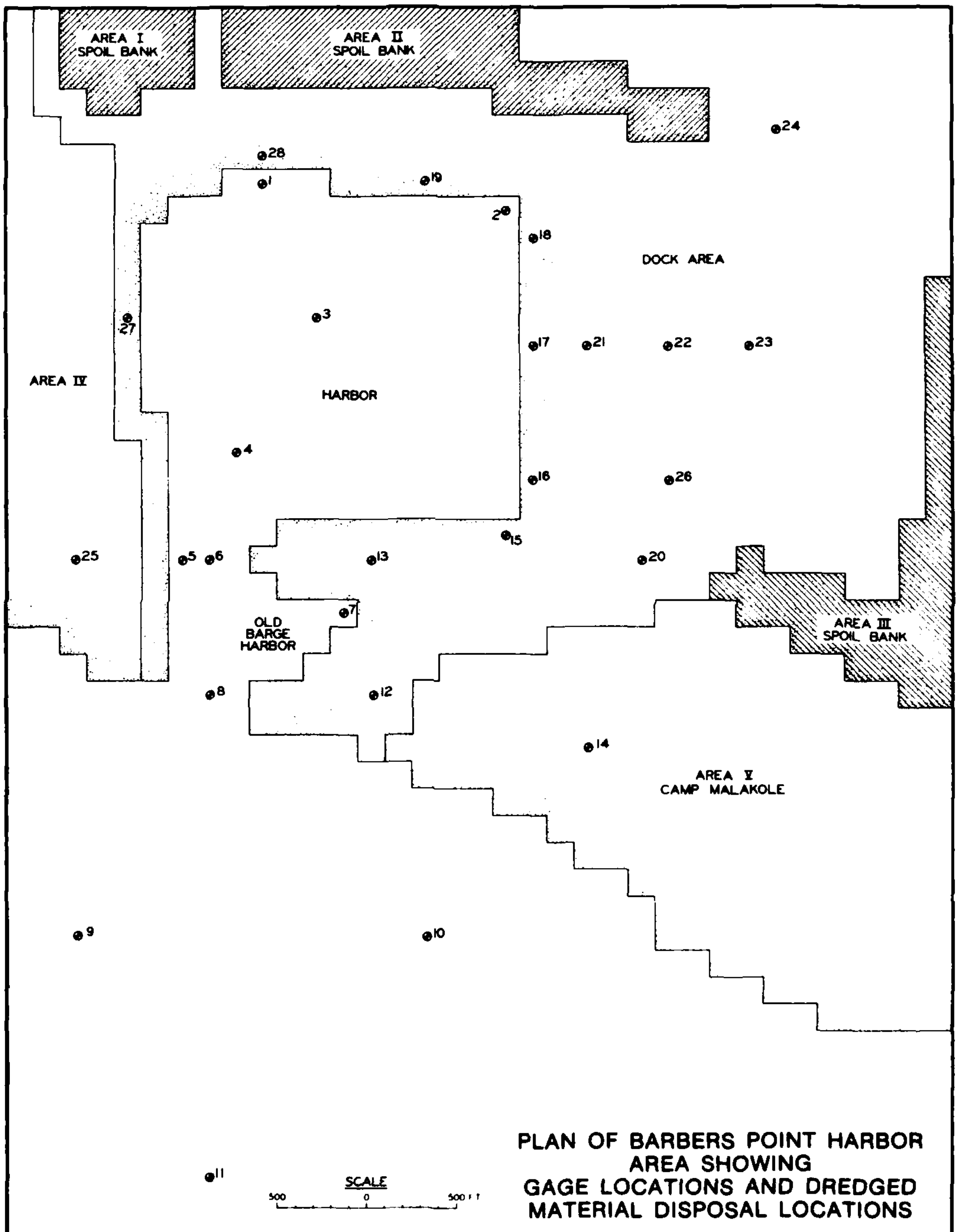

PLAN OF BARBERS POINT HARBOR
AREA SHOWING
GAGE LOCATIONS AND DREDGED
MATERIAL DISPOSAL LOCATIONS

PLATE 3

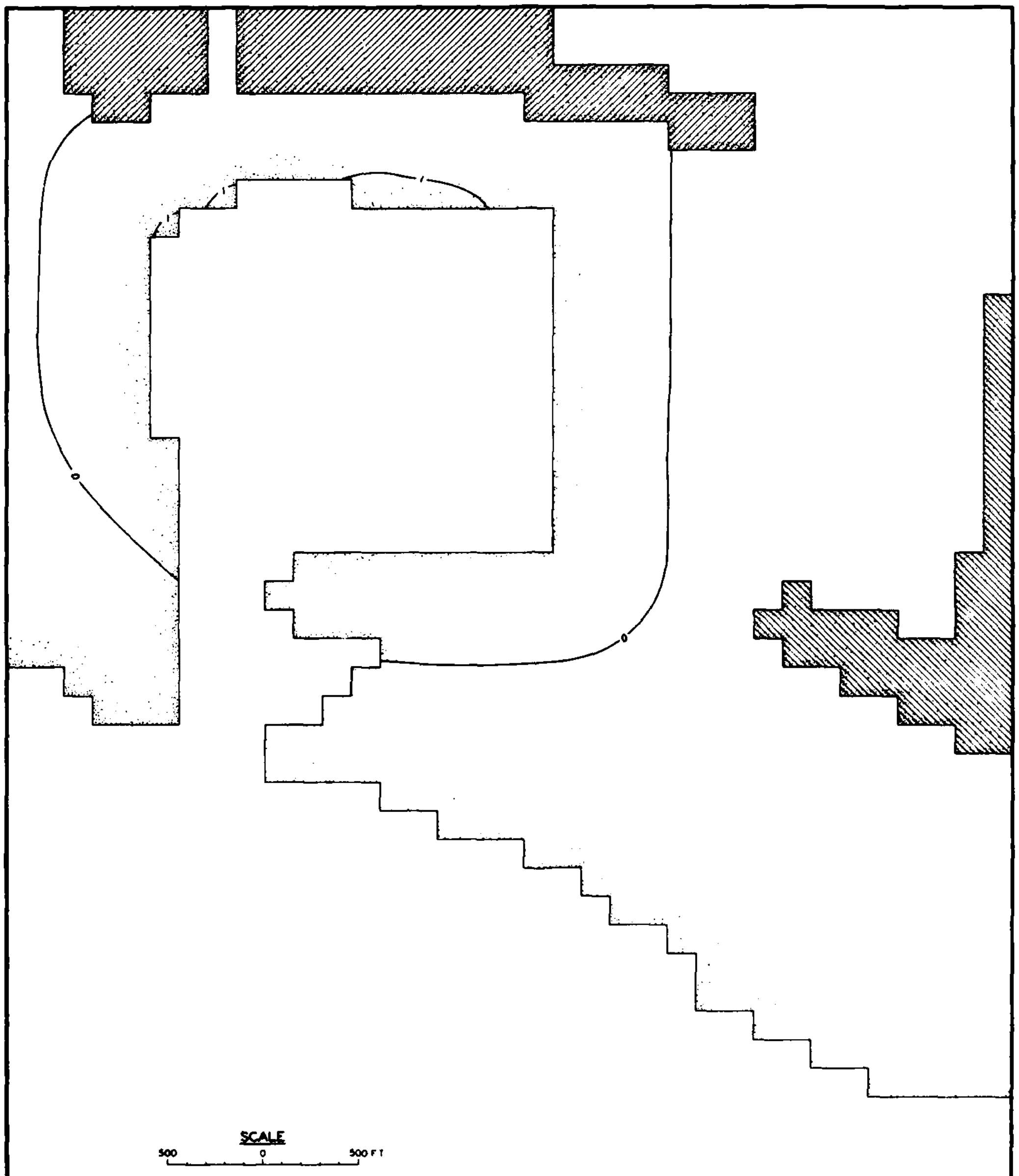

BARBERS POINT HARBOR
CONTOURS OF
MAXIMUM DEPTH OF OVERLAND FLOODING
800-SEC WAVE PERIOD
3-FT INCIDENT WAVE AMPLITUDE
4-FT LAND ELEVATION

PLATE 4

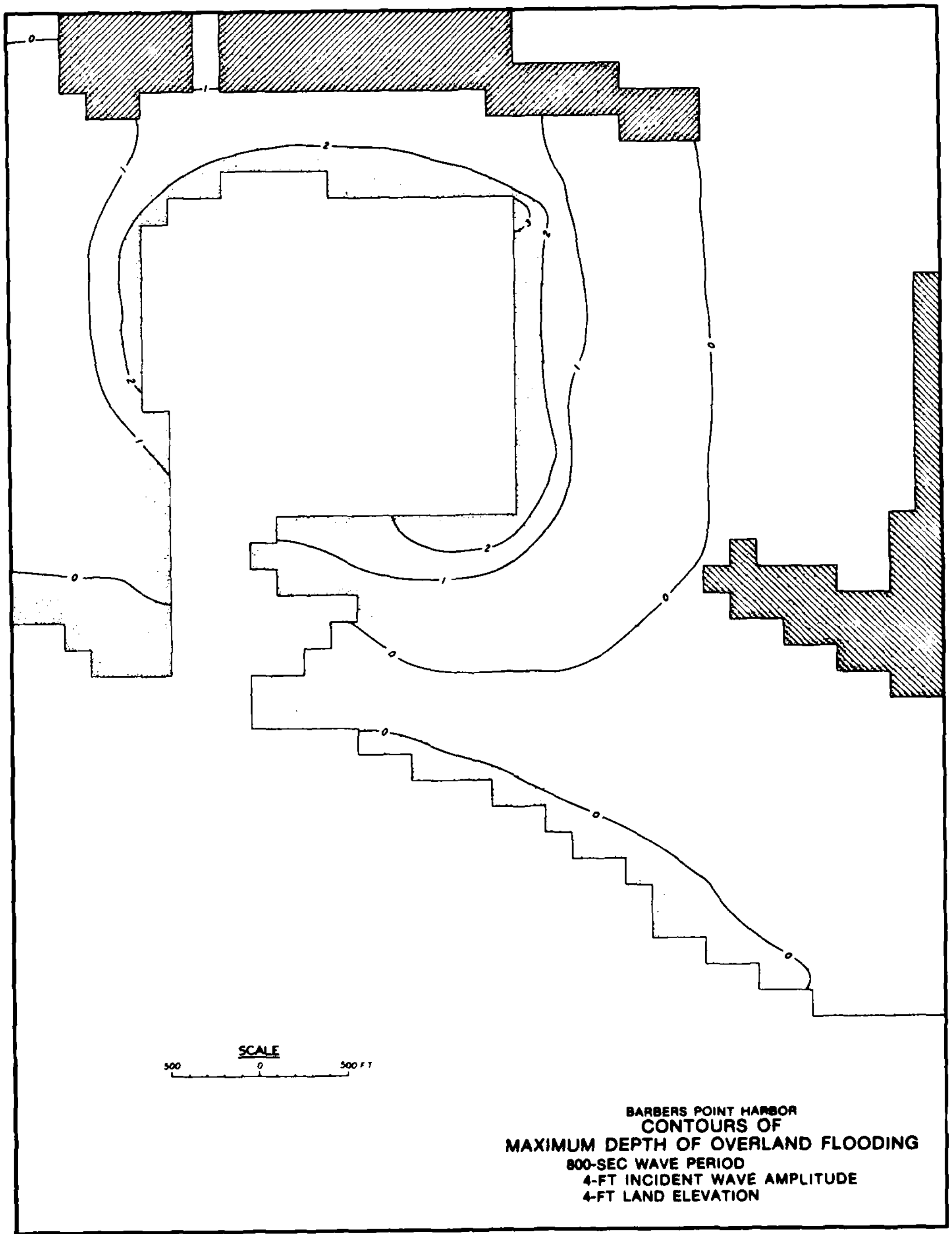

BARBERS POINT HARBOR
CONTOURS OF
MAXIMUM DEPTH OF OVERLAND FLOODING
800-SEC WAVE PERIOD
4-FT INCIDENT WAVE AMPLITUDE
4-FT LAND ELEVATION

PLATE 5

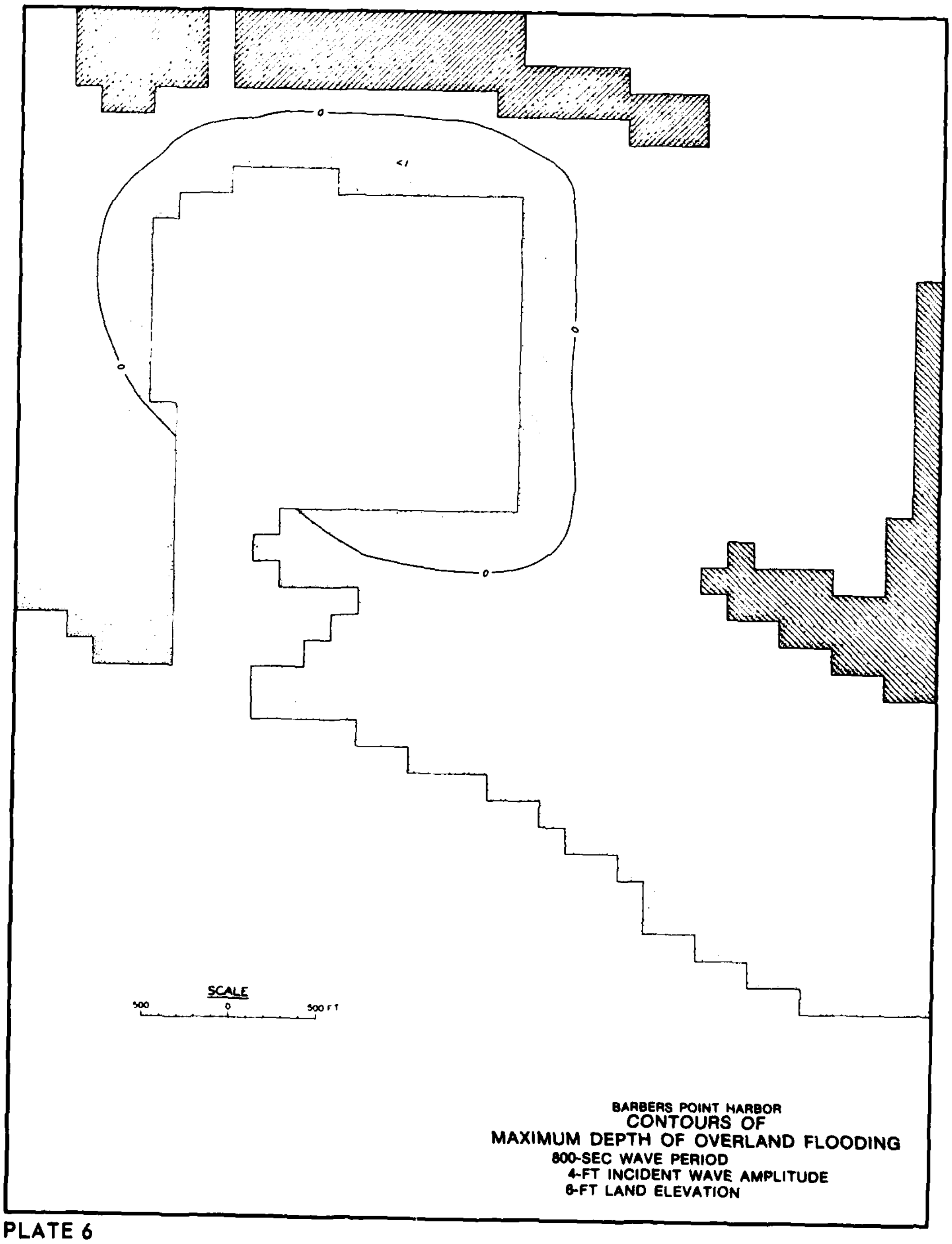

BARBERS POINT HARBOR
CONTOURS OF
MAXIMUM DEPTH OF OVERLAND FLOODING
800-SEC WAVE PERIOD
4-FT INCIDENT WAVE AMPLITUDE
6-FT LAND ELEVATION

PLATE 6

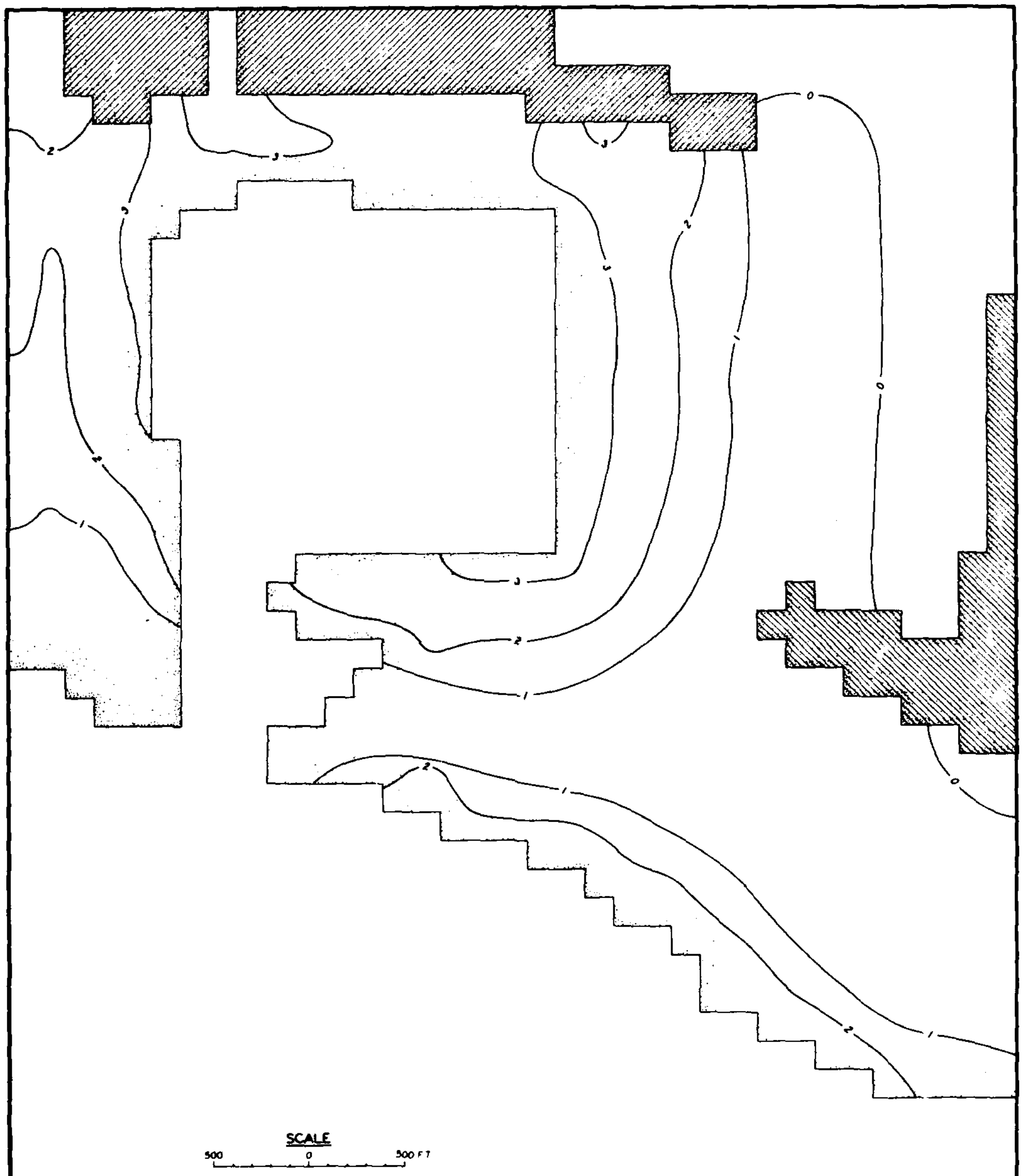

BARBERS POINT HARBOR
CONTOURS OF
MAXIMUM DEPTH OF OVERLAND FLOODING
800-SEC WAVE PERIOD
6-FT INCIDENT WAVE AMPLITUDE
4-FT LAND ELEVATION

PLATE 7

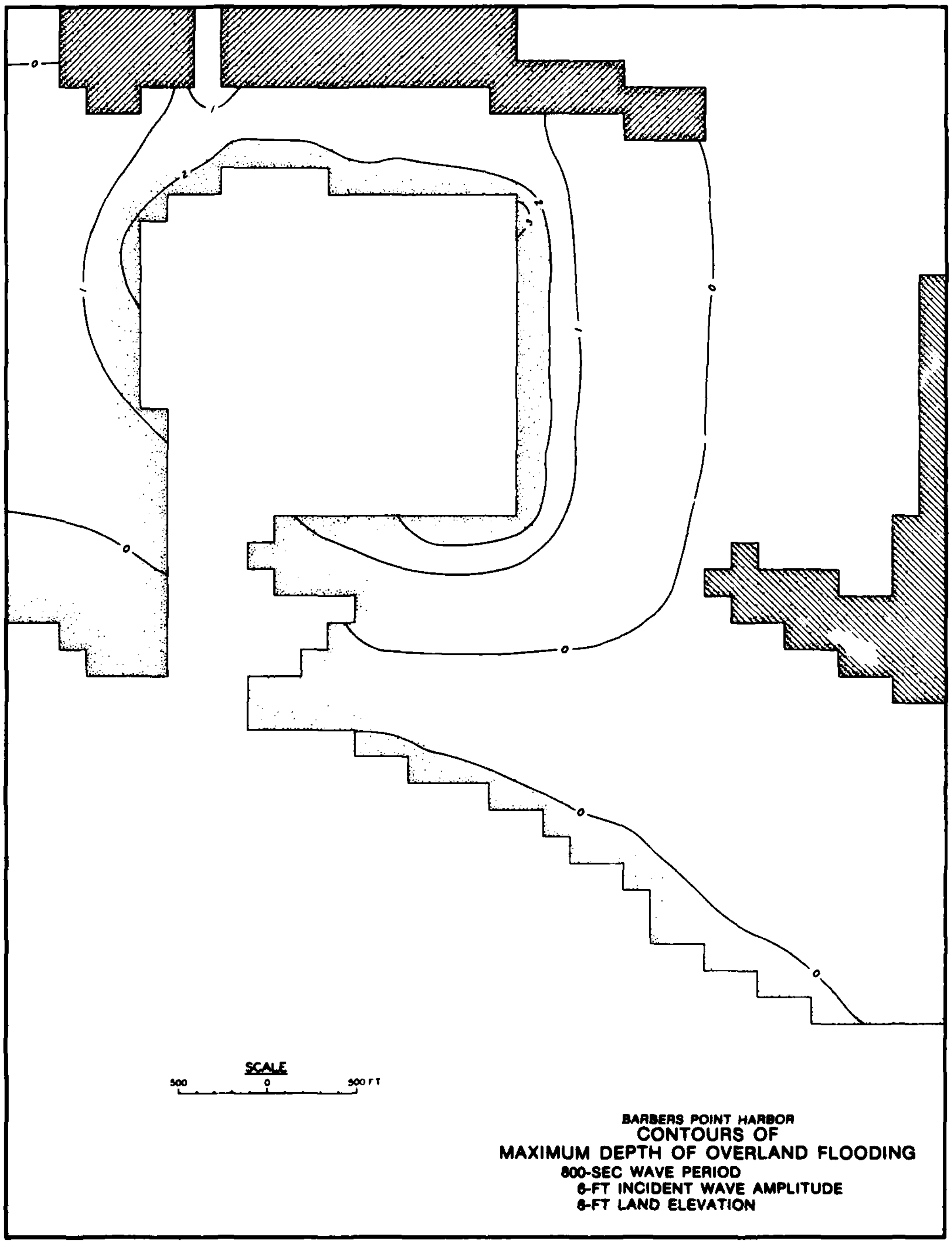

SCALE
500
0
500 FT
BARBERS POINT HARBOR
CONTOURS OF
MAXIMUM DEPTH OF OVERLAND FLOODING
800-SEC WAVE PERIOD
6-FT INCIDENT WAVE AMPLITUDE
8-FT LAND ELEVATION

PLATE 8

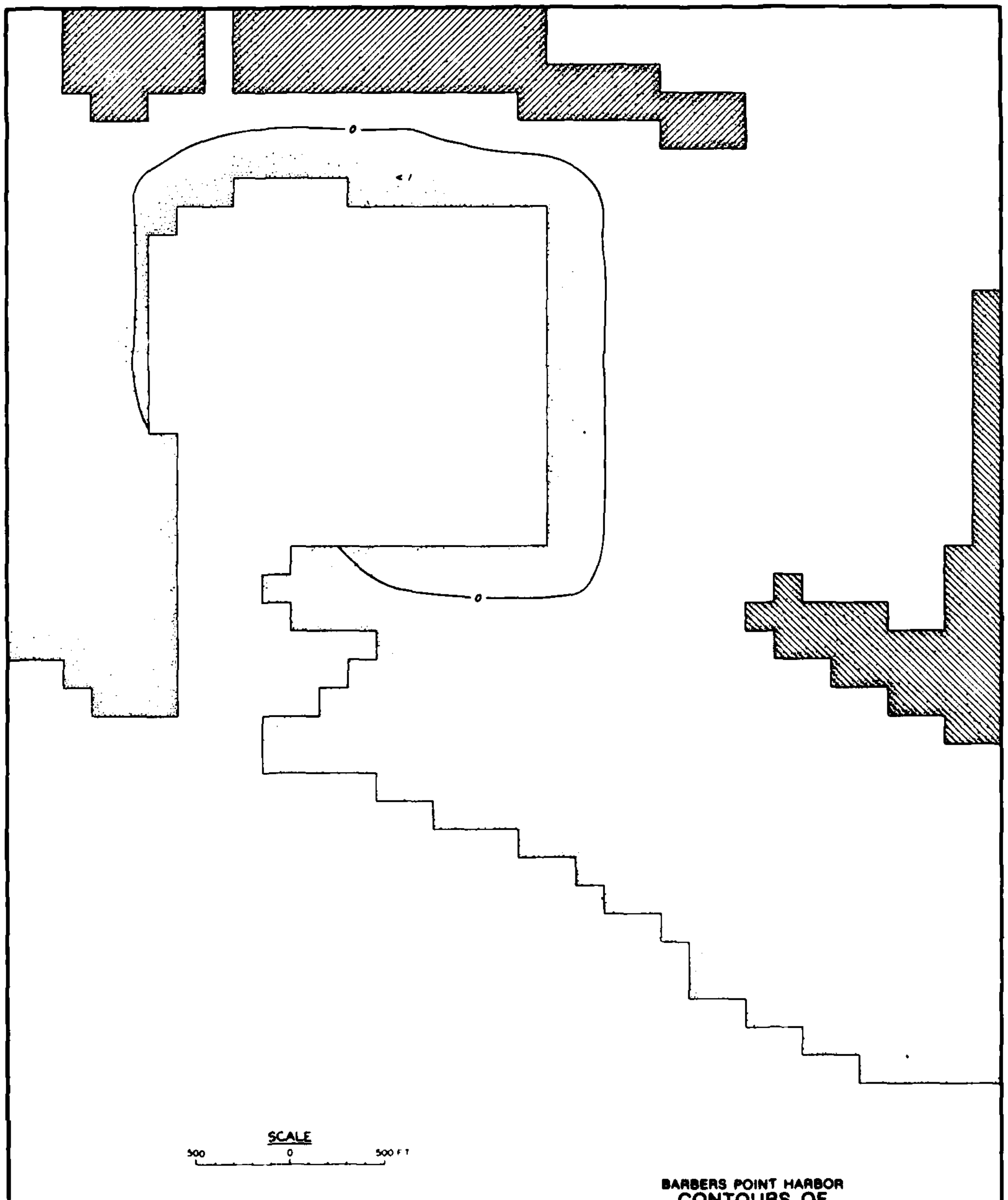

BARBERS POINT HARBOR
CONTOURS OF
MAXIMUM DEPTH OF OVERLAND FLOODING
800-SEC WAVE PERIOD
6-FT INCIDENT WAVE AMPLITUDE
8-FT LAND ELEVATION

PLATE 9

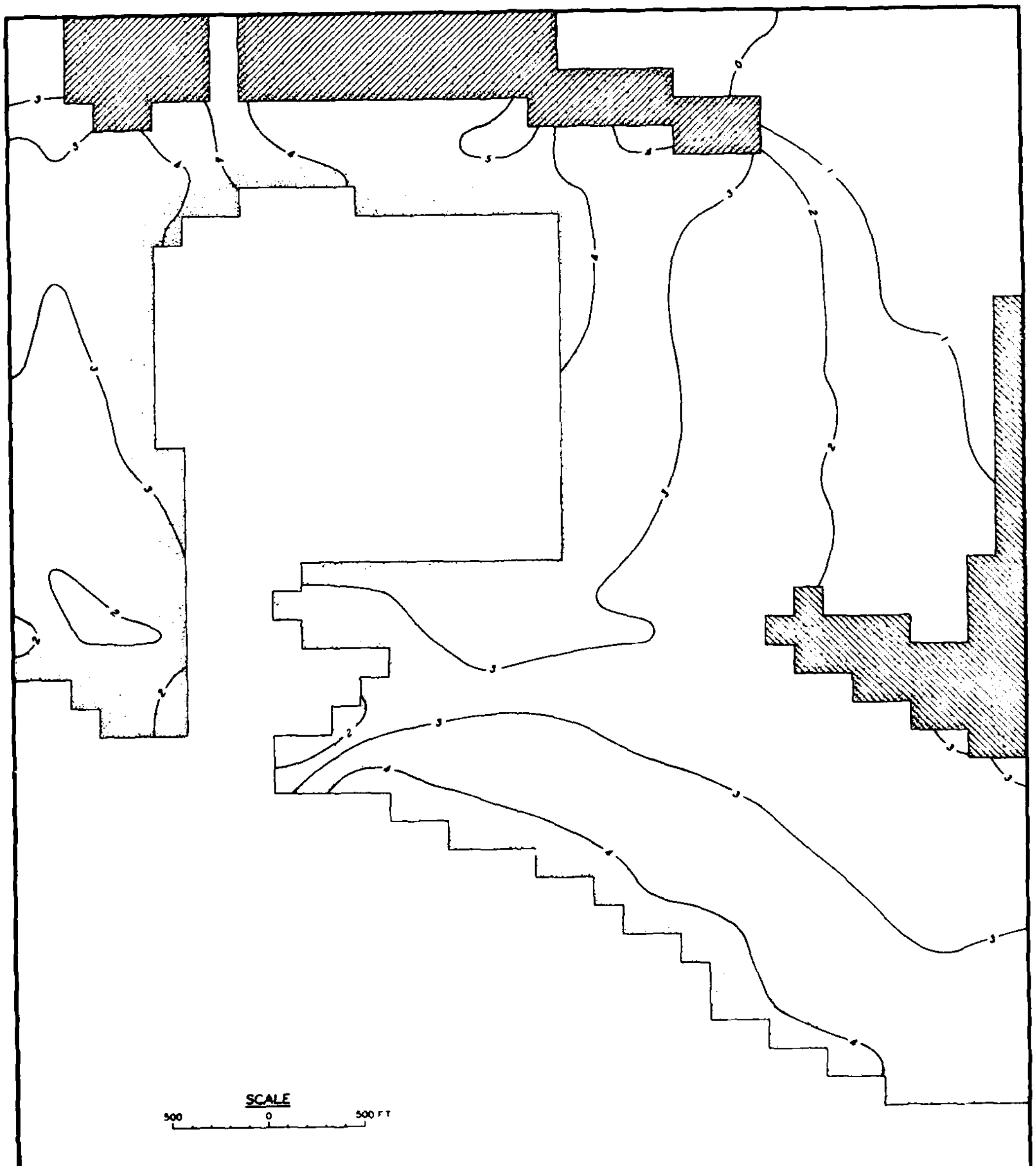

BARBERS POINT HARBOR
CONTOURS OF
MAXIMUM DEPTH OF OVERLAND FLOODING
800-SEC WAVE PERIOD
8-FT INCIDENT WAVE AMPLITUDE
4-FT LAND ELEVATION

PLATE 10

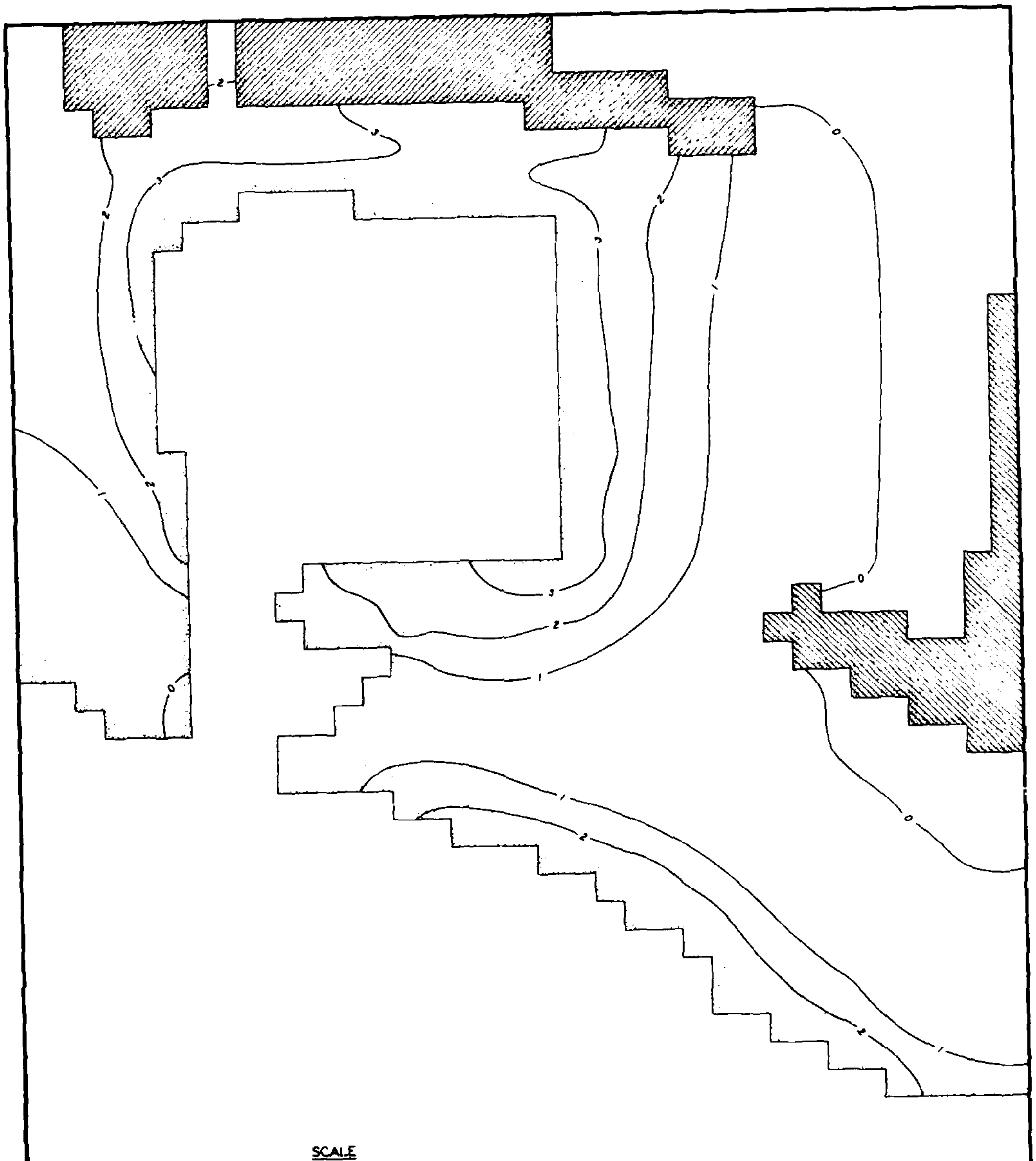

BARBERS POINT HARBOR
CONTOURS OF
MAXIMUM DEPTH OF OVERLAND FLOODING
800-SEC WAVE PERIOD
8-FT INCIDENT WAVE AMPLITUDE
6-FT LAND ELEVATION

PLATE 11

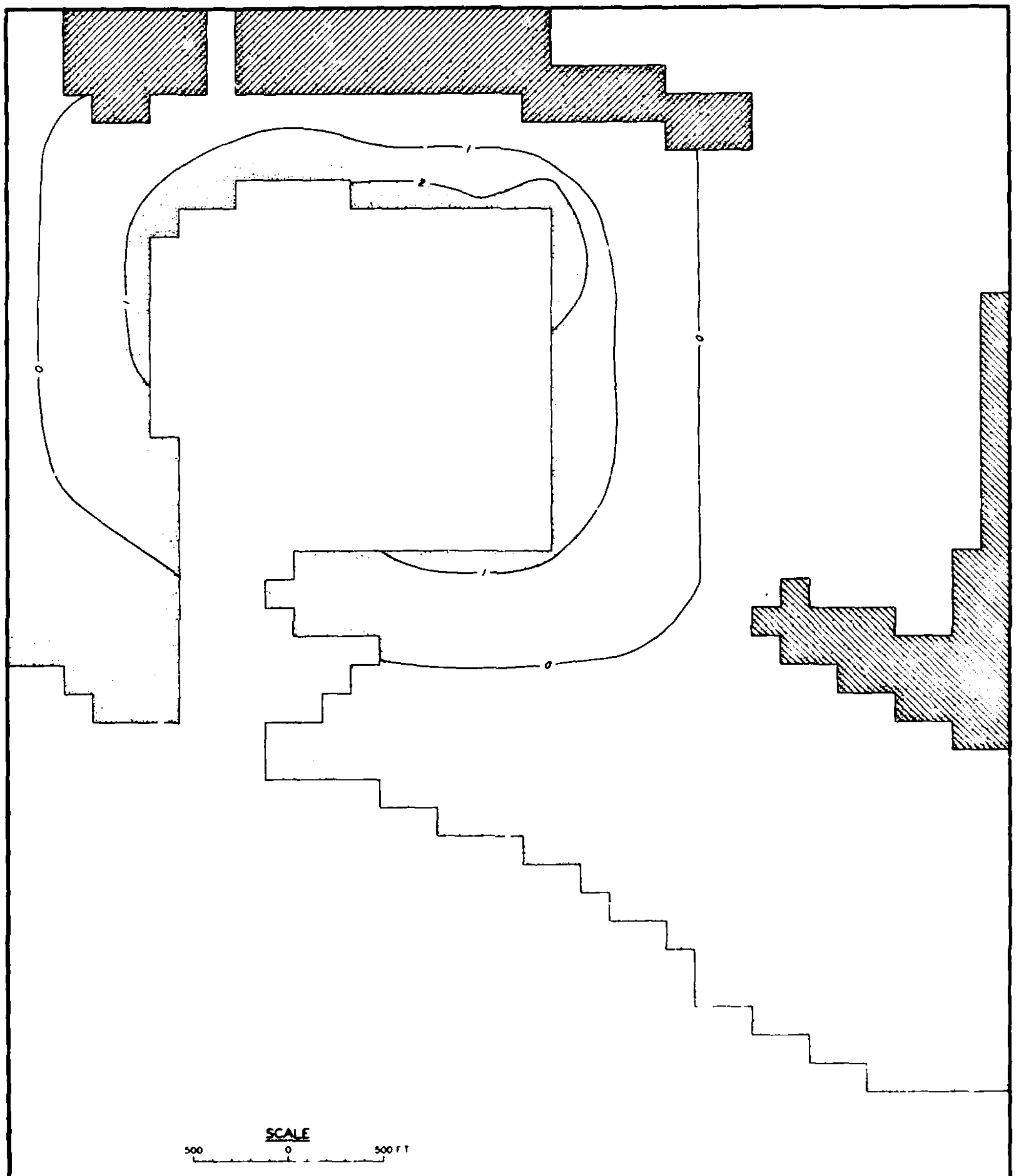

BARBERS POINT HARBOR
CONTOURS OF
MAXIMUM DEPTH OF OVERLAND FLOODING
800-SEC WAVE PERIOD
8-FT INCIDENT WAVE AMPLITUDE
8-FT LAND ELEVATION

PLATE 12

AD-A122 299 TSUNAMI RESPONSE OF BARBERS POINT HARBOR HAWAII(U) ARMY ENGINEER WATERWAYS EXPERIMENT STATION VICKSBURG MS HYDRAULICS LAB P D FARRAR ET AL. OCT 82 WES/MP/HL-82-1

2/2

UNCLASSIFIED F/G 8/3 NL

END
DATE
FILMED
2 83
DTIC

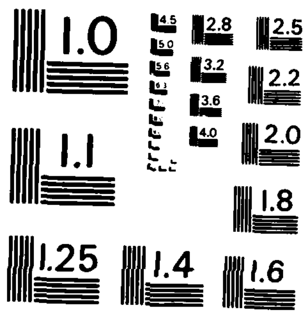

MICROCOPY RESOLUTION TEST CHART
NATIONAL BUREAU OF STANDARDS-1963-A

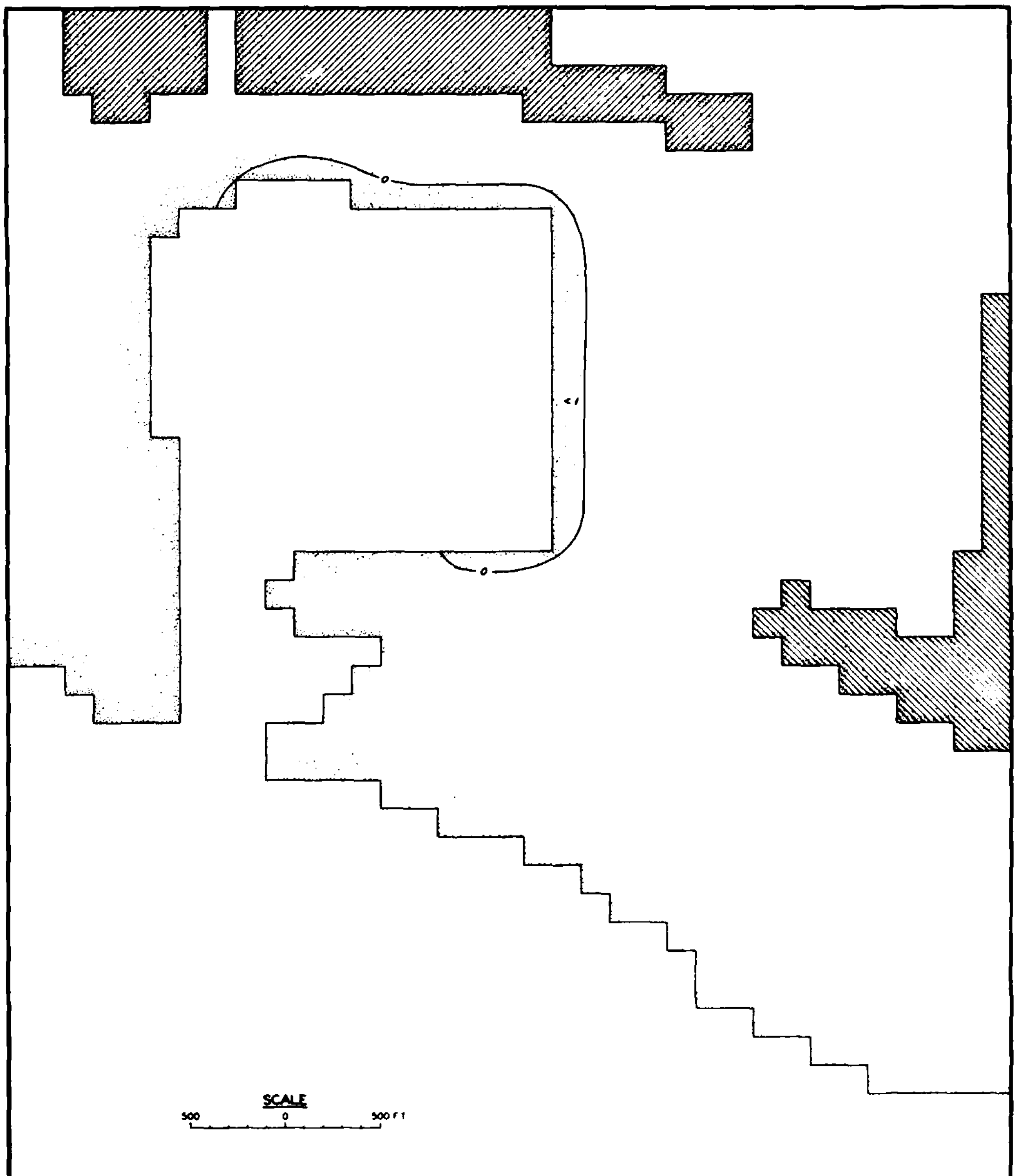

BARBERS POINT HARBOR
CONTOURS OF
MAXIMUM DEPTH OF OVERLAND FLOODING
800-SEC WAVE PERIOD
8-FT INCIDENT WAVE AMPLITUDE
10-FT LAND ELEVATION

PLATE 13

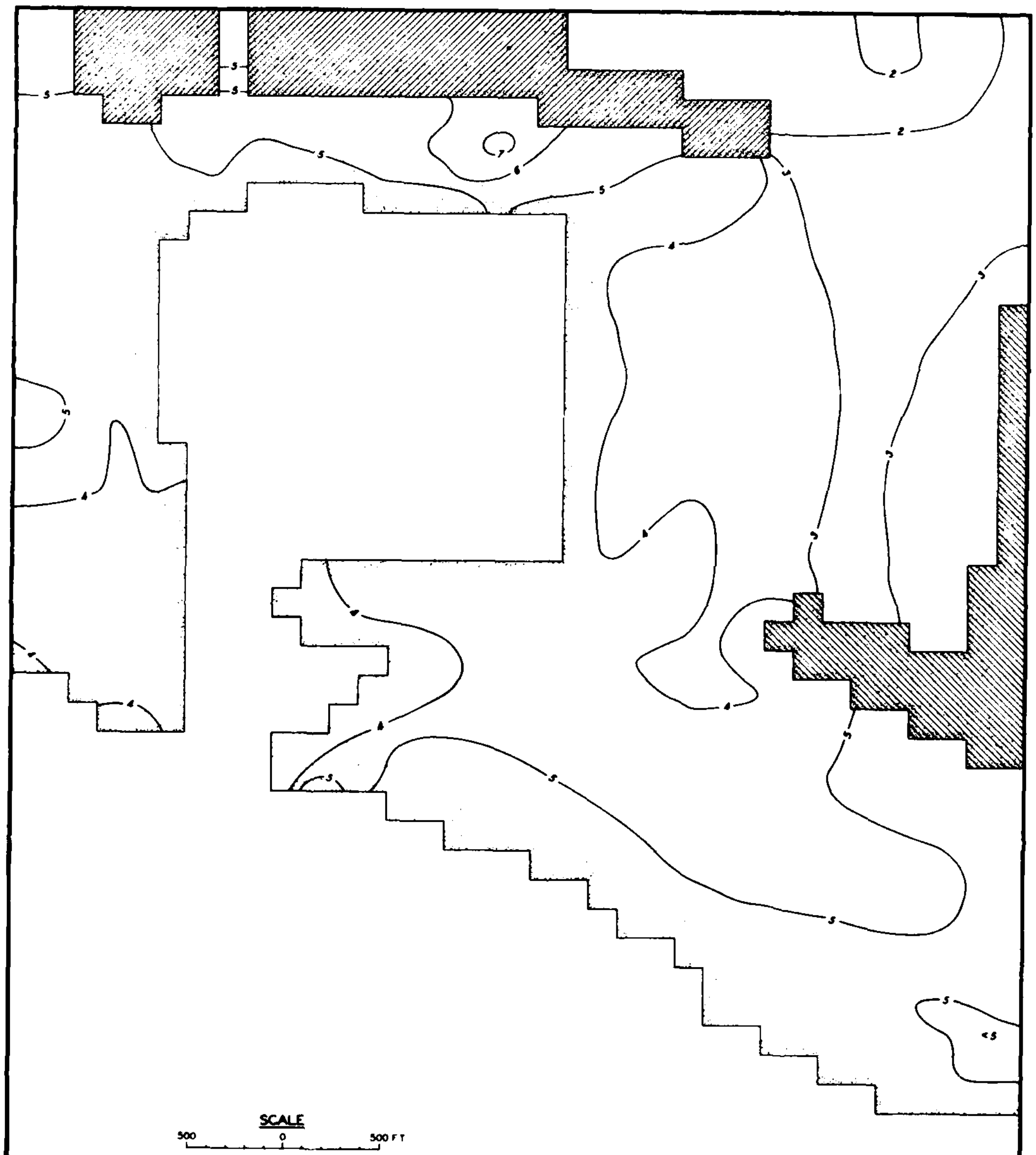

BARBERS POINT HARBOR
CONTOURS OF
MAXIMUM DEPTH OF OVERLAND FLOODING
800-SEC WAVE PERIOD
10-FT INCIDENT WAVE AMPLITUDE
4-FT LAND ELEVATION

PLATE 14

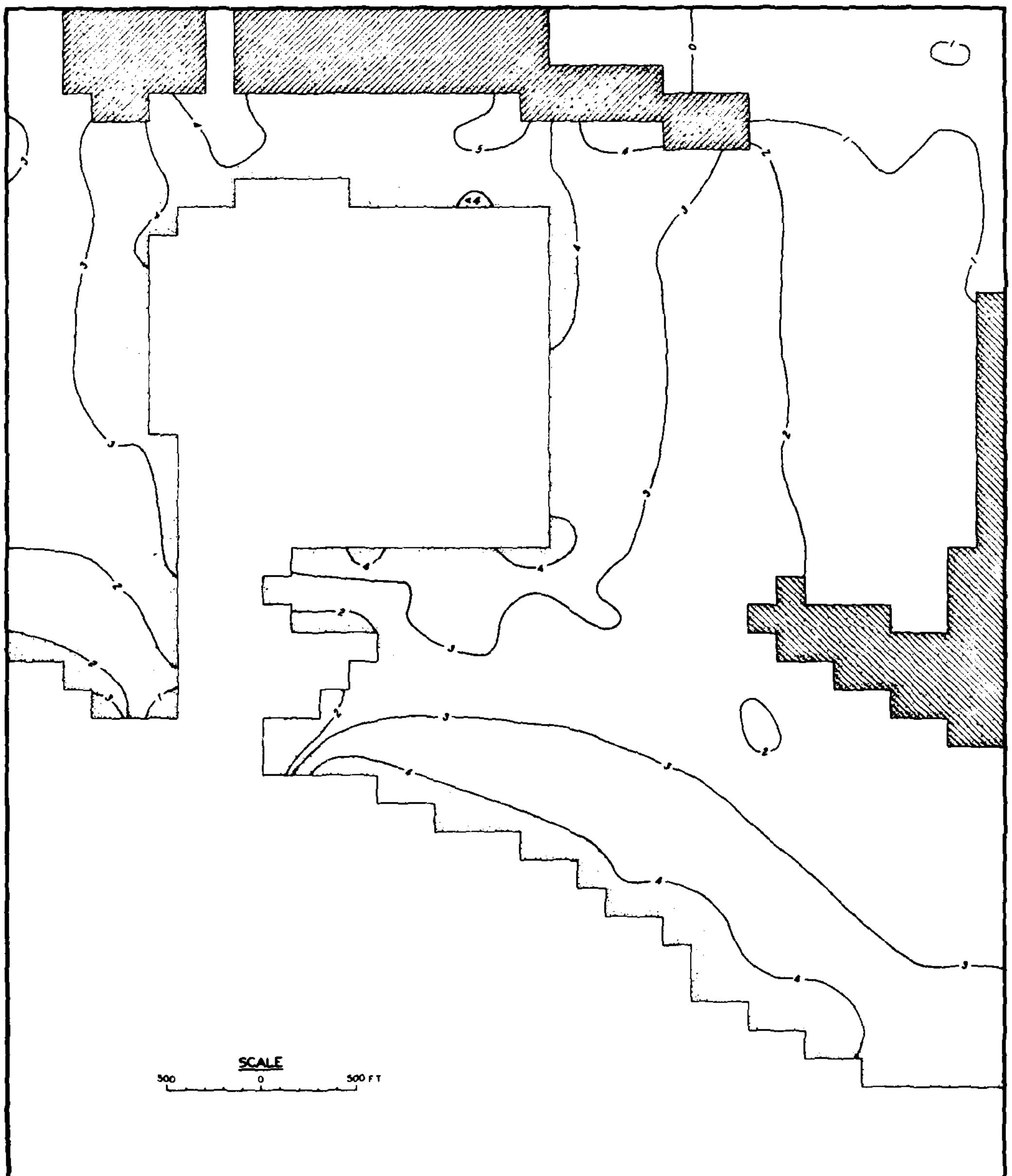

BARBERS POINT HARBOR
CONTOURS OF
MAXIMUM DEPTH OF OVERLAND FLOODING
600-SEC WAVE PERIOD
10-FT INCIDENT WAVE AMPLITUDE
6-FT LAND ELEVATION

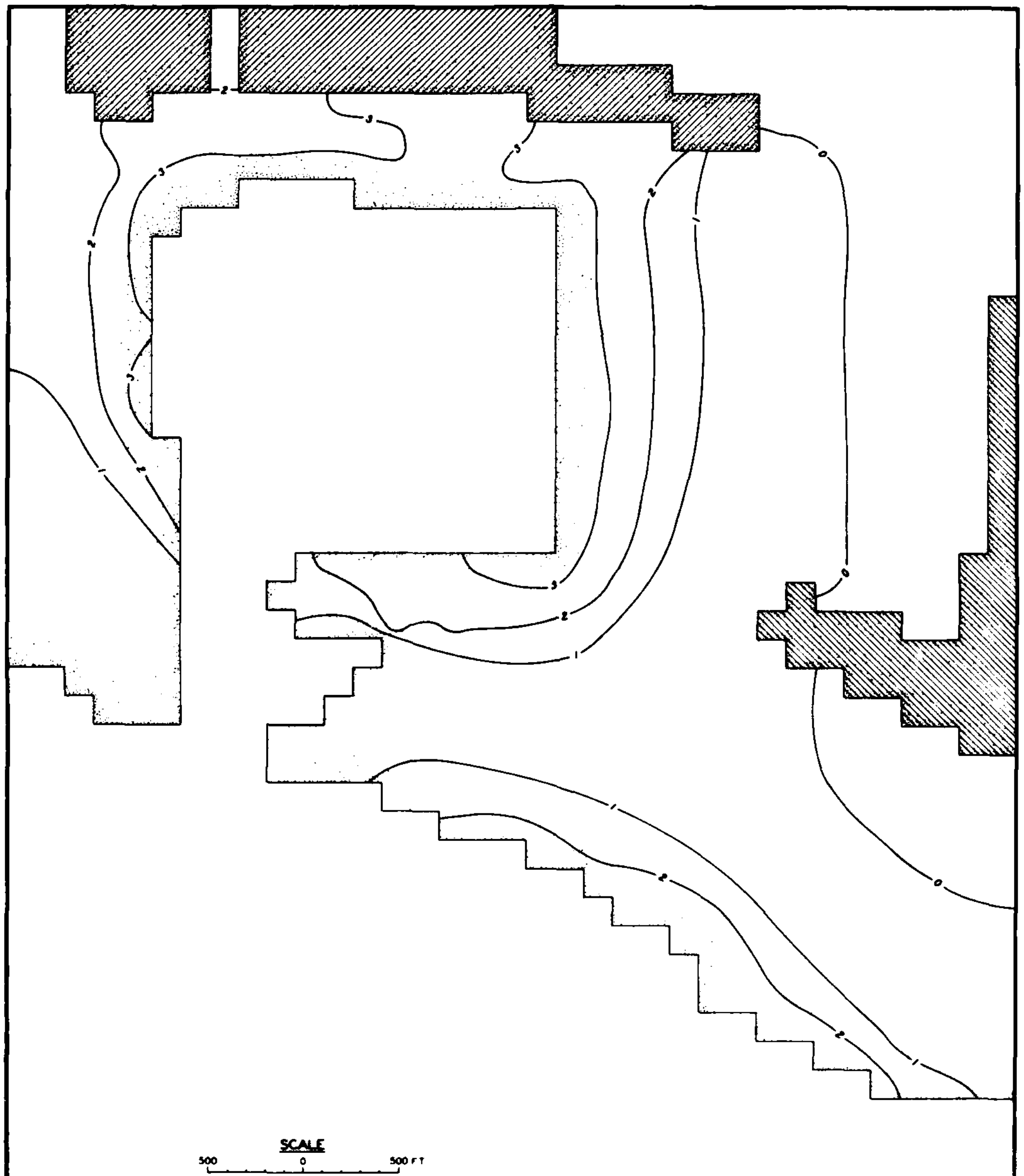

BARBERS POINT HARBOR
CONTOURS OF
MAXIMUM DEPTH OF OVERLAND FLOODING
800-SEC WAVE PERIOD
10-FT INCIDENT WAVE AMPLITUDE
8-FT LAND ELEVATION

PLATE 16

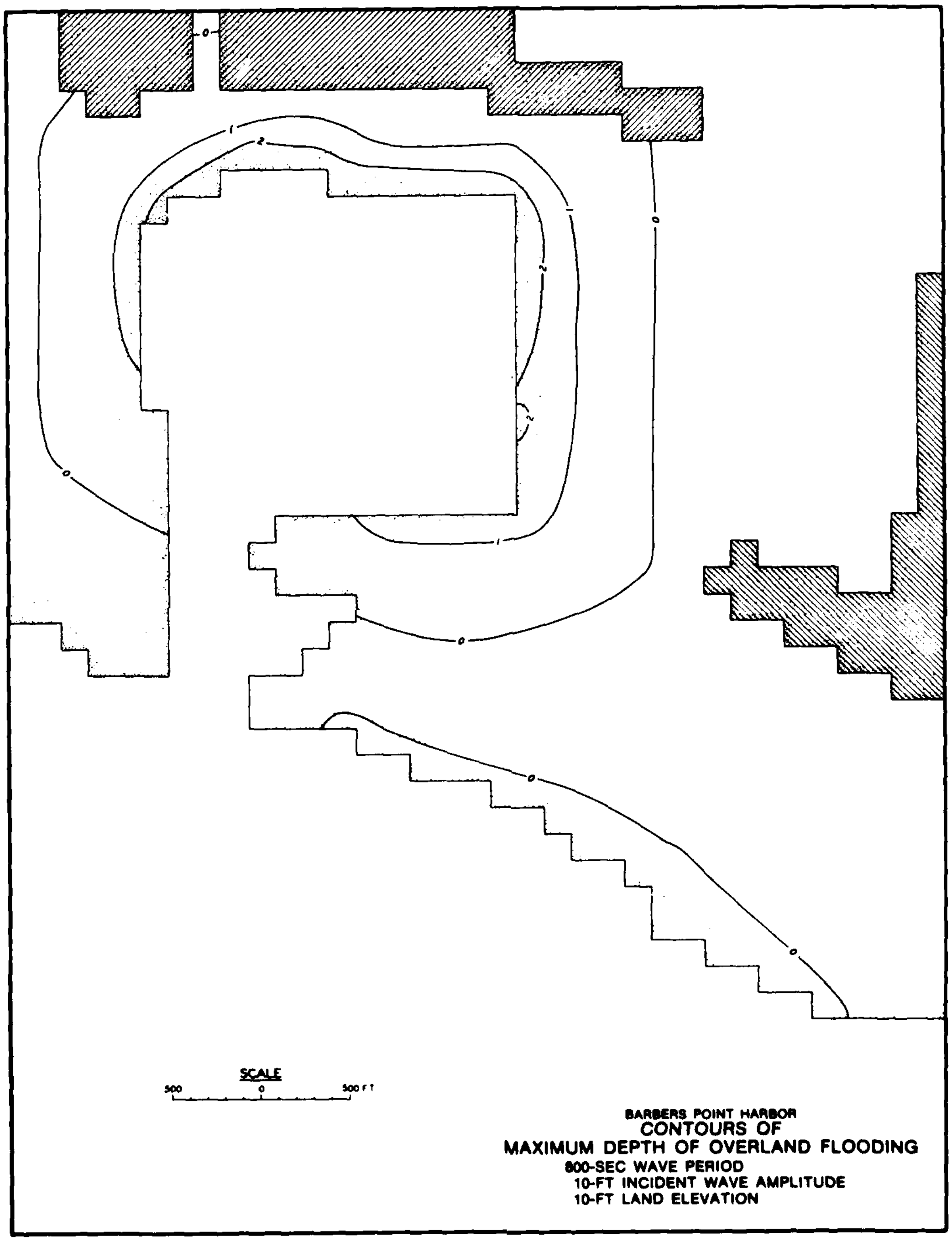
0
1
2
SCALE
500
0
500 FT
BARBERS POINT HARBOR
CONTOURS OF
MAXIMUM DEPTH OF OVERLAND FLOODING
800-SEC WAVE PERIOD
10-FT INCIDENT WAVE AMPLITUDE
10-FT LAND ELEVATION

PLATE 17

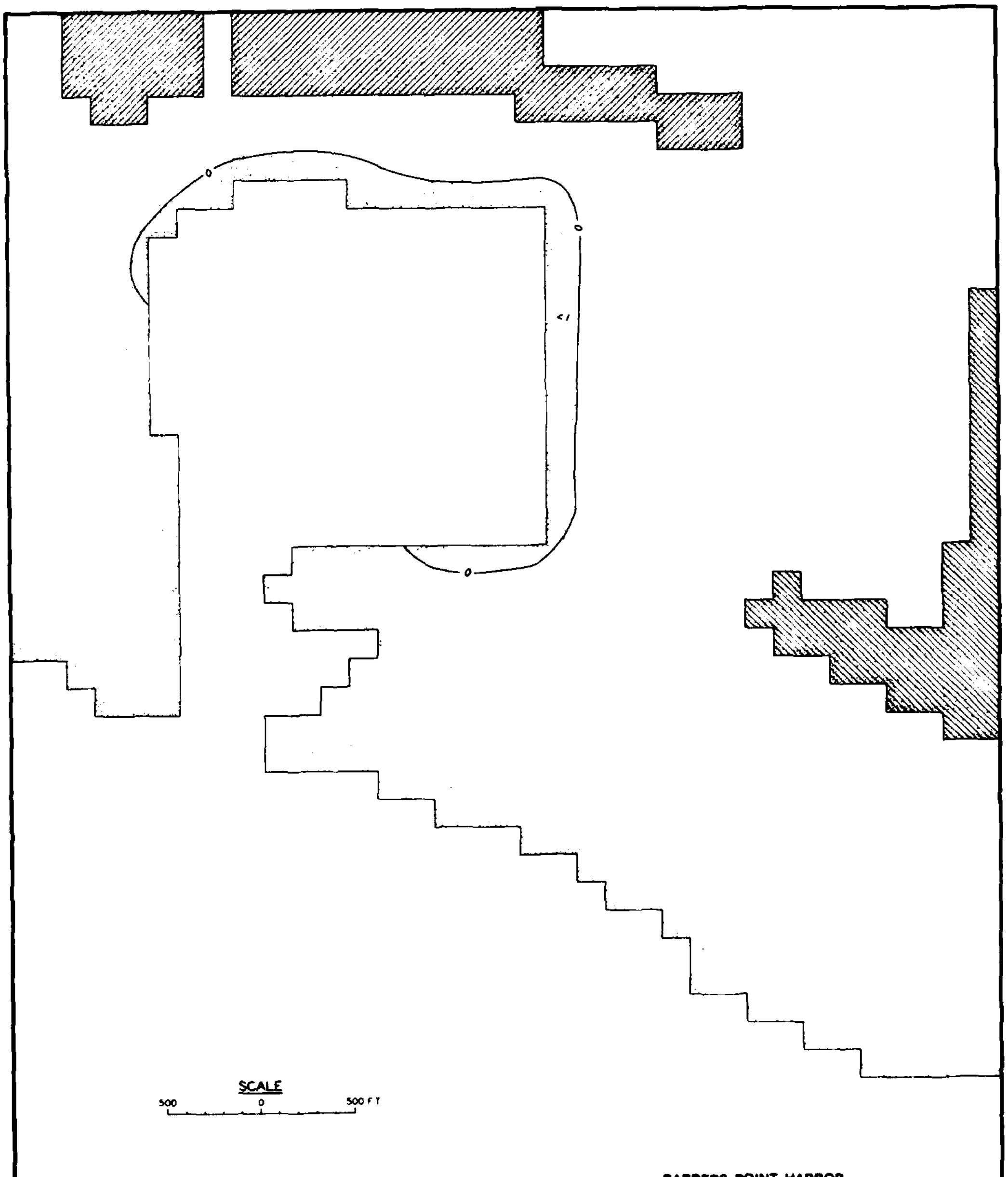

BARBERS POINT HARBOR
CONTOURS OF
MAXIMUM DEPTH OF OVERLAND FLOODING
800-SEC WAVE PERIOD
10-FT INCIDENT WAVE AMPLITUDE
12-FT LAND ELEVATION

PLATE 18

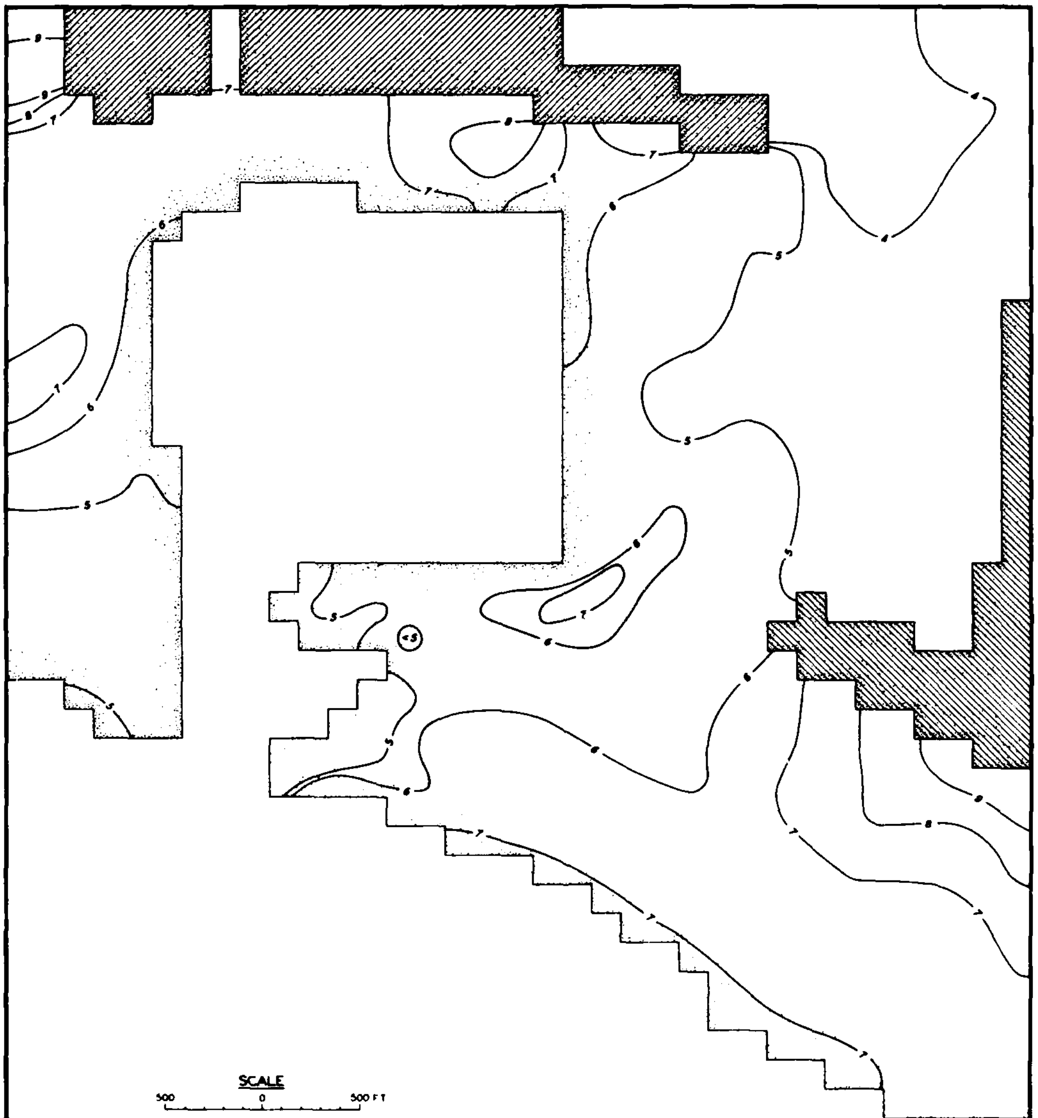

BARBERS POINT HARBOR
CONTOURS OF
MAXIMUM DEPTH OF OVERLAND FLOODING
800-SEC WAVE PERIOD
12-FT INCIDENT WAVE AMPLITUDE
4-FT LAND ELEVATION

PLATE 19

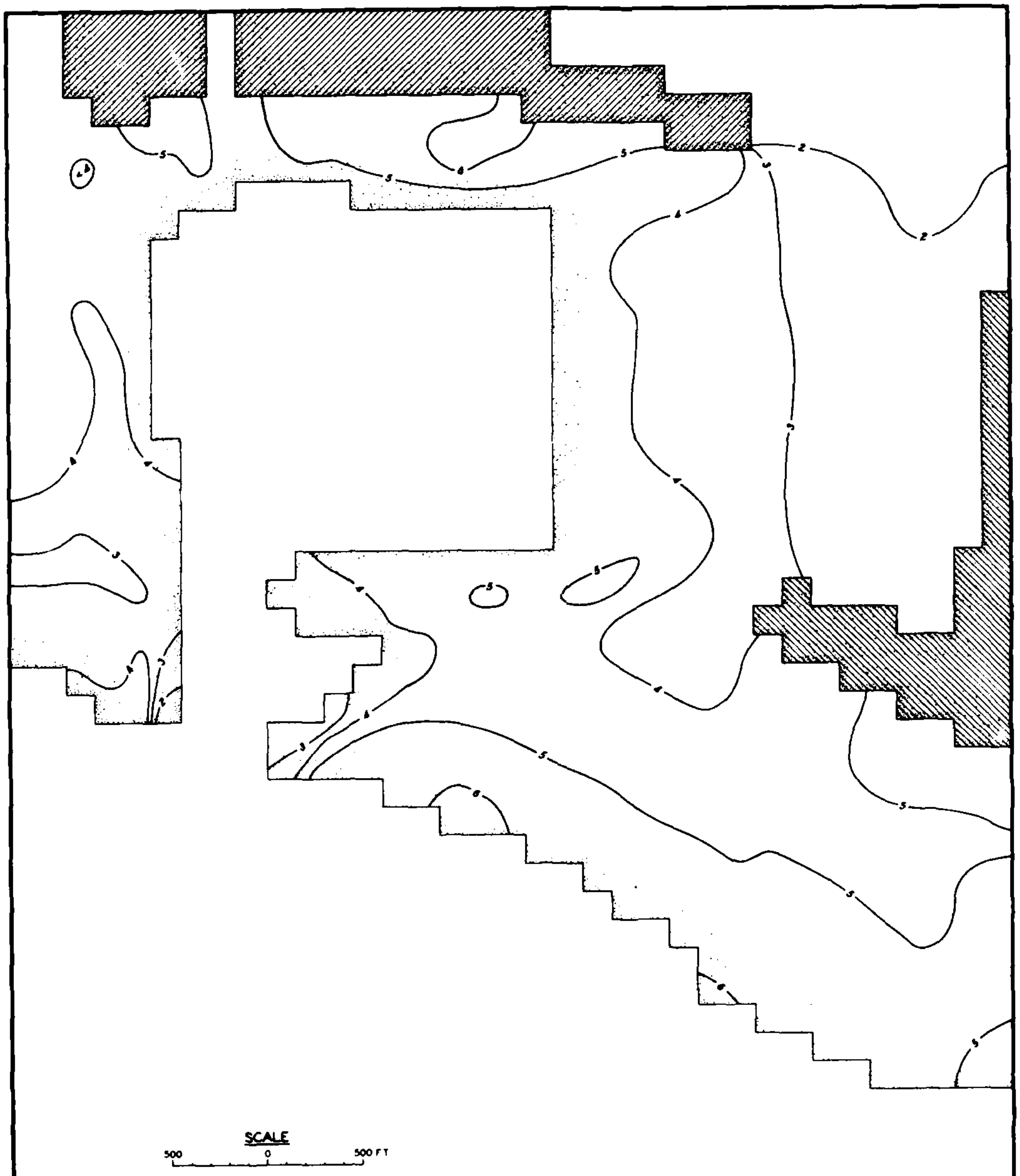

BARBERS POINT HARBOR
CONTOURS OF
MAXIMUM DEPTH OF OVERLAND FLOODING
800-SEC WAVE PERIOD
12-FT INCIDENT WAVE AMPLITUDE
6-FT LAND ELEVATION

PLATE 20

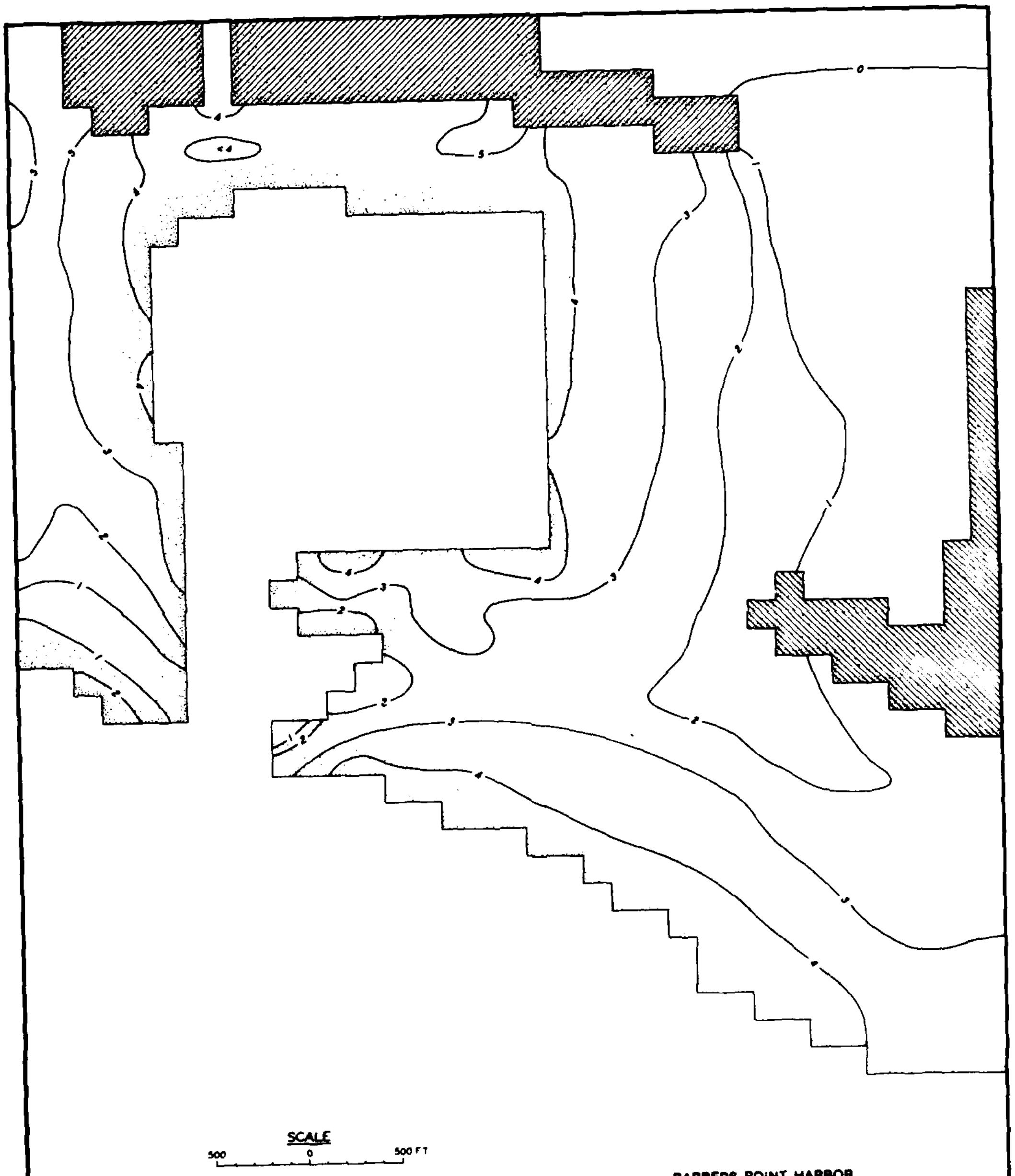

BARBERS POINT HARBOR
CONTOURS OF
MAXIMUM DEPTH OF OVERLAND FLOODING
800-SEC WAVE PERIOD
12-FT INCIDENT WAVE AMPLITUDE
8-FT LAND ELEVATION

PLATE 21

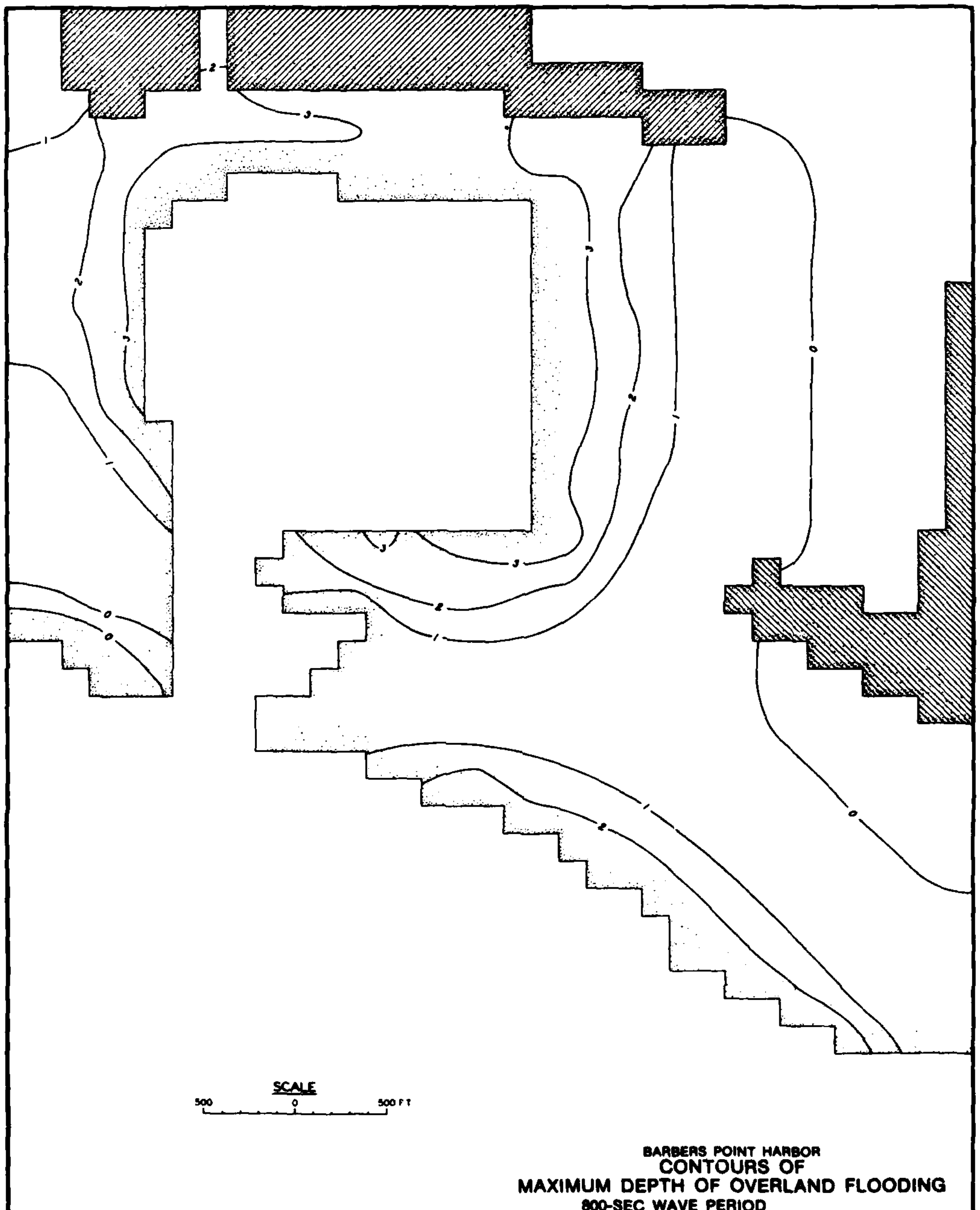

BARBERS POINT HARBOR
CONTOURS OF
MAXIMUM DEPTH OF OVERLAND FLOODING
800-SEC WAVE PERIOD
12-FT INCIDENT WAVE AMPLITUDE
10-FT LAND ELEVATION

PLATE 22

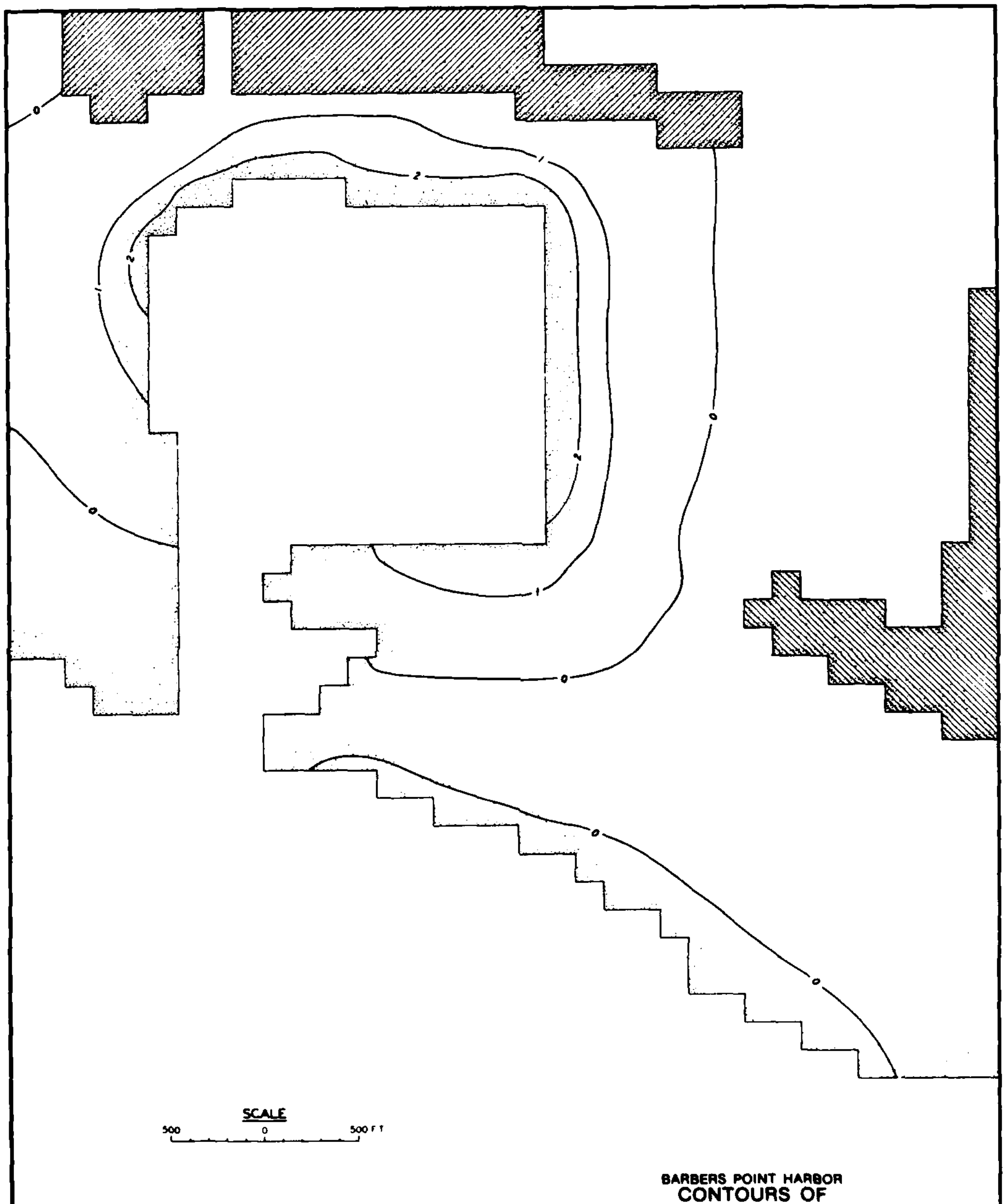

BARBERS POINT HARBOR
CONTOURS OF
MAXIMUM DEPTH OF OVERLAND FLOODING
800-SEC WAVE PERIOD
12-FT INCIDENT WAVE AMPLITUDE
12-FT LAND ELEVATION

PLATE 23

BARBERS POINT HARBOR

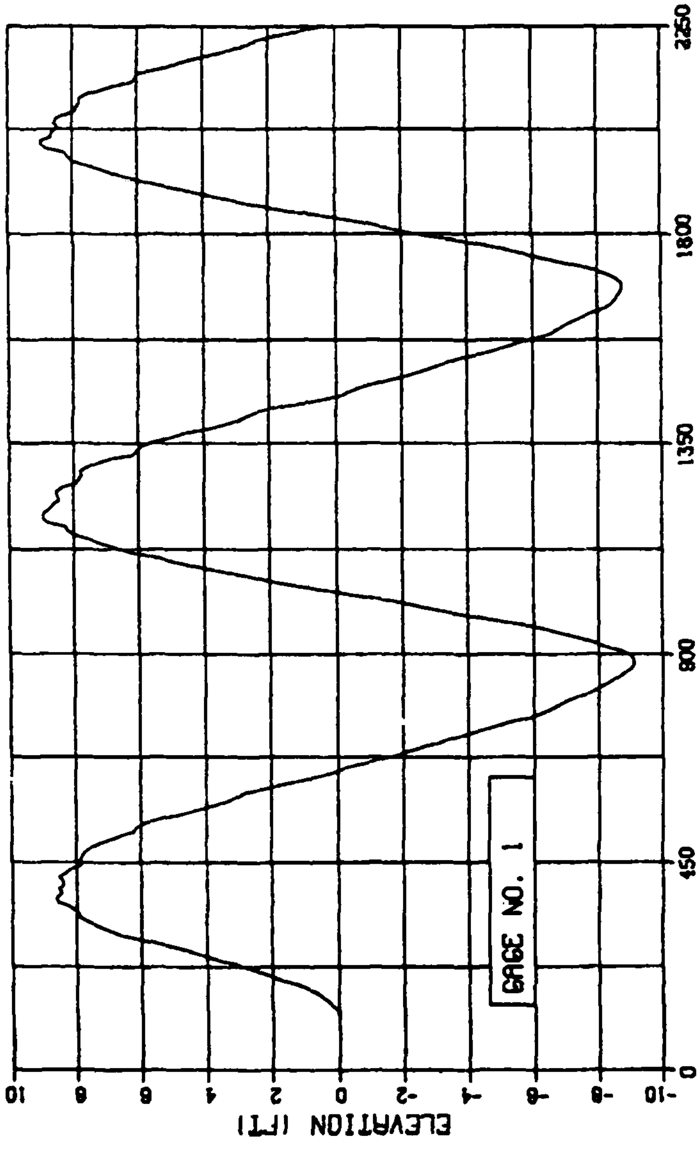

8 FT AMPLITUDE   800 SEC PERIOD   FLOODING

LAND ELEVATIONS: IV, V, DOCK AREA - 6 FT; I, II, III - 40 FT

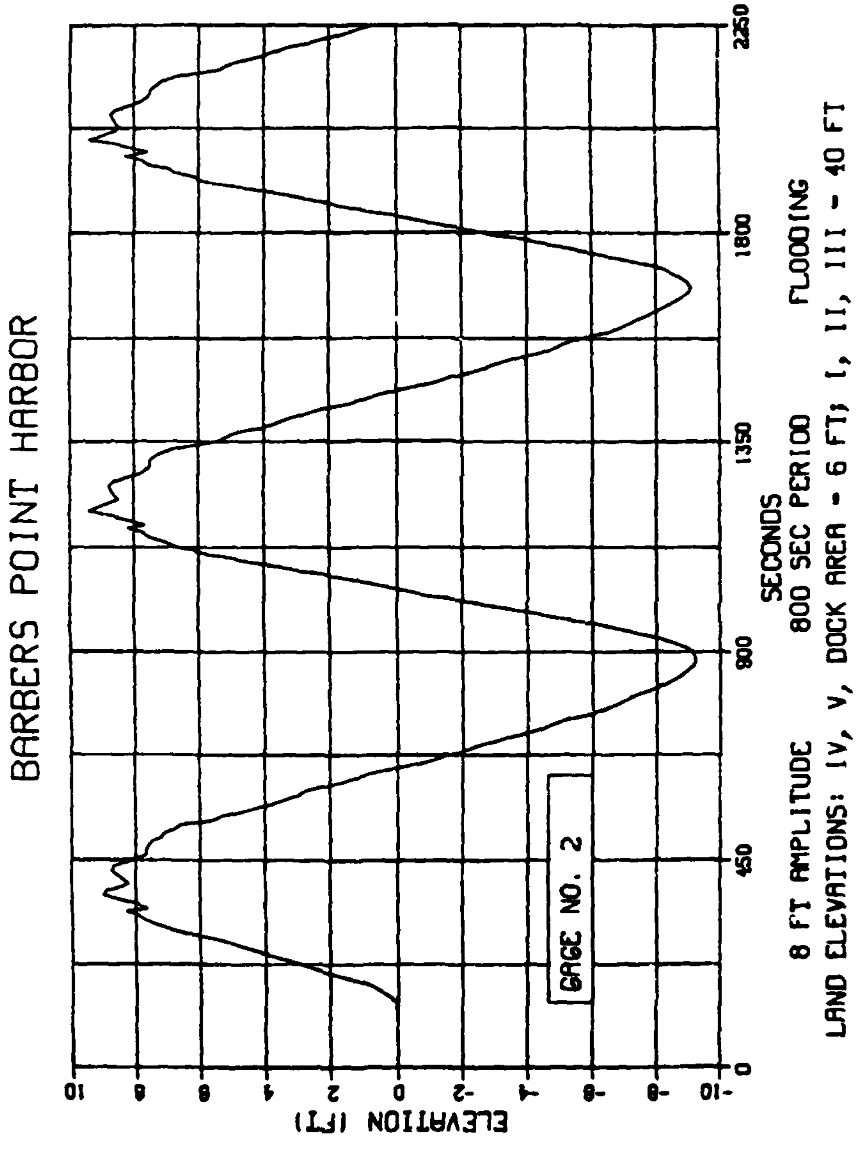

BARBERS POINT HARBOR
GAGE NO. 2
ELEVATION (FT)
10
8
6
4
2
0
-2
-4
-6
-8
-10
0
450
900
1350
1800
2250
SECONDS
8 FT AMPLITUDE
800 SEC PERIOD
FLOODING
LAND ELEVATIONS: IV, V, DOCK AREA - 6 FT; I, II, III - 40 FT

BARBERS POINT HARBOR

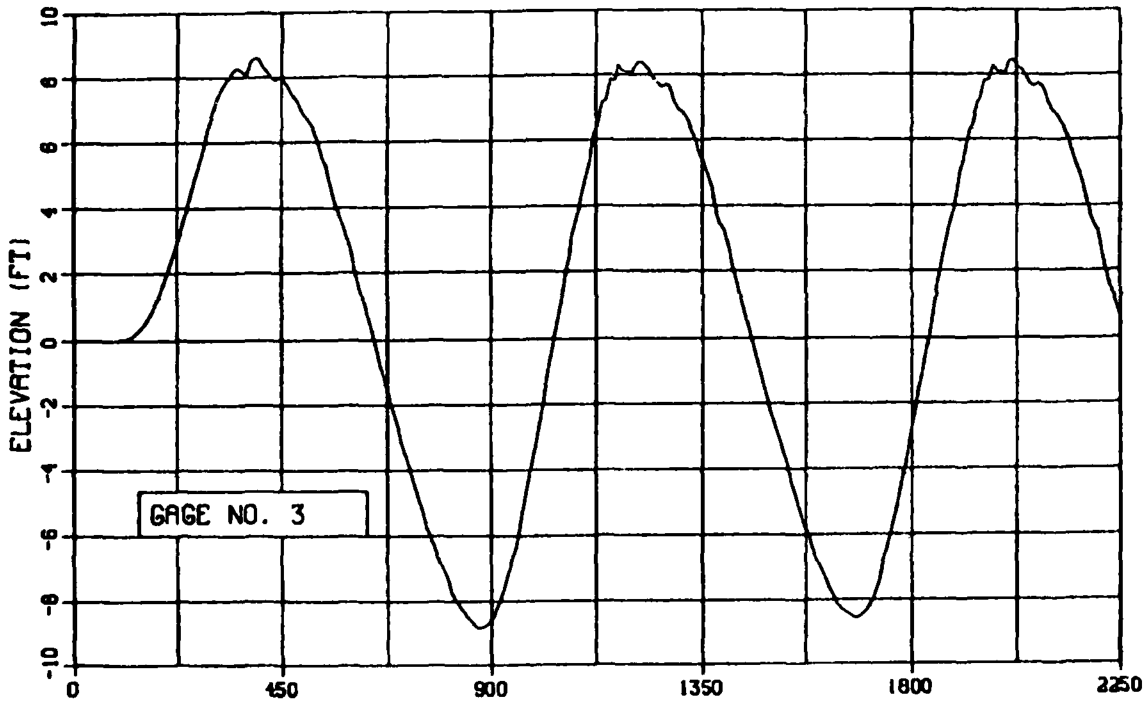

8 FT AMPLITUDE 800 SEC PERIOD FLOODING

LAND ELEVATIONS: IV, V, DOCK AREA - 6 FT; I, II, III - 40 FT

BARBERS POINT HARBOR

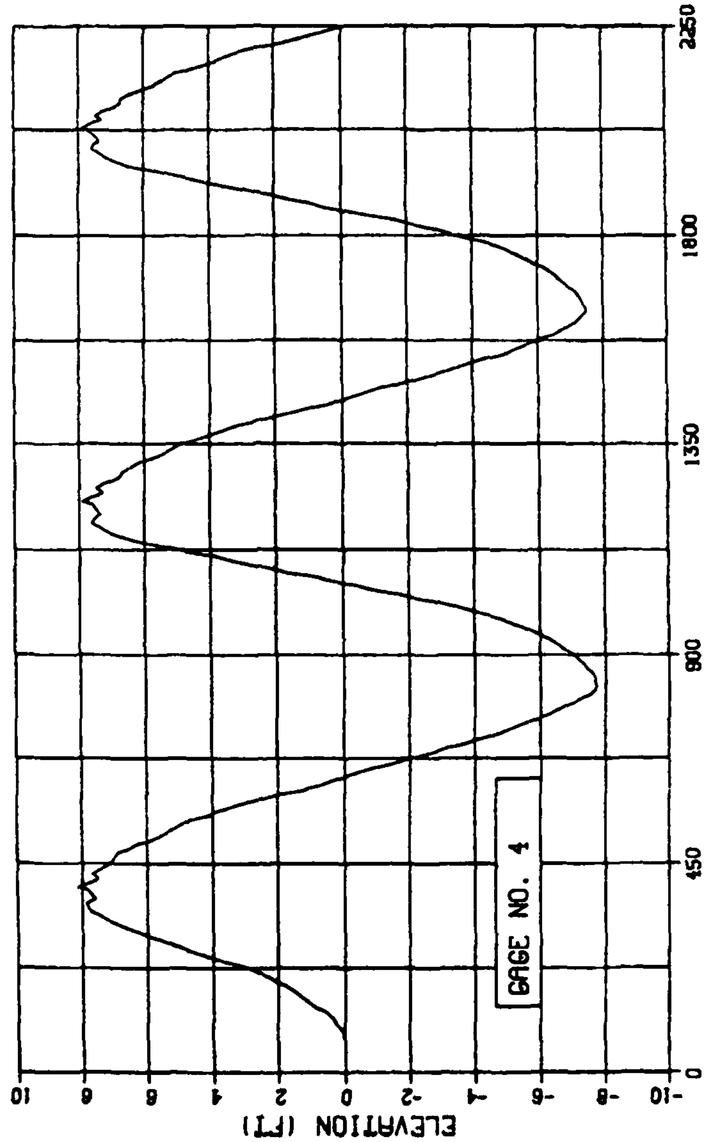

8 FT AMPLITUDE 800 SEC PERIOD FLOODING
LAND ELEVATIONS: IV, V, DOCK AREA - 6 FT; I, II, III - 40 FT

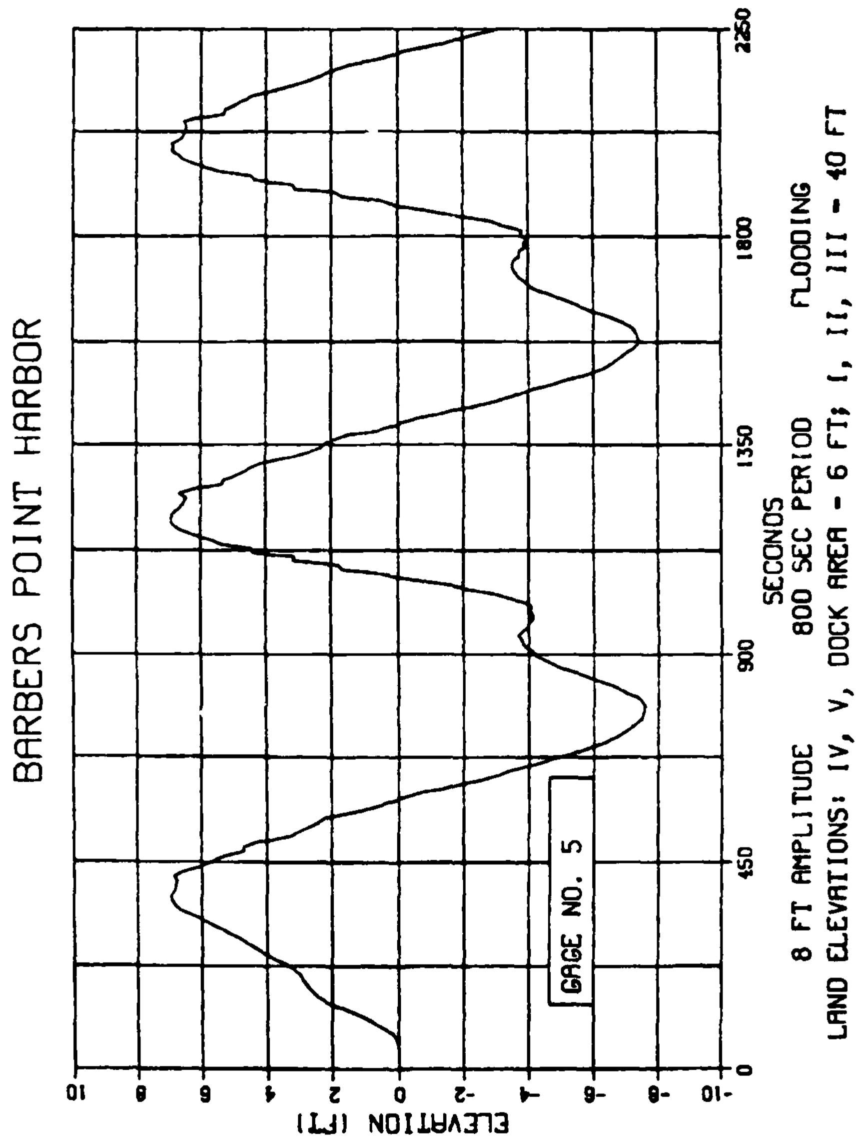

BARBERS POINT HARBOR
GAGE NO. 5
ELEVATION (FT)
10
8
6
4
2
0
-2
-4
-6
-8
-10
0
450
900
1350
1800
2250
SECONDS
8 FT AMPLITUDE 800 SEC PERIOD FLOODING
LAND ELEVATIONS: IV, V, DOCK AREA - 6 FT; I, II, III - 40 FT

PLATE 28

BARBERS POINT HARBOR

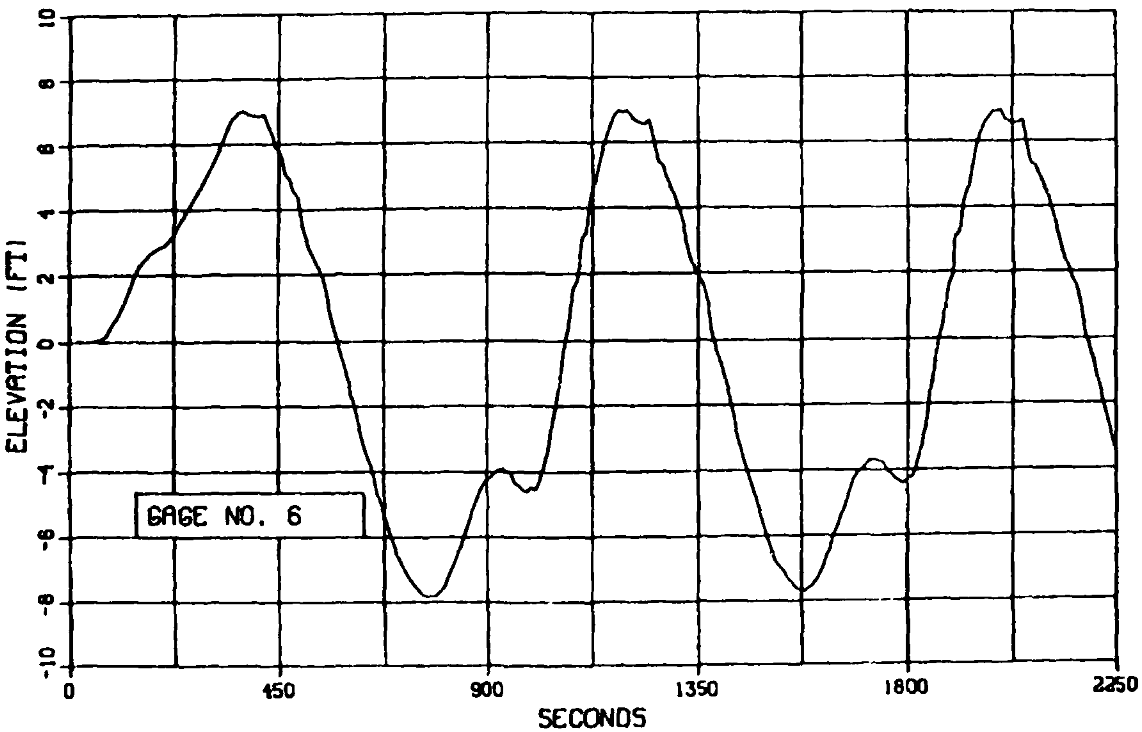

8 FT AMPLITUDE 800 SEC PERIOD FLOODING

LAND ELEVATIONS: IV, V, DOCK AREA - 6 FT; I, II, III - 40 FT

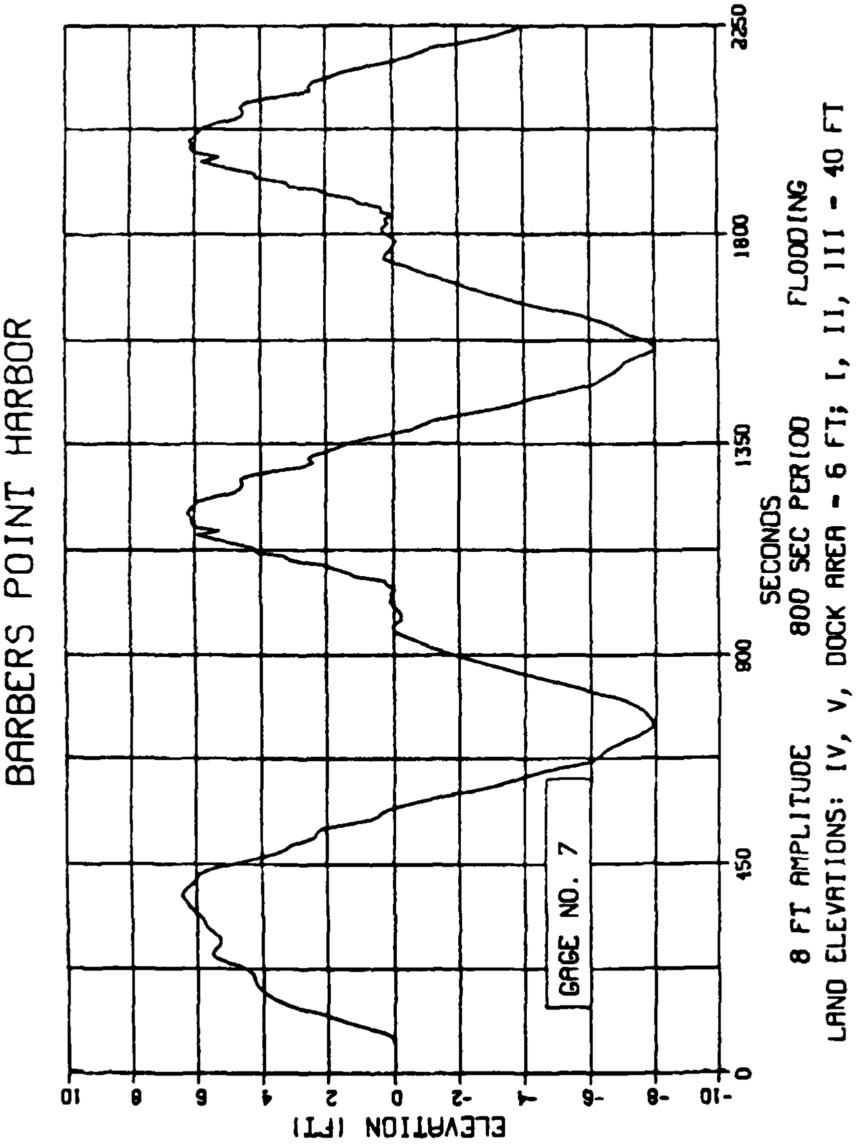

BARBERS POINT HARBOR
GAGE NO. 7
ELEVATION (FT)
10 8 6 4 2 0 -2 -4 -6 -8 -10
0 450 900 1350 1800 2250
SECONDS
8 FT AMPLITUDE
800 SEC PERIOD
FLOODING
LAND ELEVATIONS: IV, V, DOCK AREA - 6 FT; I, II, III - 40 FT

PLATE 30

BARBERS POINT HARBOR

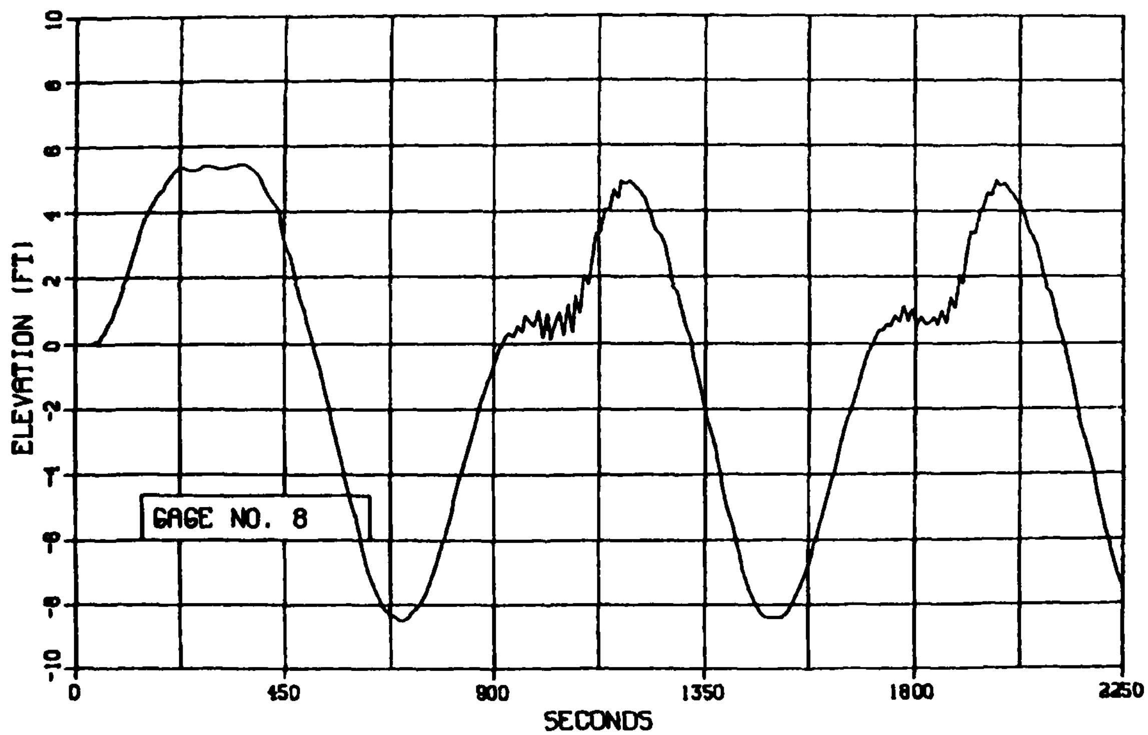

8 FT AMPLITUDE 800 SEC PERIOD FLOODING

LAND ELEVATIONS: IV, V, DOCK AREA - 6 FT; I, II, III - 40 FT

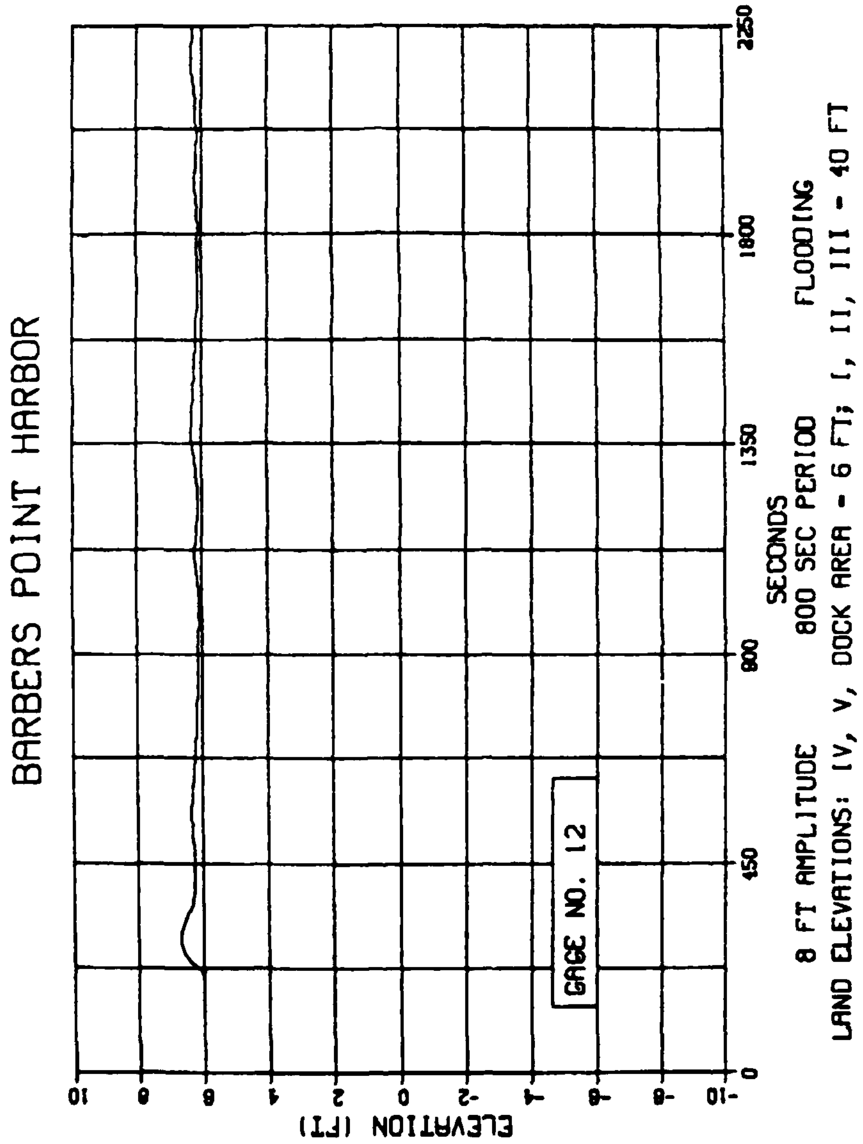
BARBERS POINT HARBOR
GAGE NO. 12
ELEVATION (FT)
10
8
6
4
2
0
-2
-4
-6
-8
-10
0
450
900
1350
1800
2250
SECONDS
8 FT AMPLITUDE
800 SEC PERIOD
FLOODING
LAND ELEVATIONS: IV, V, DOCK AREA - 6 FT; I, II, III - 40 FT

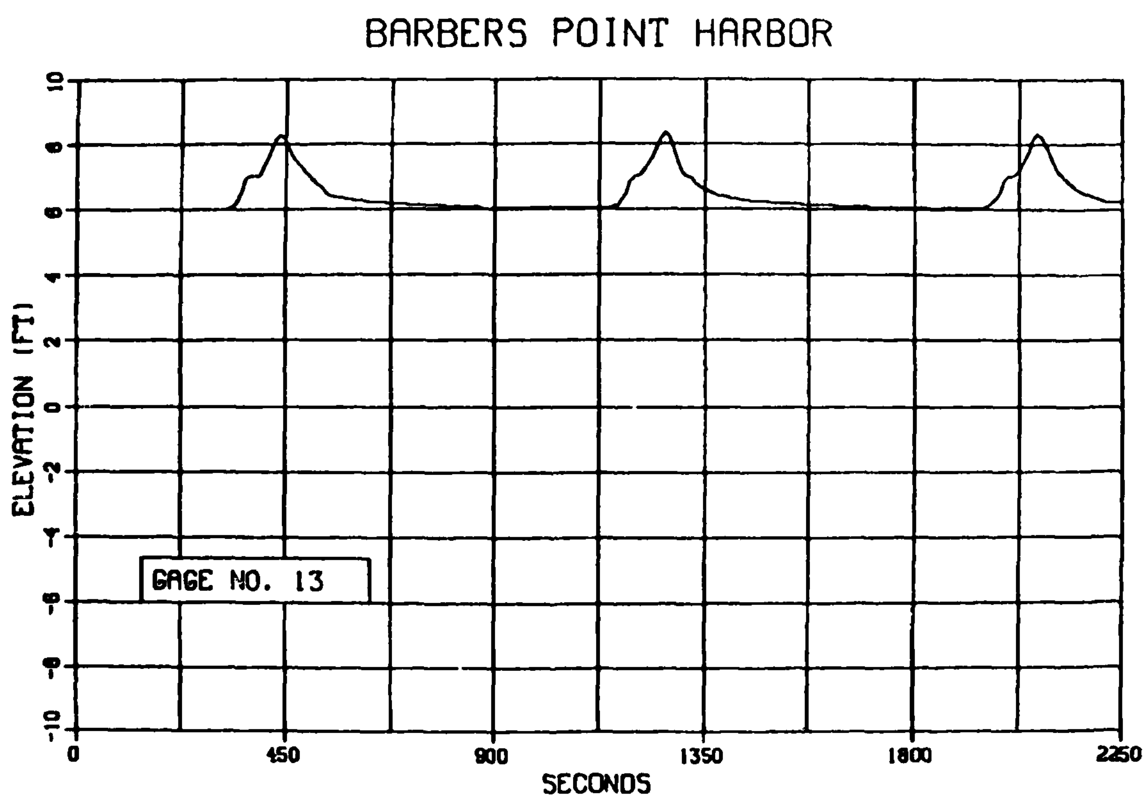

8 FT AMPLITUDE 800 SEC PERIOD FLOODING

LAND ELEVATIONS: IV, V, DOCK AREA - 6 FT; I, II, III - 40 FT

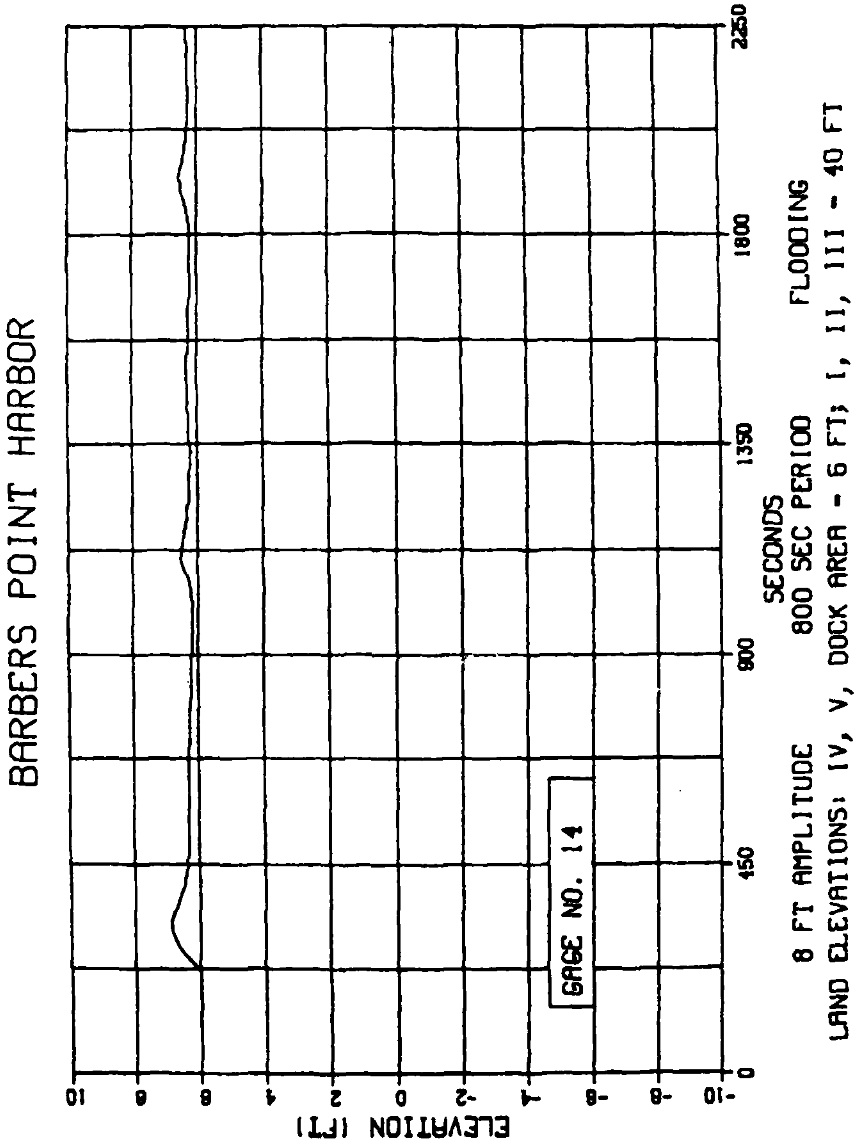
BARBERS POINT HARBOR
GAGE NO. 14
ELEVATION (FT)
10
8
6
4
2
0
-2
-4
-6
-8
-10
0
450
900
1350
1800
2250
SECONDS
8 FT AMPLITUDE 800 SEC PERIOD FLOODING
LAND ELEVATIONS: IV, V, DOCK AREA - 6 FT; I, II, III - 40 FT

PLATE 34

BARBERS POINT HARBOR

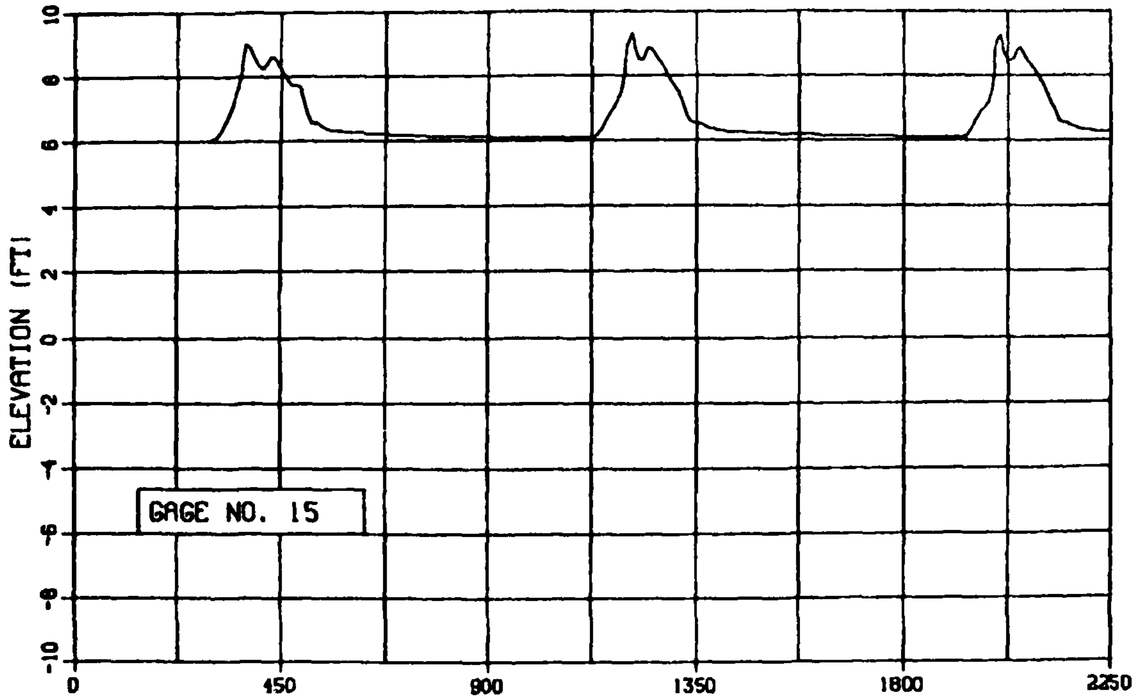

SECONDS

8 FT AMPLITUDE   800 SEC PERIOD   FLOODING

LAND ELEVATIONS: IV, V, DOCK AREA - 6 FT; I, II, III - 40 FT

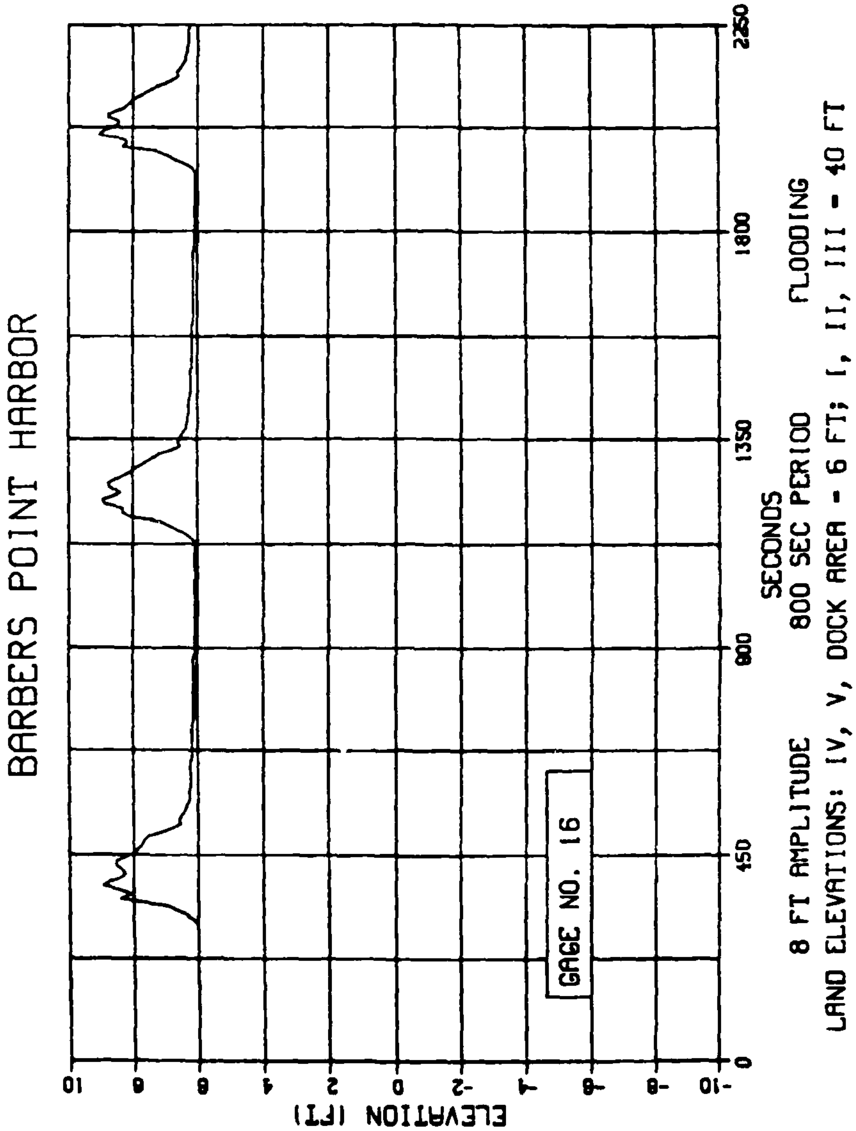
BARBERS POINT HARBOR
GAGE NO. 16
ELEVATION (FT)
10
8
6
4
2
0
-2
-4
-6
-8
-10
0
450
900
1350
1800
2250
SECONDS
8 FT AMPLITUDE
800 SEC PERIOD
FLOODING
LAND ELEVATIONS: IV, V, DOCK AREA - 6 FT; I, II, III - 40 FT

PLATE 36

BARBERS POINT HARBOR

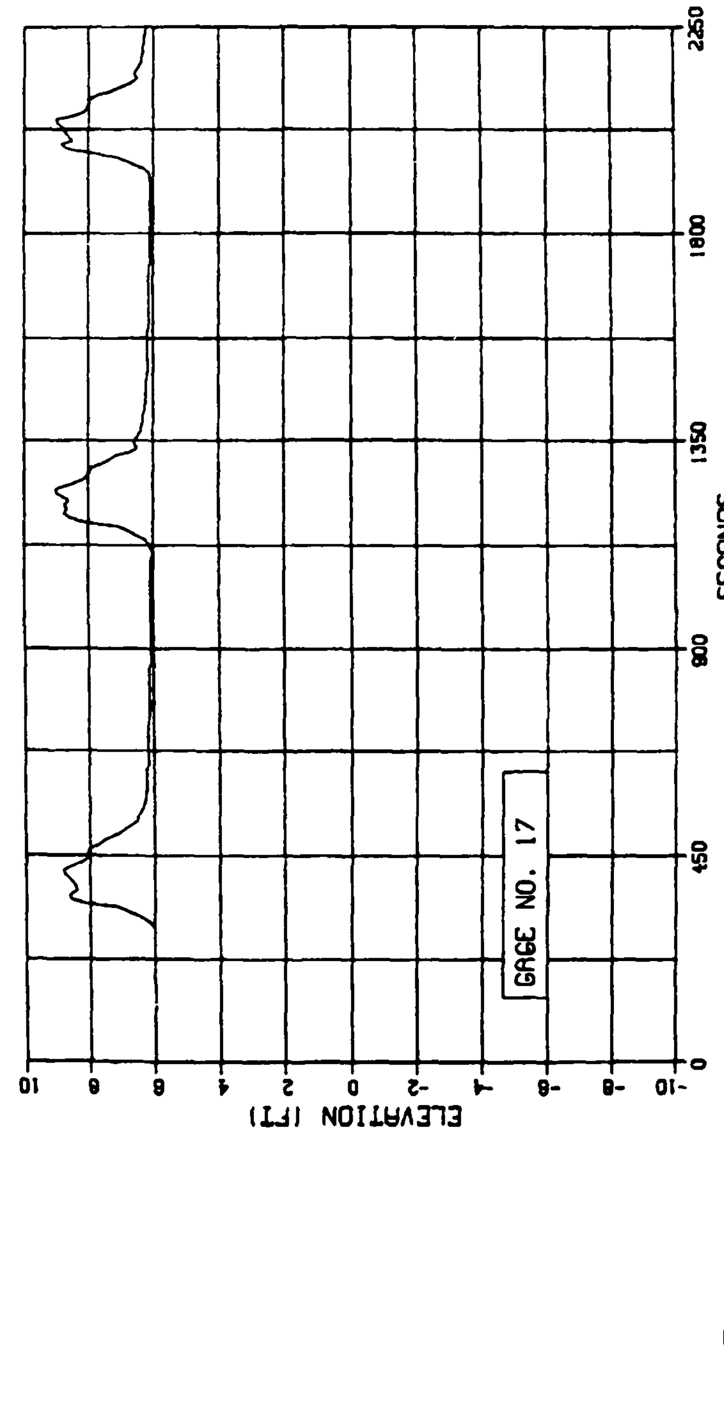

8 FT AMPLITUDE 800 SEC PERIOD FLOODING
LAND ELEVATIONS: IV, V, DOCK AREA - 6 FT; I, II, III - 40 FT

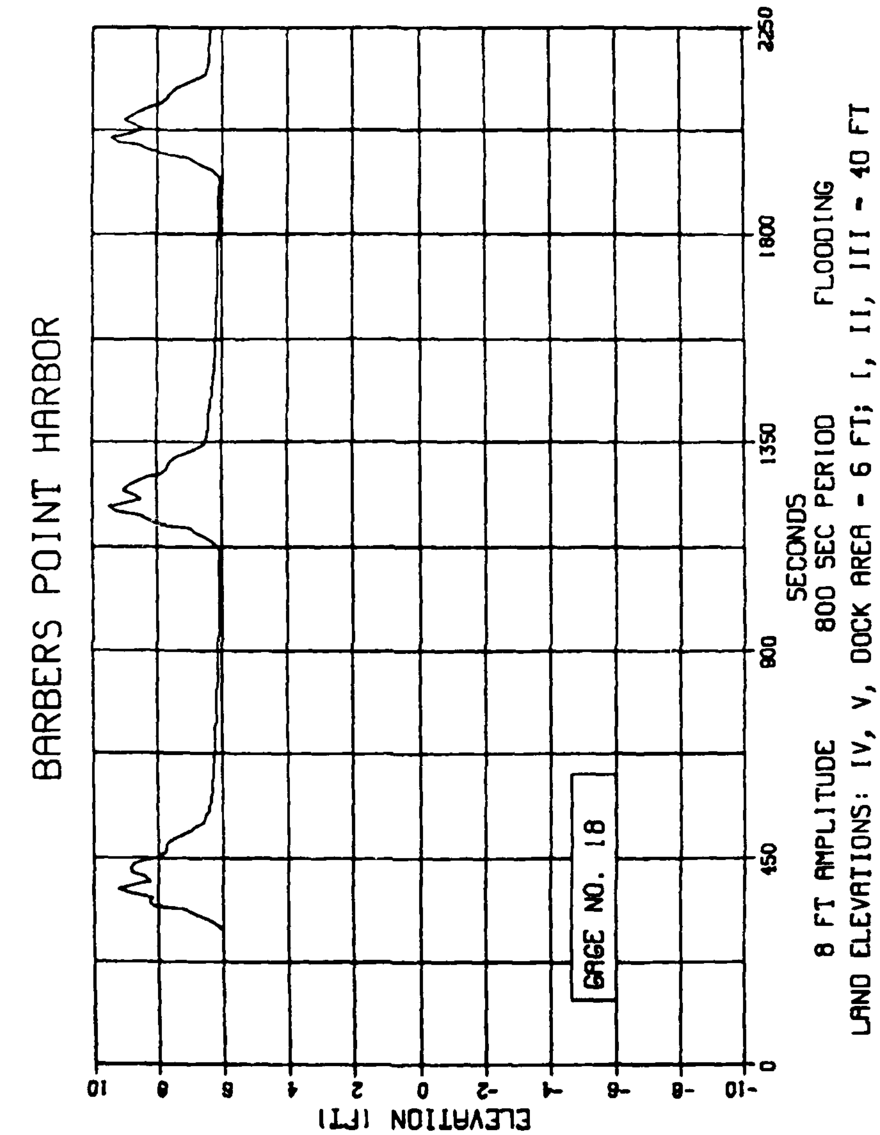
BARBERS POINT HARBOR
GAGE NO. 18
10
8
6
4
2
0
-2
-4
-6
-8
-10
ELEVATION (FT)
0
450
900
1350
1800
2250
SECONDS
8 FT AMPLITUDE
800 SEC PERIOD
FLOODING
LAND ELEVATIONS: IV, V, DOCK AREA - 6 FT; I, II, III - 40 FT

BARBERS POINT HARBOR

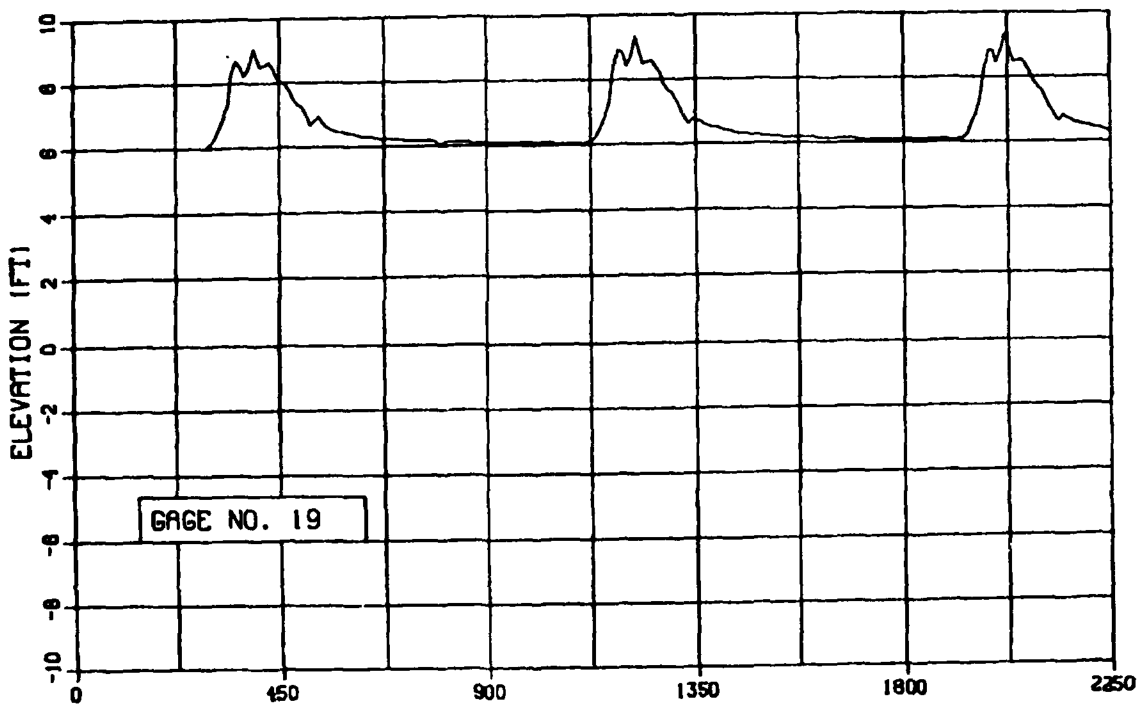

8 FT AMPLITUDE 900 SEC PERIOD FLOODING

LAND ELEVATIONS: IV, V, DOCK AREA - 6 FT; I, II, III - 40 FT

PLATE 39

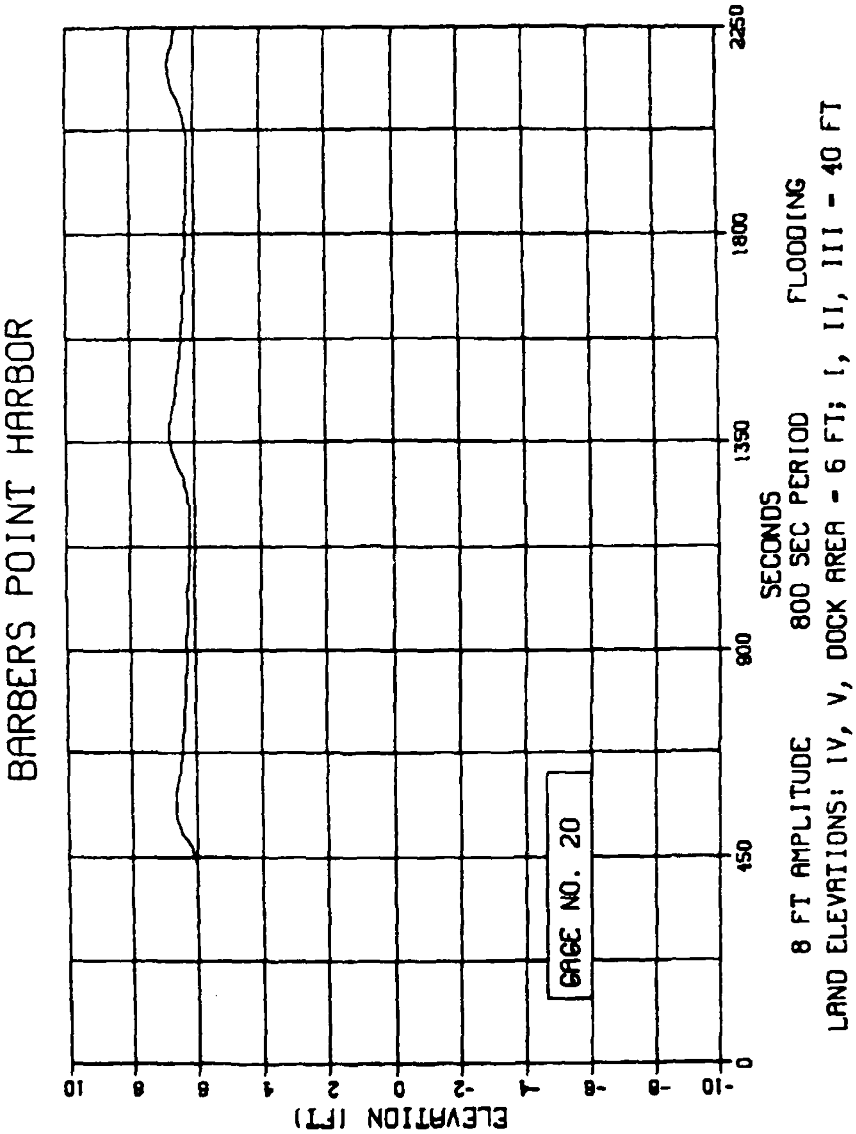
BARBERS POINT HARBOR
GAGE NO. 20
ELEVATION (FT)
10
8
6
4
2
0
-2
-4
-6
-8
-10
0
450
900
1350
1800
2250
SECONDS
8 FT AMPLITUDE 800 SEC PERIOD FLOODING
LAND ELEVATIONS: IV, V, DOCK AREA - 6 FT; I, II, III - 40 FT

PLATE 40

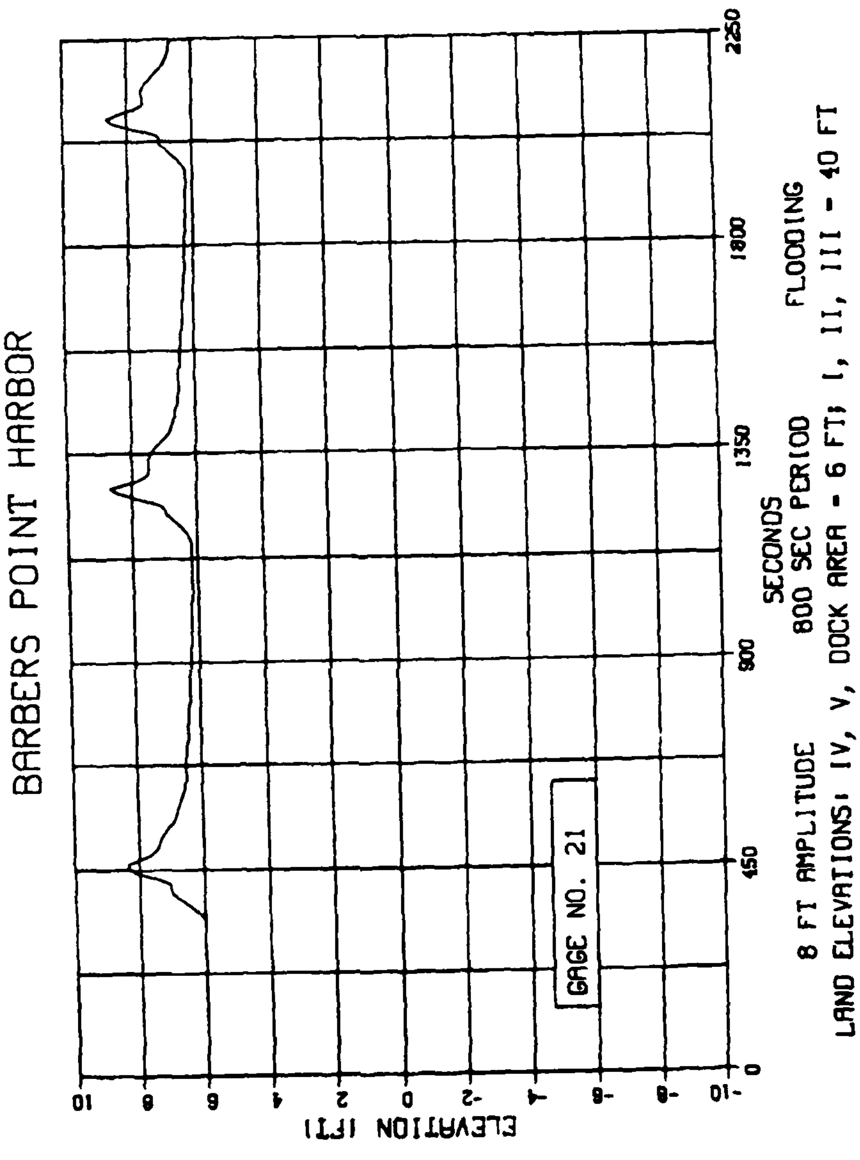
BARBERS POINT HARBOR
GAGE NO. 21
ELEVATION (FT)
10
8
6
4
2
0
-2
-4
-6
-8
-10
0
450
900
1350
1800
2250
SECONDS
8 FT AMPLITUDE
800 SEC PERIOD
FLOODING
LAND ELEVATIONS: IV, V, DOCK AREA - 6 FT; I, II, III - 40 FT

PLATE 41

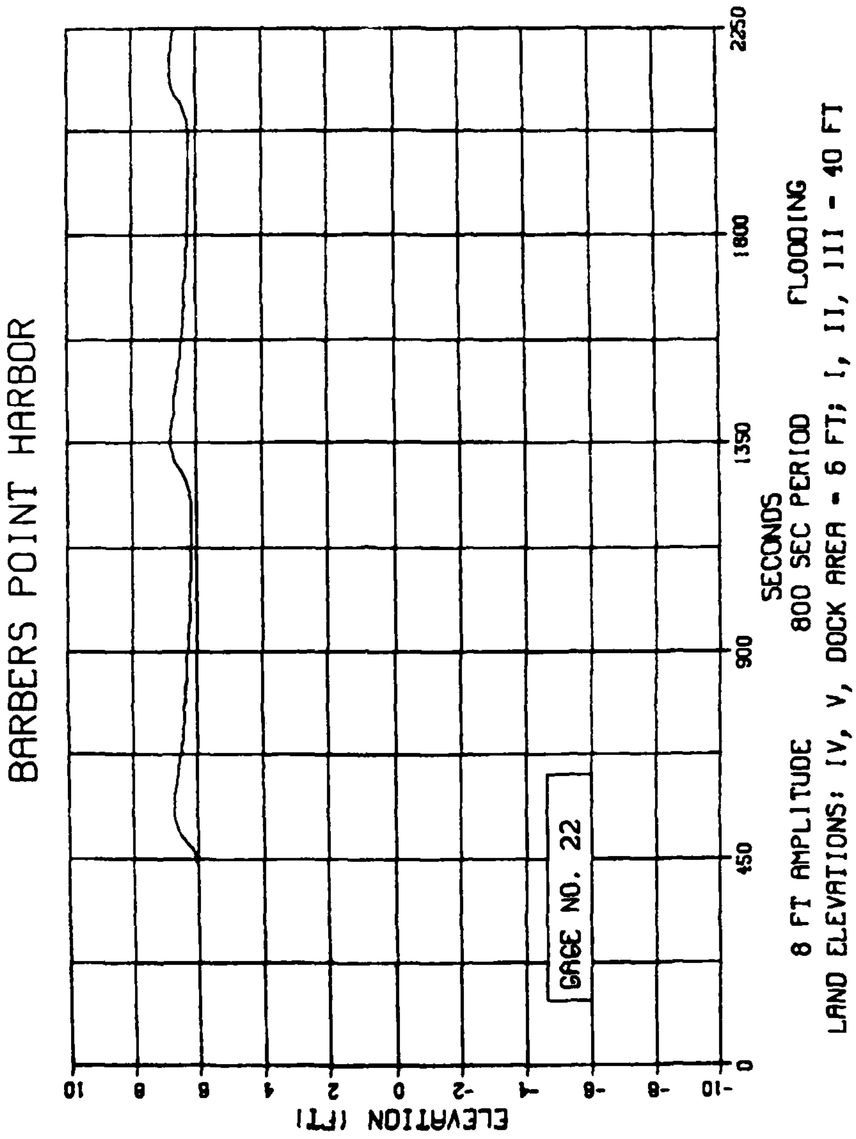
BARBERS POINT HARBOR
GAGE NO. 22
ELEVATION (FT)
10
8
6
4
2
0
-2
-4
-6
-8
-10
0
450
900
1350
1800
2250
SECONDS
8 FT AMPLITUDE
800 SEC PERIOD
FLOODING
LAND ELEVATIONS: IV, V, DOCK AREA - 6 FT; I, II, III - 40 FT

PLATE 42

BARBERS POINT HARBOR

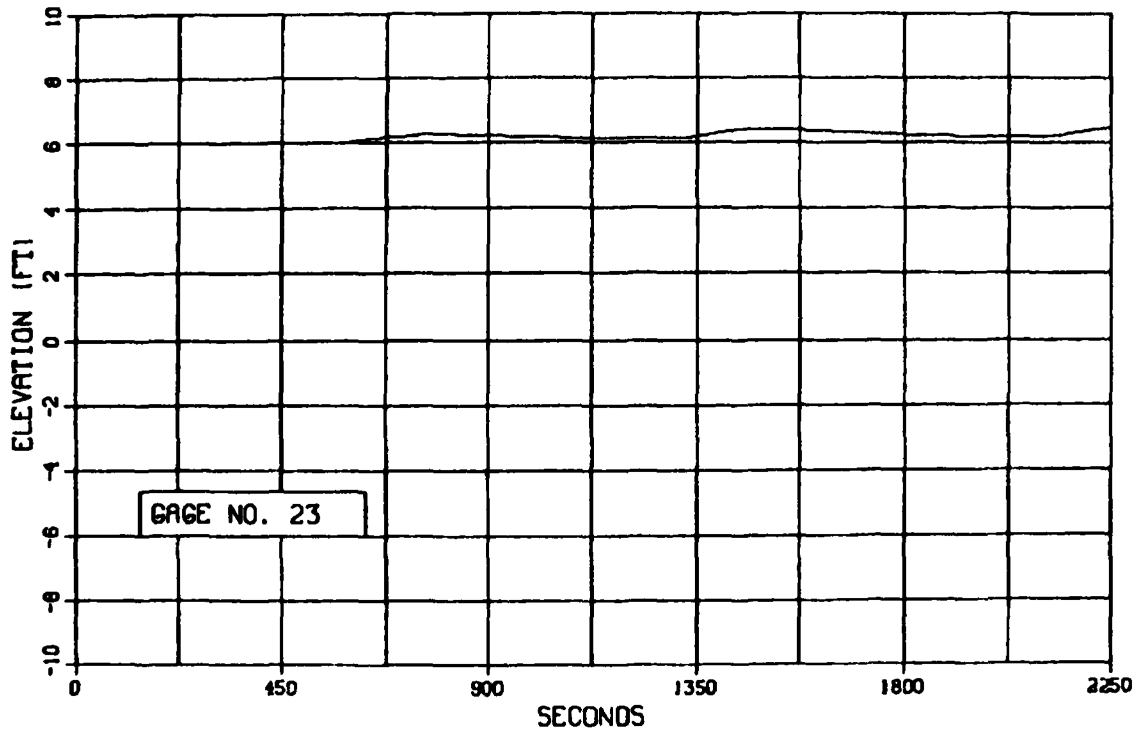

8 FT AMPLITUDE 800 SEC PERIOD FLOODING

LAND ELEVATIONS: IV, V, DOCK AREA - 6 FT; I, II, III - 40 FT

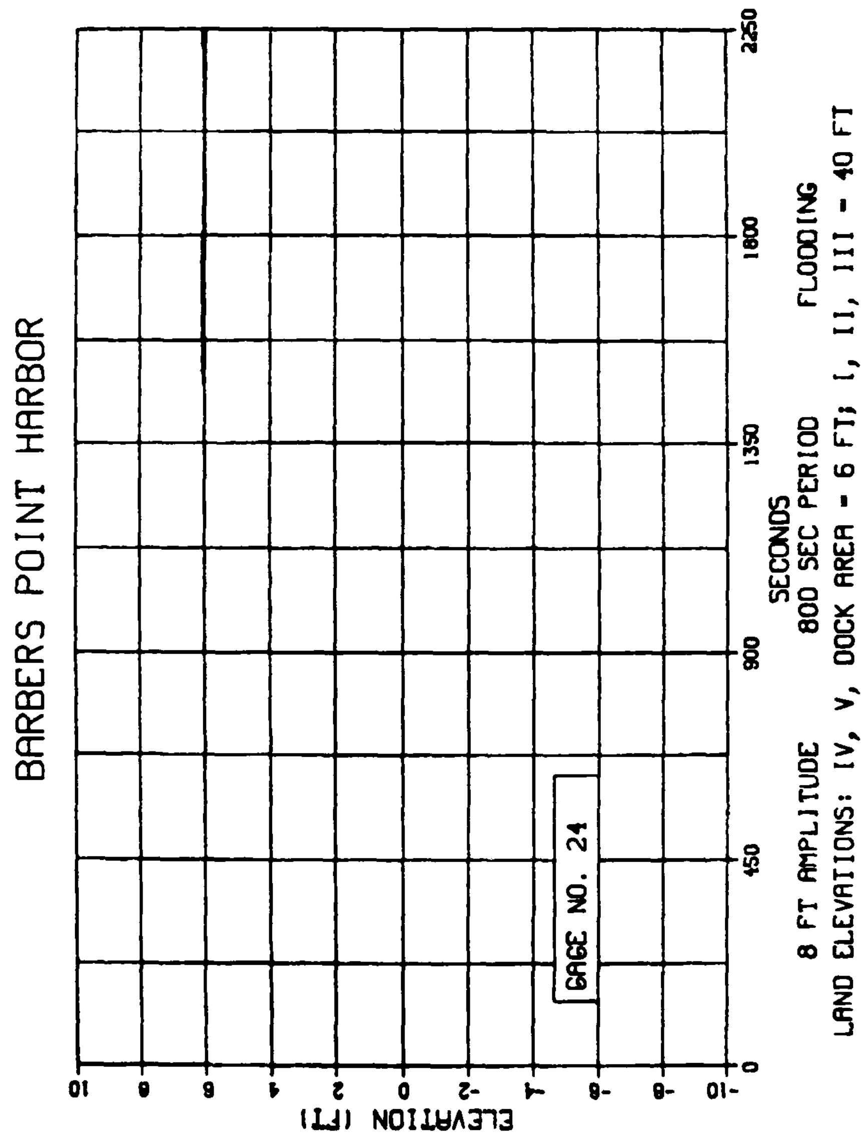
BARBERS POINT HARBOR
GAGE NO. 24
ELEVATION (FT)
10
8
6
4
2
0
-2
-4
-6
-8
-10
0
450
900
1350
1800
2250
SECONDS
8 FT AMPLITUDE
800 SEC PERIOD
FLOODING
LAND ELEVATIONS: IV, V, DOCK AREA - 6 FT; I, II, III - 40 FT

BARBERS POINT HARBOR

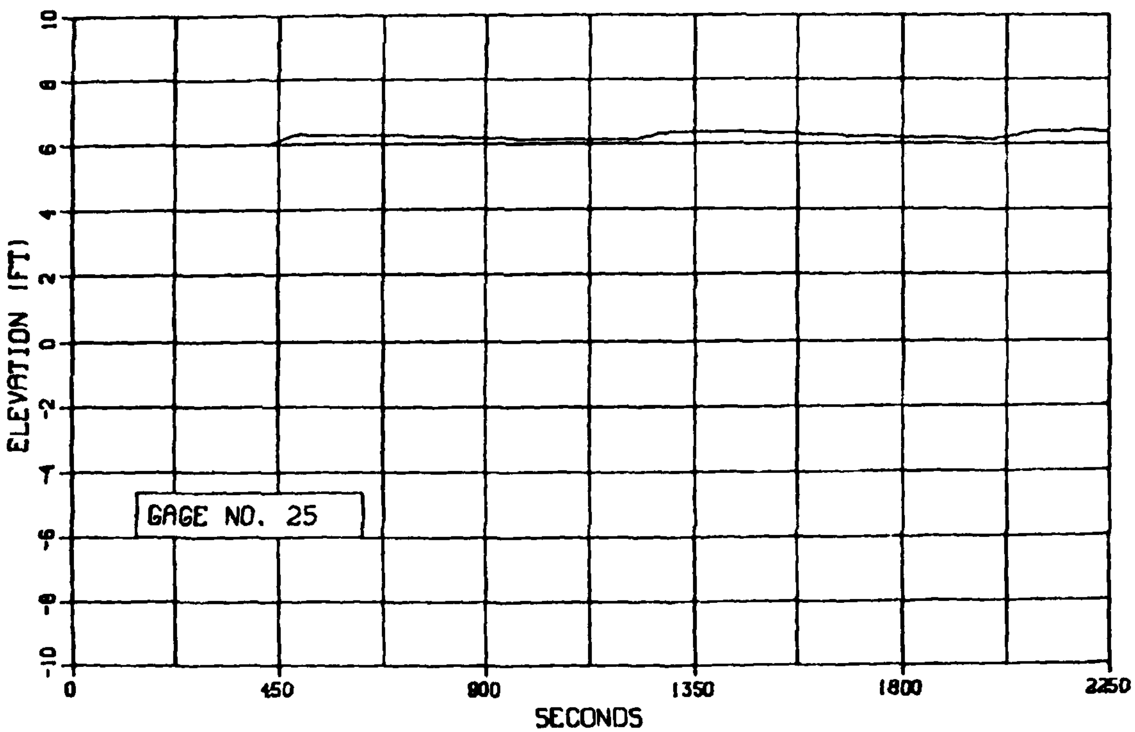

8 FT AMPLITUDE 800 SEC PERIOD FLOODING

LAND ELEVATIONS: IV, V, DOCK AREA - 6 FT; I, II, III - 40 FT

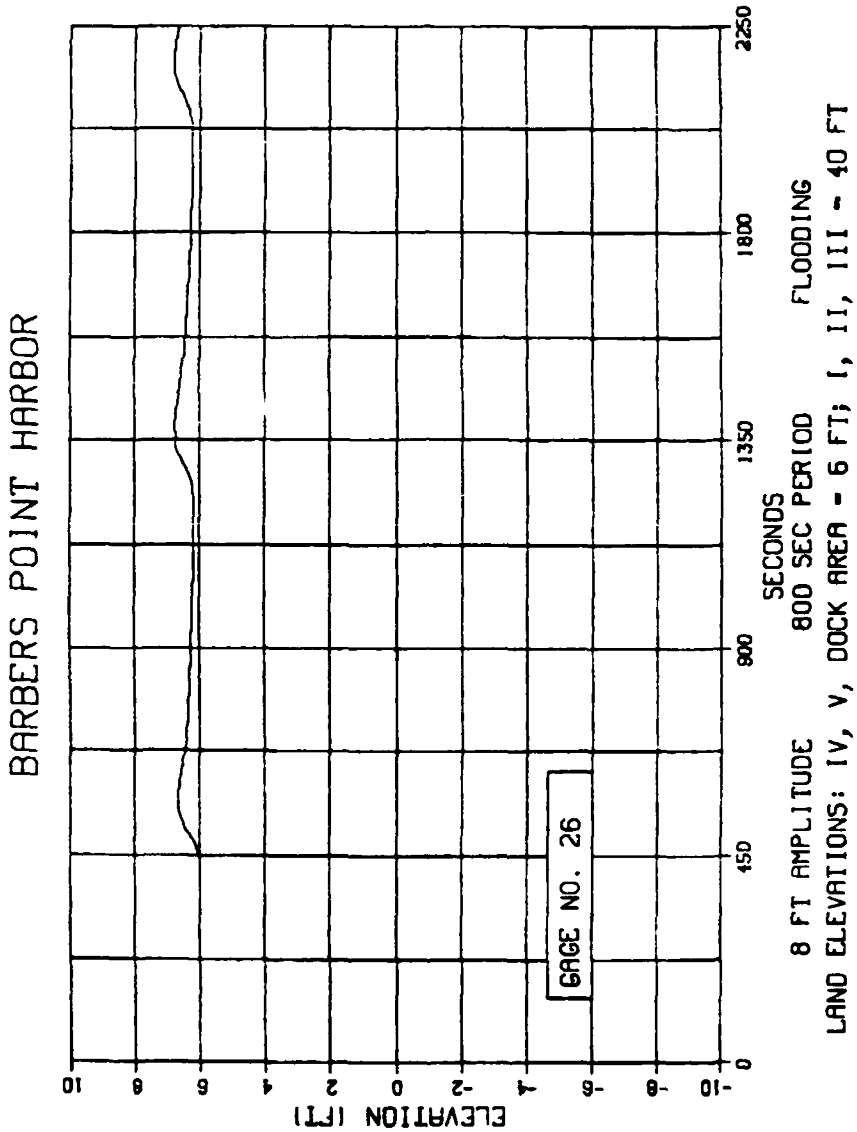
BARBERS POINT HARBOR
GAGE NO. 26
ELEVATION (FT)
10
8
6
4
2
0
-2
-4
-6
-8
-10
0
450
900
1350
1800
2250
SECONDS
8 FT AMPLITUDE
800 SEC PERIOD
FLOODING
LAND ELEVATIONS: IV, V, DOCK AREA - 6 FT; I, II, III - 40 FT

PLATE 46

BARBERS POINT HARBOR

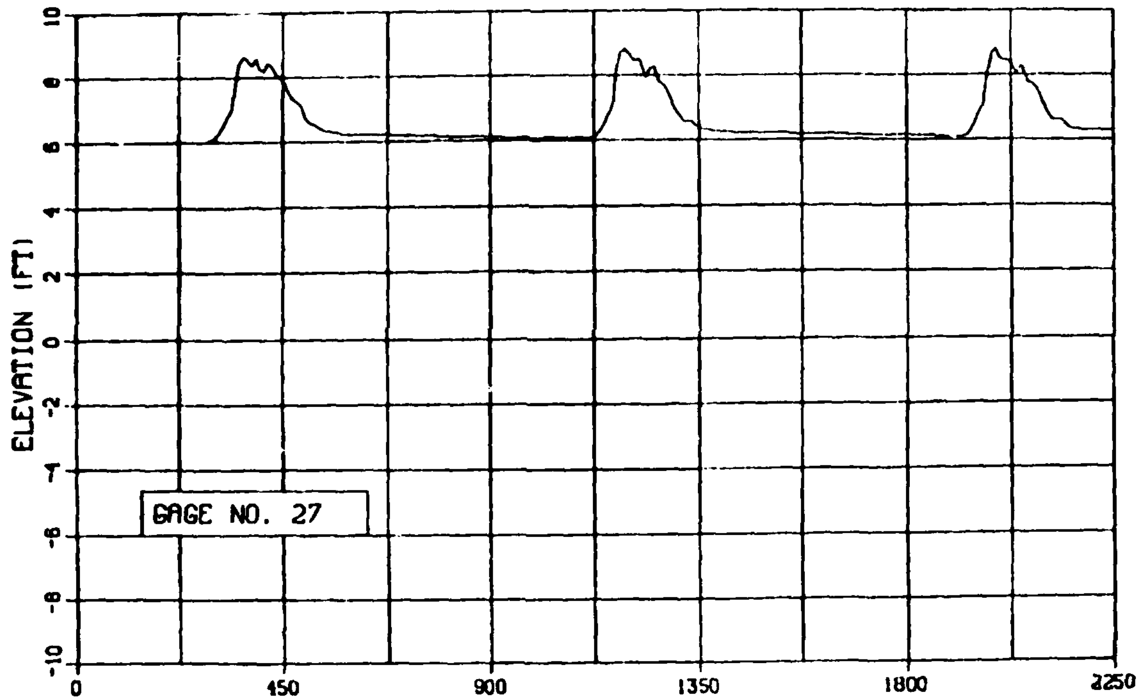

8 FT AMPLITUDE 800 SEC PERIOD FLOODING

LAND ELEVATIONS: IV, V, DOCK AREA - 6 FT; I, II, III - 40 FT

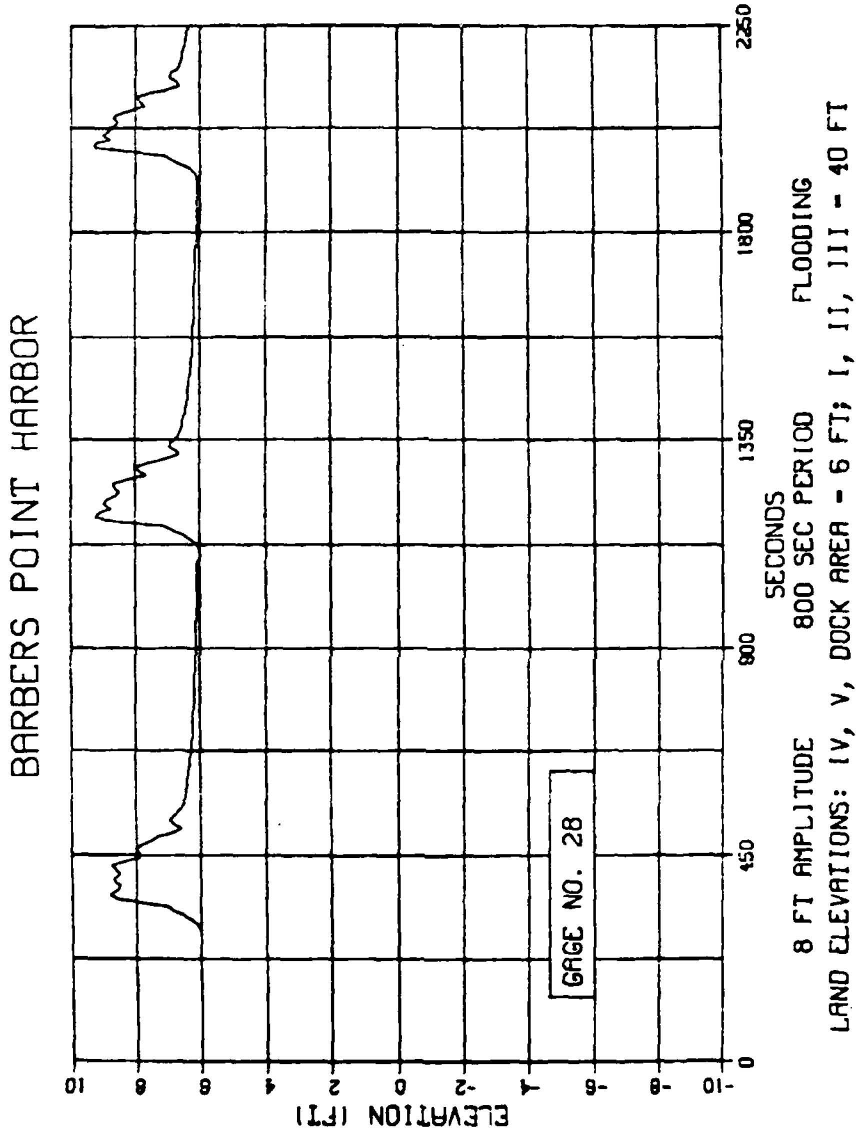
BARBERS POINT HARBOR
GAGE NO. 28
ELEVATION (FT)
10
8
6
4
2
0
-2
-4
-6
-8
-10
0
450
900
1350
1800
2250
SECONDS
8 FT AMPLITUDE
800 SEC PERIOD
FLOODING
LAND ELEVATIONS: IV, V, DOCK AREA - 6 FT; I, II, III - 40 FT

PLATE 48

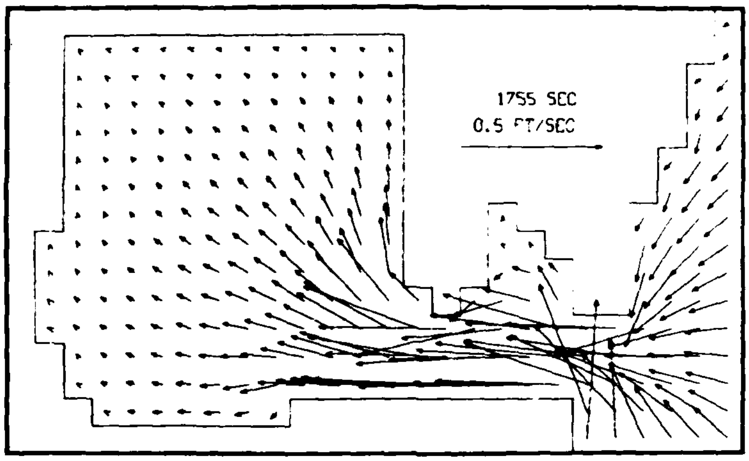

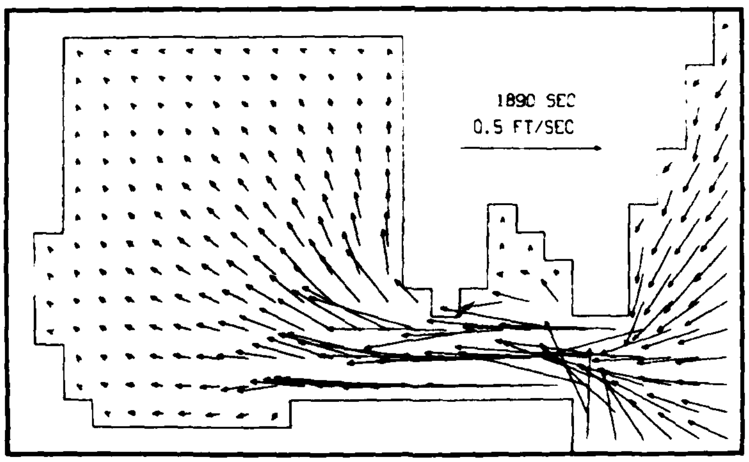

BARBERS POINT HARBOR

WATER VELOCITY

800-SEC PERIOD 0.1-FT. AMPLITUDE
NO FLOODING

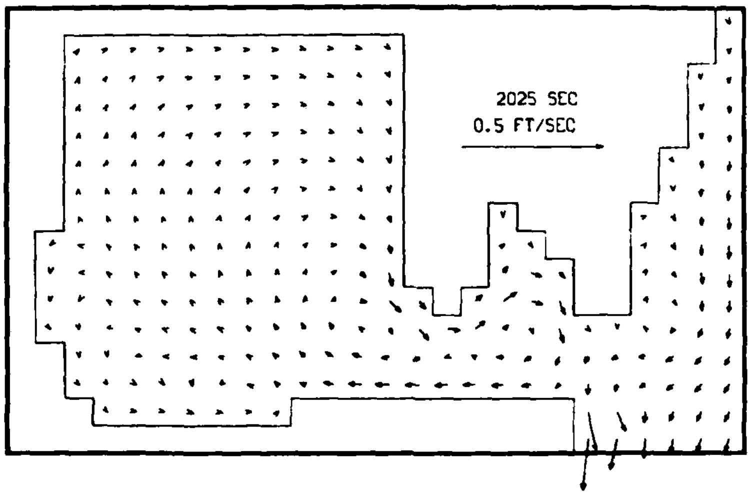

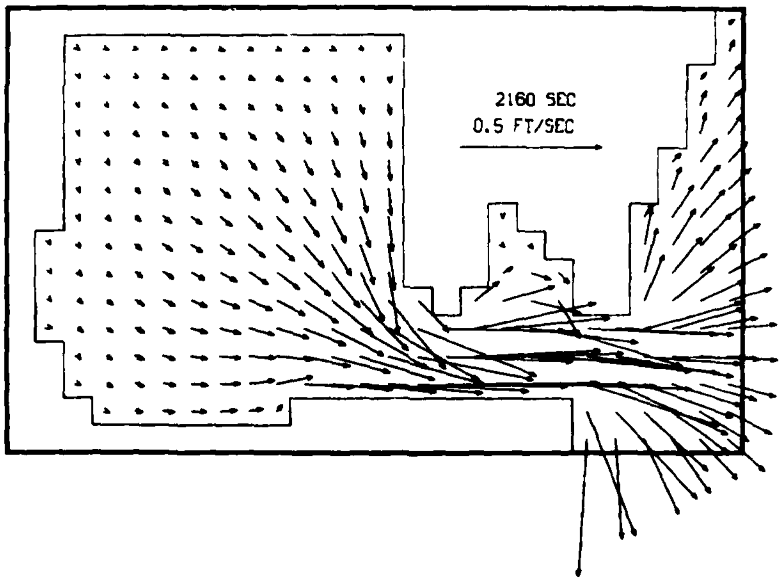

BARBERS POINT HARBOR

WATER VELOCITY

600-SEC PERIOD 0.1-FT. AMPLITUDE

NO FLOODING

PLATE 50

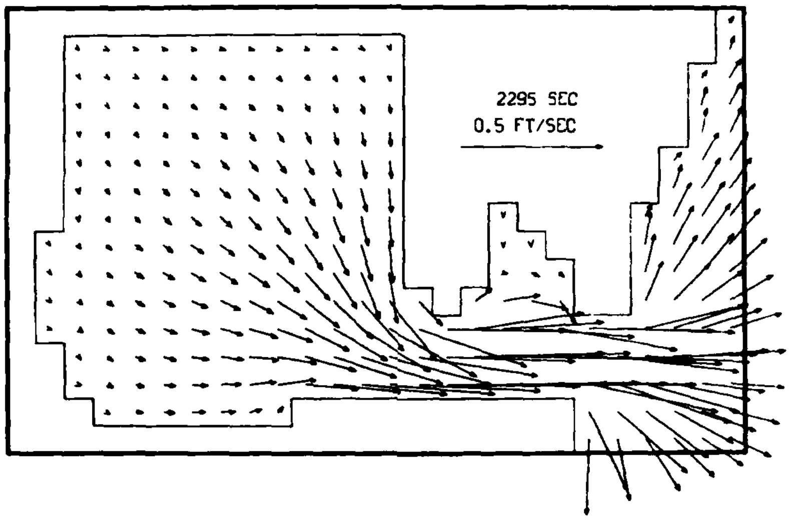

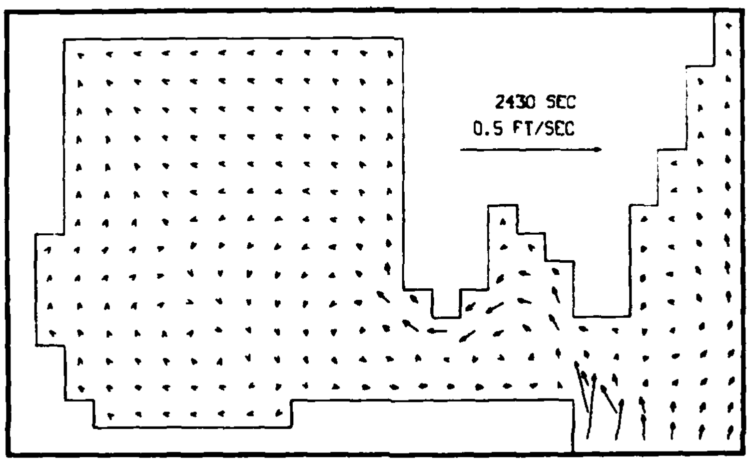

BARBERS POINT HARBOR

WATER VELOCITY

800-SEC PERIOD 0.1-FT. AMPLITUDE
NO FLOODING

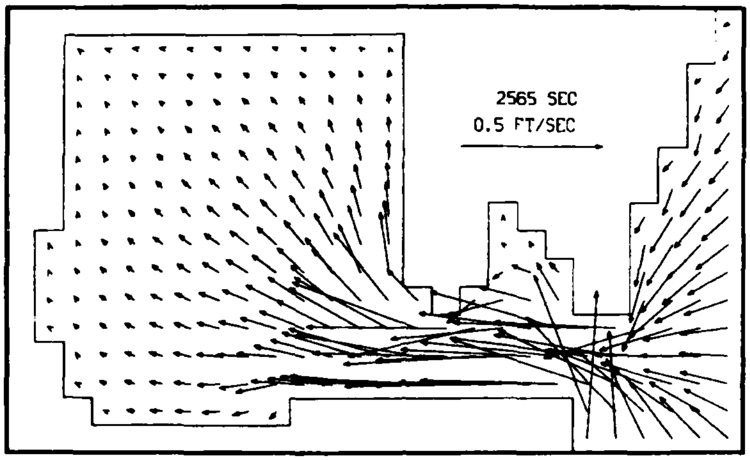

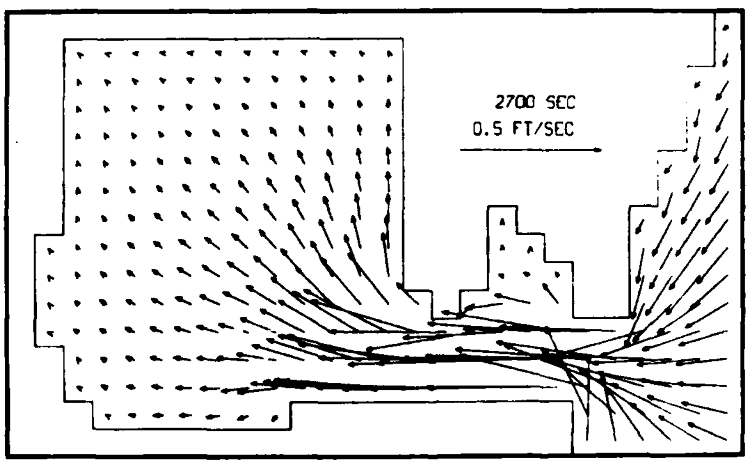

BARBERS POINT HARBOR

WATER VELOCITY

800-SEC PERIOD 0.1-FT. AMPLITUDE

NO FLOODING

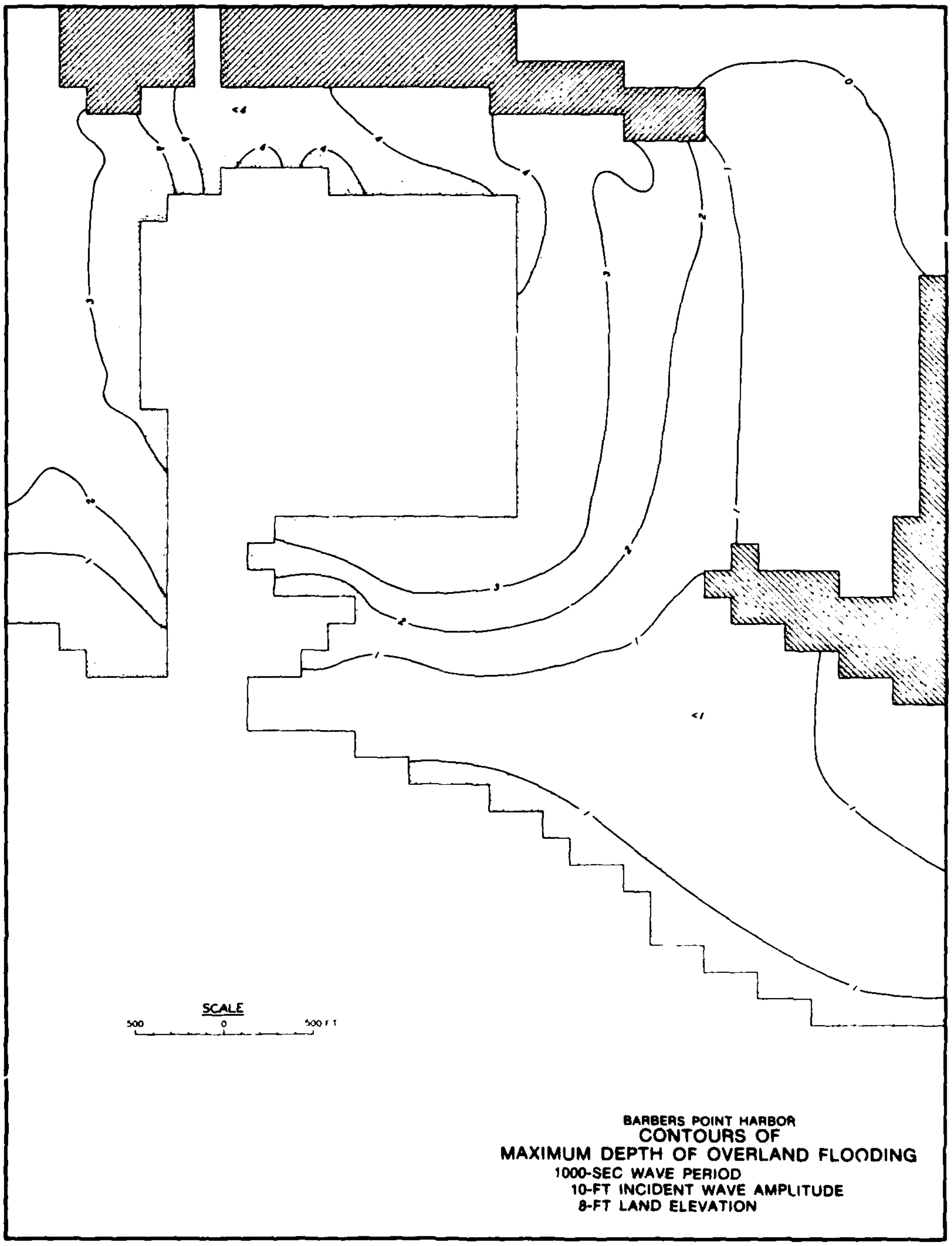

BARBERS POINT HARBOR
CONTOURS OF
MAXIMUM DEPTH OF OVERLAND FLOODING
1000-SEC WAVE PERIOD
10-FT INCIDENT WAVE AMPLITUDE
8-FT LAND ELEVATION

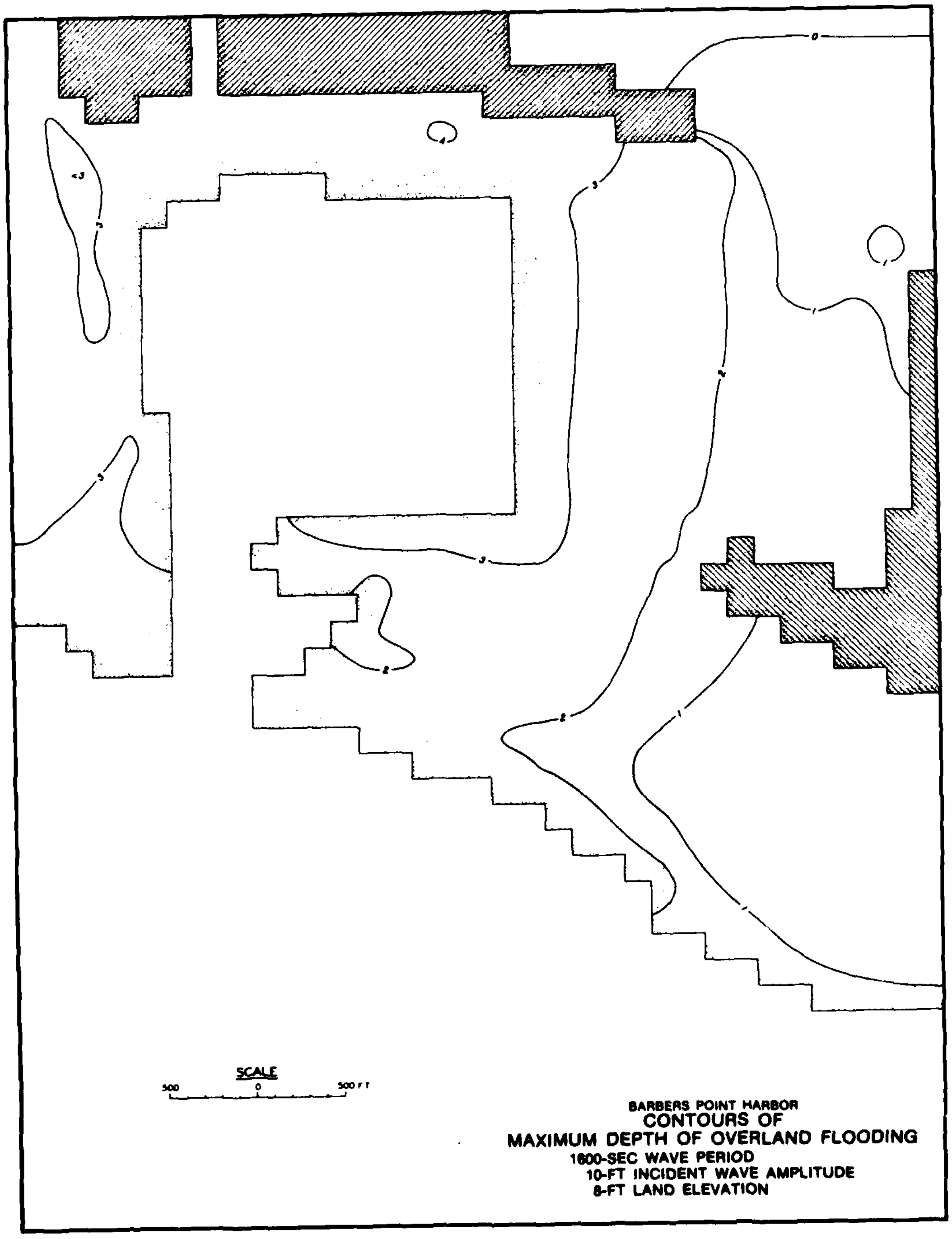
0
<3
3
4
3
2
1
3
2
1
2
1
1
SCALE
500
0
500 FT
BARBERS POINT HARBOR
CONTOURS OF
MAXIMUM DEPTH OF OVERLAND FLOODING
1600-SEC WAVE PERIOD
10-FT INCIDENT WAVE AMPLITUDE
8-FT LAND ELEVATION

PLATE 54

APPENDIX A: VERIFICATION OF MODEL FOR CRESCENT CITY TSUNAMI OF 1964

1. In order to test the model against a known case of flooding around a harbor during a tsunami, the model was run for the Crescent City, Calif., tsunami of 1964. This tsunami was generated by the Alaskan earthquake of that year. The effects have been carefully surveyed, in particular by Magoon (1965). Another study is that of Wiegel (1965). A 101 by 101 grid was set up using topographic data from Magoon and from the U. S. Geological Survey map "Sister Rocks, California," AMS 1167 IINW - Series V895, 1966. The grid encompasses all of the harbor and city area and some areas outside, including all of the Crescent City region that was flooded. The relevant parameters and constants used are $\Delta s = 100$ ft, $\Delta t = 0.75$ sec, $C_o = 2$, $c = 1$, $D_c = 1$ ft, $K = 200\ ft^2/sec^{-1}$, and $n = 0.025$.

2. The input wave rose sinusoidally from 0 to 18.8 ft in 800 sec. The harbor amplified this by a factor of around 1.1, giving an amplitude within the harbor of around 20 ft (depending, of course, on location). The tide gage at Crescent City was unable to record the actual tsunami, so the model input reproduced the inferred marigram of Wilson and Tørum (1968).

3. Figure A1 shows the depths of flooding recorded in the city area by Magoon (dashed lines) compared to model results (solid lines).

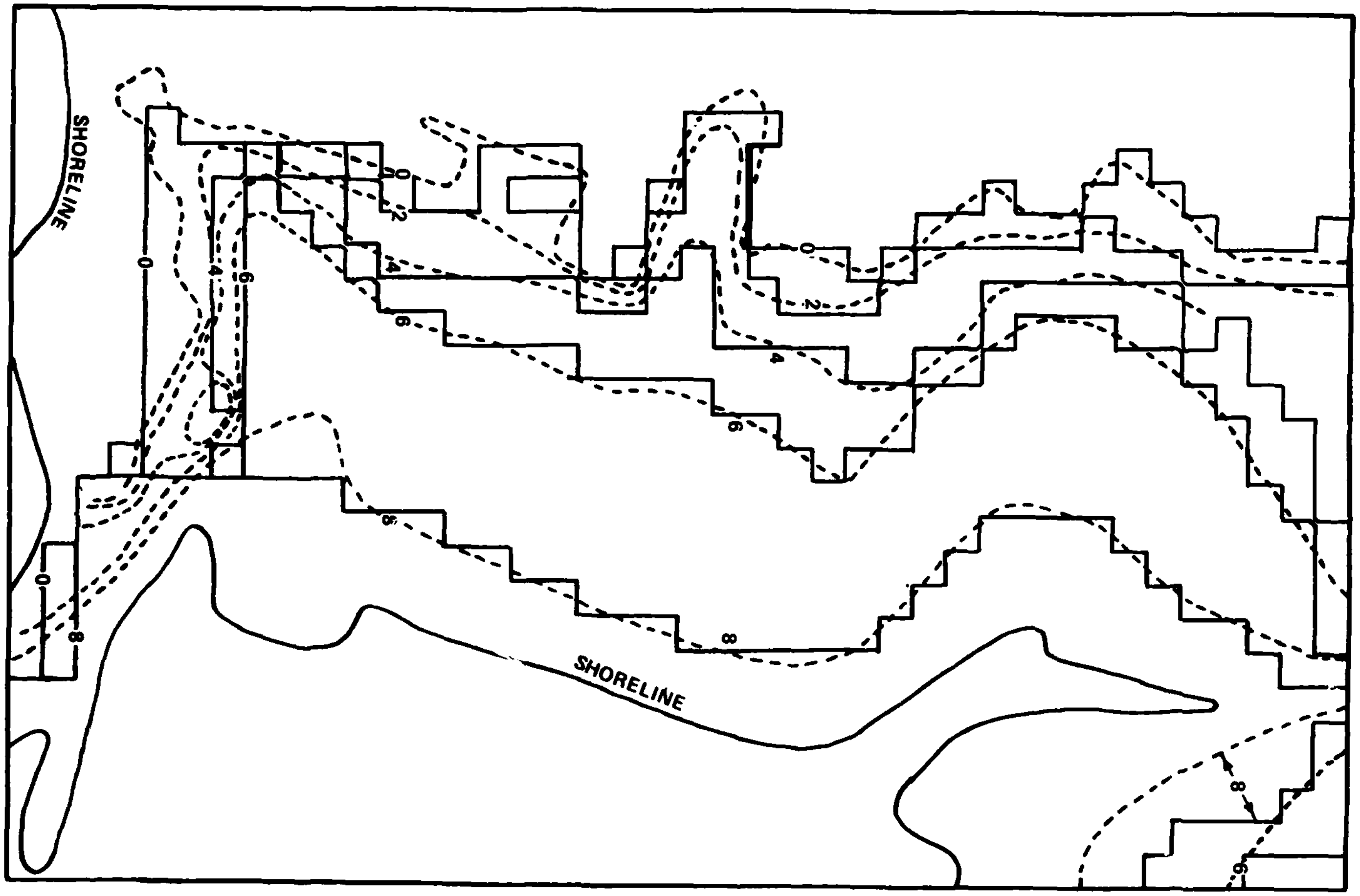

Figure A1. Comparison of Observed (dashed lines) and Computer (solid lines) Depths of Flooding for 1964 Tsunami at Crescent City, California

APPENDIX B: NOTATION

A	Coefficient, frequency-of-occurrence equation
a	Wave component amplitude
A_c	Cross-sectional area of channel
A_h	Surface area of harbor
B	Coefficient frequency-of-occurrence equation
C	Chezy coefficient
c	Arbitrary constant
C_0, C_1	Flooding and drying coefficients
D	Water depth
D_b	Water depth at boundary between cells
D_c	Water depth for using wave equations
F	Event frequency
$F(\omega)$	Wave function
g	Gravitational force/mass
H	Event amplitude, frequency-of-occurrence equation
h	Water depth
h_{max}	Maximum water depth
i, j	Subscripts denoting location of variable
K	Lateral eddy diffusion coefficient
k	Subscript denoting time of variable
ℓ	Channel length
n	Manning's coefficient
Q	Current speed
Q_n	Transport normal to a boundary

$R(x,y,\omega)$	Response function
R_h	Hydraulic radius
S	Water surface slope
T	Wave period
T_0	Fundamental mode period
t	Time
u	x-direction velocity
$\bar{u}$	Average u in a cell
$\underline{u}$	u interpolated to posiiton of v
v	y-direction velocity
$\bar{v}$	Average v in a cell
$\underline{v}$	v interpolated to position of u
z,y,z	Spatial dimensions
Δs	Spatial increment
Δt	Time increment
∇	Gradient operator
η	Surface elevation
ω	Radian frequency

In accordance with letter from DAEN-RDC, DAEN-ASI dated 22 July 1977, Subject: Facsimile Catalog Cards for Laboratory Technical Publications, a facsimile catalog card in Library of Congress MARC format is reproduced below.

Farrar, Paul D.
  Tsunami response of Barbers Point Harbor, Hawaii / by Paul D. Farrar, James R. Houston (Hydraulics Laboratory, U.S. Army Engineer Waterways Experiment Station). -- Vicksburg, Miss. : The Station ; Springfield, Va. ; available from NTIS, 1982.
  82 p. in various pagings, 54 p. of plates : ill. ; 27 cm. -- (Miscellaneous paper ; HL-82-1)
  Cover title.
  "October 1982."
  Final report.
  "Prepared for U.S. Army Engineer Division, Pacific Ocean."
  Bibliography: p. 53.

  1. Barbers Point Harbor (Hawaii). 2. Harbors--Hawaii. 3. Mathematical models. 4. Ocean waves. 5. Tsunamis. I. Houston, James R. II. United States.

Farrar, Paul D.
  Tsunami response of Barbers Point Harbor : ... 1982.
(Card 2)

Army. Corps of Engineers. Pacific Ocean Division. III. U.S. Army Engineer Waterways Experiment Station. Hydraulics Laboratory. IV. Title V. Series: Miscellaneous paper (U.S. Army Engineer Waterways Experiment Station) ; HL-82-1.
TA7.W34m no.HL-82-1

DATE

FILMED

8